FLUIDIZED-BED DRYING AND MICROWAVE-ASSISTED FLUIDIZED-BED DRYING OF CARROT SLICES

XUE HU

Department of Bioresource Engineering

Faculty of Agricultural and Environmental Sciences

McGill University

Sainte-Anne-de-Bellevue, Quebec, Canada

January 2016

Thesis submitted to McGill University in partial fulfilment of the requirement of the degree of

Master of Science

In

Bioresource Engineering

ABSTRACT

Essential nutrients such as minerals, vitamins and fibre are mainly obtained from vegetables and fruits. However, the industrial processing and marketing of fresh fruits and vegetables produce a lot of residues to be disposed. These residues contain nutritional compounds to be recovered for the human consumption. Drying technology can be applied to transform these residues into high-value by-products to enhance the agricultural income and protect the environment. Drying process is used to remove free water from the drying material by the efficient supply of thermal energy and produce dried products of desired quality. Different drying methods have been investigated for drying of vegetables and fruits, such as hot air drying, microwave-assisted drying, microwave-assisted hot air drying and combined microwave-vacuum and freeze drying. In this study, the drying performance of fluidized-bed drying and microwave-assisted fluidized-bed drying were analyzed and optimized. Carrot slices were used as the drying material.

In the first study, the fluidized-bed drying (FBD) of carrot slices without any pre-treatment at controlled inlet air temperatures of 40°C, 50°C and 60°C and with pre-treatment methods of water blanching (WB), osmotic drying 20% sugar solution (SS) and 1% citric acid (CAS) at 60°C were conducted. The drying duration significantly decreased with the increase of drying temperature for carrot slices without any pre-treatment. At the drying temperature of 60°C, there was 60% reduction in drying time for carrot slices with pre-treatment. The best fitting mathematical models to the experimental data were selected and analyzed. The pre-treatment helped to retain the natural color in the dried carrot slices. Textural strength of the dried carrot slices increased with the increase in inlet air temperature and the application of pre-treatments before drying.

In the second study, the microwave-assisted fluidized-bed drying (MWFBD) of carrot slices at different initial microwave power densities and inlet air temperatures were investigated. The drying conditions such as the initial microwave power density and inlet air temperature were optimized. The drying performance of pre-treated carrot slices with

WB, SS and CAS was estimated under the optimized drying conditions. The drying kinetics and physical properties of the dried carrot slices were analyzed. The mathematical models to fit the experimental data and the moisture diffusion were established and analyzed.

RÉSUMÉ

Les nutriments essentiels tels que les minéraux, les vitamines et les fibres sont principalement obtenus à partir de fruits et légumes. Cependant, la transformation industrielle et la commercialisation des fruits et légumes frais produisent beaucoup de résidus à éliminer. Ces résidus contiennent des composés nutritionnels qui peuvent être récupérés pour la consommation humaine. Le séchage est une technologie qui permet de transformer les résidus végétaux dans des sous-produits à valeur ajoutés, créant ainsi une source de revenue tout en réduisant l'impact sur l'environnement. Différentes méthodes ont été étudiées pour réduire la teneur en eau des fruits et légumes. Parmi les méthodes le plus utilisées, on retrouve le séchage à air chaud, le séchage par micro-ondes, séchage à air chaud assistée par micro-ondes, le vide, les lits fluidisés, et la lyophilisation. Dans cette étude, la cinétique de séchage en lit fluidisé et le séchage en lit fluidisé assistée par micro-ondes ont été analysé et optimisé la déshydratation des carottes déclassées.

Dans la première partie de l'étude, des carottes tranchées on été séchées à des températures de l'air d'admission de 40, 50 et 60 °C dans un séchoir à lit fluidisé conventionnel (FBD). Comme on s'y attendait, la durée de séchage a diminué avec l'augmentation de la température et les meilleurs résultats ont été obtenus à 60 °C. Des modèles mathématiques ont été développés pour représenter la cinétique de séchage des tranches de carottes dans un lit fluidisé. Par la suite, des essais ont permis de comparer l'efficacité de différents prétraitements sur le temps de séchage et la qualité des carottes séchées à une température de 60 °C. Les différents prétraitements évalués étaient: le blanchiment à l'eau chaude (WB), trempage dans une solution osmotique contenant 20% de sucre (SS) ou dans une solution contenant 1% d'acide citrique (CAS). Les résultats ont démontré que l'utilisation d'un prétraitement, quel qu'il soit, permettait de réduire de près de 60% le temps de séchage tout en aidant à conserver la couleur naturelle des carottes séchées. De plus, il a été démontré que la texture des tranches de carotte réhydratées était plus élevée lorsque le la température de séchage était plus élevée et lorsque les prétraitements étaient utilisés.

Dans la seconde partie de l'étude, des essais on été effectués pour comparer la cinétique de séchage des tranches de carottes dans un lit fluidisé assisté par micro-ondes (MWFBD) opérant avec différentes densités de puissance micro-ondes et de températures d'air. Des essais ont permis de comparer l'efficacité de différents prétraitements. Les résultats obtenus ont conduit à l'optimisation des conditions de séchage et de prétraitement en fonction du temps de séchage et de la qualité des produits séchés. Des modèles mathématiques ont été développés pour représenter la cinétique de séchage des tranches de carottes dans un lit fluidisé utilisant l'effet combiné de l'air chaud et de l'énergie micro-ondes.

ACKNOWLEDGEMENTS

I would like to express my deep gratitude to my supervisor Dr. G.S.V. Raghavan for his guidance, initiation and encouragement throughout my Mater's project. It is my great honor and pleasure to be in such research group with excellent faculty and teammates, and work under the supervision of Dr. Raghavan.

Special thanks to Mr. Yvan Gariépy for helping with all the technical problems. My project could not be finished successfully without his contributions. And I have really learned a lot of the engineering technologies from him. I am also appreciative of the on and off campus help of Dr. Darwin Lyew.

I would like to gratefully appreciate the support of Dr. Jiby Kurian with the data analysis and drying conditions optimization. And I am really thankful for his patience to assist me in my scientific writing.

I also would like to thank all my teammates in our lab: Sai Kranthi, Brinda, Priyanka, Lanrewaju, and Ademola. Thank you all so much for your motivation during my thesis project. I would like to express my thanks to my friends Kacey, Wenjun, Nani, Madhi, Anisha, and Olivia for their love and support.

I would like to thank my parents and all family members for their unconditional love and support. I will always remember the pleasant memories with all of you in Canada.

CONTRIBUTION OF THE AUTHORS

The work reported in this Thesis was performed by Xue Hu under the supervision of Dr. Vijaya Raghavan of the Department of Bioresource Engineering, Macdonald Campus of McGill University, Montreal. The entire work was conducted at the Machine Shop, Macdonald Campus of McGill University, Montreal.

The following are the manuscripts prepared and submitted for publication:

1. Xue Hu, Jiby Kurian, Yvan Gariépy, G.S. Vijaya Raghavan. 2016. "Fundamentals and Applications of Microwave-Assisted Fluidized-Bed Drying of Fruits and Vegetables: A Review" (submitted).
2. Xue Hu, Jiby Kurian, Yvan Gariépy, G.S. Vijaya Raghavan. 2016. "Fluidized-Bed Drying of Carrot Slices at Controlled Temperatures" (submitted).
3. Xue Hu, Jiby Kurian, Yvan Gariépy, G.S. Vijaya Raghavan. 2016. "Optimization of Microwave-Assisted Fluidized-Bed Drying of Carrot Slices" (submitted).

Co-authors, Dr. Raghavan provided the scientific suggestions in the development of the manuscripts. Dr. Kurian from the Department of Bioresource Engineering was involved in the data analysis and editing of the manuscripts. Mr. Gariépy from the Department of Bioresource Engineering provided the technical suggestions and facilities for carrying out the experiments.

TABLE OF CONTENTS

LIST OF FIGURES

LIST OF TABLES

CHAPTER 1

INTRODUCTION

One third of the global food produced is lost or wasted (Gustavsson et al., 2011), and the industrial processing and marketing of fruits and vegetables produce a lot of residues which are needed to be disposed-off. Fresh fruits and vegetables are an important part of a healthy diet as they are rich in essential nutrients such as minerals and vitamins and fibre (Orsat et al., 2007). Carrot is one of the most widely consumed vegetables and is high in vitamins and fibre content (Doymaz, 2004). One way to reclaim the value out of the carrot residues is to dry them into by-products with added value. This approach will make our agriculture more sustainable and help to protect the environment.

Drying is the oldest method of food preservation and it removes water to a certain degree from food materials in order to increase the shelf life by preventing spoilage and decay (Kendall et al., 2004). The drying of fruits and vegetables is done not only to maintain their quality but also to offer the possibility of adding value to the harvested commodities and providing an opportunity to increase the farm revenues. Drying process is applied to produce dried materials in desired quality and at minimum cost by the efficient supply of thermal energy (Mujumdar, 2014). As the degree of acceptance of dehydrated vegetables and fruits in the market is rising, the demand for a large quantity of dehydrated foods with better quality and longer shelf-life has also increased (Krokida et al., 1998). Production of dehydrated carrots, which could be used in instant soup, have been studied using various drying methods. For example, convective air drying of carrots was conducted by Doymaz (2004), Maskan (2001) has investigated the microwave drying of carrots, solar drying was applied on carrot slices by Şevik (2013), Baysal et al. (2002) have studied the final quality of carrots dried by using the combined microwave and hot air drying.

Fluidized-bed drying (FBD) has been considered as one of the most economical drying methods with fast and uniform drying, high thermal efficiency and short drying time

(Hovmand, 1995). During the fluidized-bed drying process, the hot air is blown through the fluidized-bed chamber at a high velocity in order to maintain the food particles in suspension. Thus the rapid heat and mass transfer can be realized by fast mixing between food particles and the hot air (Doymaz, 2004). Reyes et al. (2002) have studied the effects of the drying conditions and modelled the drying of carrots in a fluidized-bed dryer. Hatamipour and Mowla (2002) have conducted researches on the shrinkage of carrots during FBD. Nazghelichi et al. (2010) did thermodynamic analysis of the drying of carrot cubes in FBD to investigate the energy utilization, the energy utilization ratio, the exergy loss, and the exergy efficiency.

In order to generate heat directly within the material and to achieve faster heating rate, shorter drying time and lower energy consumption (Orsat et al., 2006), microwave energy has been applied to the fluidized-bed drying process and is called as the microwave-assisted fluidized-bed drying (MWFBD). Microwaves have frequencies range from 300 MHz to 30 GHz, with 915 MHz and 2450 MHz being the most commonly used for dielectric heating. which reflects commercial emphasis on home microwave ovens (Venkatesh and Raghavan, 2004). During the MWFBD, microwave energy is usually combined with the hot air to help transport the water vapor away from the drying food material. Investigations were carried to demonstrate the benefit of using microwave energy in combination with the fluidized-bed for drying of carrots. Souraki et al. (2009) have developed the mathematical models of MWFBD of cylindrical carrot samples. Similarly, Stanisławski (2005) has studied the effect of microwave energy on fluidized-bed drying of diced carrots.

The conduction of heat from the surface of the product to the interior results in hardness of the products. In addition, drying with high temperature causes poor appearance and wilt on the products (Sanga et al., 2002). The application of pre-treatments to fruits and vegetables before drying is often recommended to enhance the quality and safety of the dried materials. For example, blanching in boiling water slows down or stops the enzyme activity that can cause undesirable changes during storage and helps in the retention of some vitamins and color (Kingsly et al., 2007).

1.1 Hypothesis

A lot of residues rejected by the fruits and vegetables industries are considered as waste and are need to be disposed of either in landfill, composted, or used as feed for livestock. Drying these residues into by-products with added value is an optimal way to reclaim the value of these residues. Conventional drying methods are widely used for this purpose but they are energy intensive with long drying time. With the application of microwave-assisted fluidized-bed dryer, the surface area for heat and mass transfer can be maximized due to the fluidization of the drying materials, and the heat can be generated directly from the interior of the food material. By the combination of microwave energy and fluidized-bed dryer, faster and more uniform drying of the materials with higher thermal efficiency, shorter drying time and better quality of dried products can be achieved.

1.2 Objectives

1.2.1 Overall Objectives

In this study, a microwave-assisted fluidized-bed dryer was designed, built, and tested to process vegetable and fruit residues under the optimized conditions for human and animal consumption. Carrot slices were used as the drying material. Mathematical models of drying process were developed and analyzed. The physical quality of the dried carrot slices was analyzed.

1.2.2 Specific Objectives

1) To investigate the effect of different inlet air temperatures and the application of pre-treatments on the drying time and the quality of the dried carrot slices in the fluidized-bed drying.
2) To optimize the initial microwave power density and the inlet air temperature in the microwave-assisted fluidized-bed drying, and to evaluate the quality of the dried carrot slices with pretreatment which were dried under the optimized drying conditions.

References

Baysal, T., Ersus, S., Icier, F. 2002. Effects of microwave and hot air combination drying on the quality of carrots. *Food Science and Biotechnology*, **11**(1), 19-23.

Doymaz, I. 2004. Convective air drying characteristics of thin layer carrots. *Journal of Food Engineering*, **61**(3), 359-364.

Gustavsson, J., Cederberg, C., Sonesson, U., Van Otterdijk, R., Meybeck, A. 2011. Global food losses and food waste. *Food and Agriculture Organization of the United Nations, Rom*.

Hatamipour, M., Mowla, D. 2002. Shrinkage of carrots during drying in an inert medium fluidized bed. *Journal of Food Engineering*, **55**(3), 247-252.

Hovmand, S. 1995. Fluidized bed drying. *Handbook of Industrial Drying*, **1**, 195-248.

Kendall, P.A., DiPersio, P.A., Sofos, J.N. 2004. *Drying vegetables*. Colorado State University Cooperative Extension.

Kingsly, A., Singh, R., Goyal, R., Singh, D. 2007. Thin-layer drying behaviour of organically produced tomato. *Am. J. Food Technol*, **2**, 71-78.

Krokida, M., Karathanos, V., Maroulis, Z. 1998. Effect of freeze-drying conditions on shrinkage and porosity of dehydrated agricultural products. *Journal of Food Engineering*, **35**(4), 369-380.

Maskan, M. 2001. Drying, shrinkage and rehydration characteristics of kiwifruits during hot air and microwave drying. *Journal of food engineering*, **48**(2), 177-182.

Mujumdar, A.S. 2014. *Handbook of industrial drying*. CRC Press.

Nazghelichi, T., Kianmehr, M.H., Aghbashlo, M. 2010. Thermodynamic analysis of fluidized bed drying of carrot cubes. *Energy*, **35**(12), 4679-4684.

Orsat, V., Changrue, V., Raghavan, G. 2006. Microwave drying of fruits and vegetables. *Stewart Postharvest Review*, **2**(6), 1-7.

Orsat, V., Yang, W., Changrue, V., Raghavan, G. 2007. Microwave-assisted drying of biomaterials. *Food and Bioproducts Processing*, **85**(3), 255-263.

Reyes, A., Alvarez, P., Marquardt, F. 2002. Drying of carrots in a fluidized bed. I. Effects of drying conditions and modelling. *Drying technology*, **20**(7), 1463-1483.

Sanga, E., Mujumdar, A., Raghavan, G. 2002. Simulation of convection-microwave drying for a shrinking material. *Chemical Engineering and Processing: Process Intensification*, **41**(6), 487-499.

Şevik, S. 2013. Design, experimental investigation and analysis of a solar drying system. *Energy Conversion and Management*, **68**, 227-234.

Souraki, B.A., Andres, A., Mowla, D. 2009. Mathematical modeling of microwave-assisted inert medium fluidized bed drying of cylindrical carrot samples. *Chemical Engineering and Processing: Process Intensification*, **48**(1), 296-305.

Stanisławski, J. 2005. Drying of diced carrot in a combined microwave–fluidized bed dryer. *Drying Technology*, **23**(8), 1711-1721.

Venkatesh, M., Raghavan, G. 2004. An overview of microwave processing and dielectric properties of agri-food materials. *Biosystems Engineering*, **88**(1), 1-18.

CHAPTER 2

FUNDAMENTALS AND APPLICATIONS OF MICROWAVE-ASSISTED FLUIDIZED-BED DRYING OF FRUITS AND VEGETABLES: A REVIEW**

Xue Hu*, Jiby Kurian, Yvan Gariépy, Vijaya Raghavan

Department of Bioresource Engineering, McGill University, 21111 Lakeshore Rd., Ste-Anne-de-Bellevue, QC, H9X 3V9, Canada

* Correspondence author:

Xue Hu, Department of Bioresource Engineering, McGill University, QC, H9X 3V9, Canada.

Phone: (438)-881-0425, Email: xue.hu@mail.mcgill.ca

**Submitted to Journal of Agricultural Science and Technology.

Abstract

Drying is the process of removing free water from substances and it can be applied to dehydrate horticultural produces and their residues to meet the increasing demand for dehydrated foods and materials. A variety of drying methods have been developed for the industrial applications and they can be used to make value-added products from vegetable residues. In order to compensate for the drawbacks of a particular drying method and to achieve high efficiency and high-quality products, an integration of different drying methods has to be investigated. This literature review comprehensively introduces the microwave-assisted fluidized-bed drying, which is a combination of fluidized-bed drying and microwave-assisted drying. The uniformity in temperature distribution can be achieved with fluidization of the material, and the drying duration can be significantly reduced by using microwave energy. Drying kinetics and mathematical models of moisture diffusion in fluidized-bed drying, microwave drying and microwaved-assisted fluidized bed drying are described in this review.

Keyword: drying, kinetics, fluidization, moisture content, microwave drying, microwave-assisted fluidized bed drying

2.1 Introduction

Fresh fruits and vegetables are an important part of a healthy diet as they are rich in vitamins, minerals and fiber. Food safety is considered as protecting the food from microbial, physical (drying out, infestation) and chemical (rancidity, browning) damage or contamination that may occur during processes of food growing, harvesting, processing, transporting, distribution and storage.

Drying is one of the oldest and most common engineering unit operations (Dufour, 2006; Mujumdar, 2014) and has been used in many industries for the processing of agricultural products, minerals, wood and many other natural biological materials (Kowalski, 2010). The most widely applied drying technology is the thermal drying, which involve three different heat transfer mechanisms; conduction, convection and radiation (Goodenough et al., 2007). During thermal drying process, heat is added to increase the vapor pressure of the moisture within the substances to enhance moisture migration and also to substantially decrease the relative humidity of the drying air to increase its moisture carrying capacity (Dincer, 2002; Dincer et al., 2002; Dincer and Sahin, 2004).

The importance of storing dried food materials for future consumption has been widely acknowledged and traditionally large quantities of food resources are being dried under sunlight (May and Perré, 2002). The basic objective of drying of food is removing water to a certain level at which microbial spoilage will be prevented (Drouzas and Schubert, 1996). Even though drying of materials has been practiced for millennia, a detailed understanding of the drying mechanisms of biological materials is required for the efficient management and utilization of agricultural products and energy resources (Scherer, 1990). Thermal decomposition takes place during drying which causes defects in final products. Therefore other non-conventional drying techniques such as acoustic drying, osmosis drying and freeze drying, etc., have to be applied to dry the heat-sensitive materials (Gayot et al., 2003). The drying process conditions are to be carefully controlled to maintain the food safety as well as high nutritional values for the long storage of fruits and vegetables to achieve a positive impact on the health of the consumers.

At present, the demand for dehydrated fruits and vegetables has increased in the global market (Villagran et al., 2003). Furthermore, industrial processing and marketing of fresh vegetables produce large volumes of residues (about 1.3 billion tons per year) that need to be disposed (Laufenberg et al., 2003) to avoid pollution problems. This large quantity of vegetable wastes can be converted into dehydrated products to reclaim their value (Lopez et al., 2000). These dehydrated vegetables are high in nutrient content, free of chemicals and preservatives, have an improved appearance and taste (Lakshmi and Vimala, 2000) and have an indefinite storage life (Rockstrom, 2000).

Various drying methods such as fluidized-bed drying, microwave-assisted drying, vacuum drying, freeze drying and solar drying are widely used to make dried fruits and vegetables (Van Arsdel et al., 1973). The fluidized-bed drying can be used to produce high-quality dried products with low capital investment (Senadeera et al., 2003). Vacuum drying method uses steam or radiation for moisture removal under low pressure conditions and the oxidation will be low in the dried products (Drouzas and Schubert, 1996). Freeze drying can reduce the quality degradation as it takes place under low temperatures and pressure conditions (Marques et al., 2006). The selection of drying methods is dependent on the properties of the raw food material, desired properties of the dried products, capital investments required and the operation conditions. Table 2.1 shows the drying method selection with respect to the physical nature of the food item.

Table 2. 1: Selection of drying methods for liquid and solid foods (Raghavan and Orsat, 2007)

Drying method	Food type
Air convection dryer	Pieces
Cabinet	Pieces, slurries, liquids
Tunnel	Pieces
Air lift	Small pieces, granules
Fluidized bed	Small pieces, granules
Spray	Liquid, slurries
Vacuum	Pieces, slurries, liquids
Freeze dryer	Pieces, liquids

However, drying of fruits and vegetables cause some undesired effects such as change in color and flavor and vitamin degradation in the final products (Gutoff et al., 1995). Therefore, further insights on drying mechanisms are required for the production of safe and high quality foods with longer storage life for local and global markets (De la Fuente-Blanco et al., 2006).

This paper reviews the fundamentals of fluidized-bed, microwave-assisted and microwave-assisted fluidized-bed (MAFB) drying methods. The application of MAFB for the drying of fruits and vegetables is also described.

2.2 General Kinetics of Material Drying

There are two stages in the drying of a material. The first stage takes place at a constant rate and removes moisture from the surface of the drying material into the ambient atmosphere. The second stage transfers moisture from the interior of the drying material to its surface at a decreasing drying rate and is dependent on the properties of the drying materials (Midilli and Kucuk, 2003). Energy is transferred from the surrounding environment to the drying material that evaporate the surface moisture and transfer the internal moisture to the surface of the drying material. The overall drying rate is governed by all these processes (Krokida et al., 2003; Mujumdar, 2014).

The dynamic factors such as moisture ratio, heat and mass transfer coefficients, and thermal diffusivity can be used to describe the drying kinetics (Giri and Prasad, 2007). The moisture ratio (*MR*), which is the ratio of free water to be removed at time *t* to the total free water initially available (Babalis and Belessiotis, 2004), can be calculated by using Equation 1.

$$MR = \frac{M_t - M_e}{M_0 - M_e} \quad (1)$$

Where M_t is the moisture content at time *t*, M_e is the equilibrium moisture content and M_0 is the initial moisture content (Akpinar et al., 2003).

Different mathematical models given in Table 2.2 can be used to simulate the drying kinetics and describe the drying process.

Table 2. 2: Mathematical models for describing the drying kinetics.

Name	Model equation	Reference
Page	$MR = \exp(-kt^n)$	(Batchelor et al., 2008; Toğrul and Pehlivan, 2002)
Modified Page	$MR = \exp(-(kt)^n)$	(Overhults et al., 1973)
Newton	$MR = \exp(-kt)$	(Midilli and Kucuk, 2003)
Wang and Singh	$MR = bt^2 + at + 1$	(Mohapatra and Rao, 2005)
Henderson and Pabis	$MR = aexp(-kt)$	(Thompson et al., 1968; Yaldiz et al., 2001)
Thomson	$t = aln(MR) + b(ln(MR))^2$	(Ertekin and Yaldiz, 2004)
Two-term	$MR = aexp(-k_0t) + bexp(-k_1t)$	(Ertekin and Yaldiz, 2004; Midilli et al., 2002)
Logarithmic	$MR = aexp(-kt^n) + C$	(Xanthopoulos et al., 2007)

One of the primary criteria in selecting the suitable model to describe the drying kinetics is the correlation coefficient *(r).* Other parameters like the reduced chi-square (χ^2), mean bias error (MBE) and root mean square error (RMSE) are also used to decide the quality of fitting the mathematical models to the observations. Equations for the chi-square, MBE and RMSE are the following:

$$\chi^2 = \frac{\sum_{i=1}^{N}\left(MR_{exp,i} - MR_{pre,i}\right)^2}{N - n} \tag{2}$$

$$MBE = \frac{1}{N}\sum_{i=1}^{N}\left(MR_{pre,i} - MR_{exp,i}\right) \tag{3}$$

$$RMSE = \left[\frac{1}{N}\sum_{i=1}^{N}\left(MR_{pre,i} - MR_{exp,i}\right)^2\right]^{1/2} \tag{4}$$

Where $MR_{exp,i}$ is the experimental moisture ratio, $MR_{pre,i}$ is the predicted moisture ratio, N and n are observations number and constant number respectively (Toğrul and Pehlivan, 2003).

Drying of material requires supply of energy and the energy that must be overcome for chemical reactions (such as free amino acid changing and sugar reducing) to occur during drying process is defined as the energy barrier (D_{eff}). The energy barrier can be calculated from the Arrhenius equation (Laidler, 1984) given in Equation 5.

$$D_{eff} = D_0 \exp\left(-\left(\frac{E_a}{RT}\right)\right) \tag{5}$$

Where D_0 is a pre-exponential factor, E_a is activation energy (kJ/kg mol), R is the universal gas constant (8.314 kJ/kg mol·K) and T is the absolute temperature (K) (Galwey and Brown, 2002).

2.3 Fluidized-Bed Drying of Materials

Fluidization is defined as an operation in which solid particles are transformed from their static state into a dynamic fluid-like state through contact with a stream of gas or liquid (Kunii and Levenspiel, 2013). Fluidization systems have been applied in many industries involving physical, chemical, electrochemical, petrochemical and biochemical operations (Brenner, 2013).

In a fixed-bed system, a gas flow will be passed at a low velocity upwards through the bed of solid particles to be percolated through the voids between the stationary particles (Dwivedi and Upadhyay, 1977). At this time, the aerodynamic drag forces on each particle will be low and the solid particles will remain in a fixed state. By gradually increasing the air velocity, the aerodynamic forces will start to counteract the gravitational forces, causing the solid particles to move away from each other and an incipient-fluidized-bed will be formed (Wang and Chen, 2000). Further increasing the air velocity to a critical value, the aerodynamic forces will be equal to the gravitational forces and the solid particles will be suspended within the fluid to create a fluidized-bed system (Kunii and Levenspiel, 2013). The different stages in the fluidization process is depicted in Fig. 2.1.

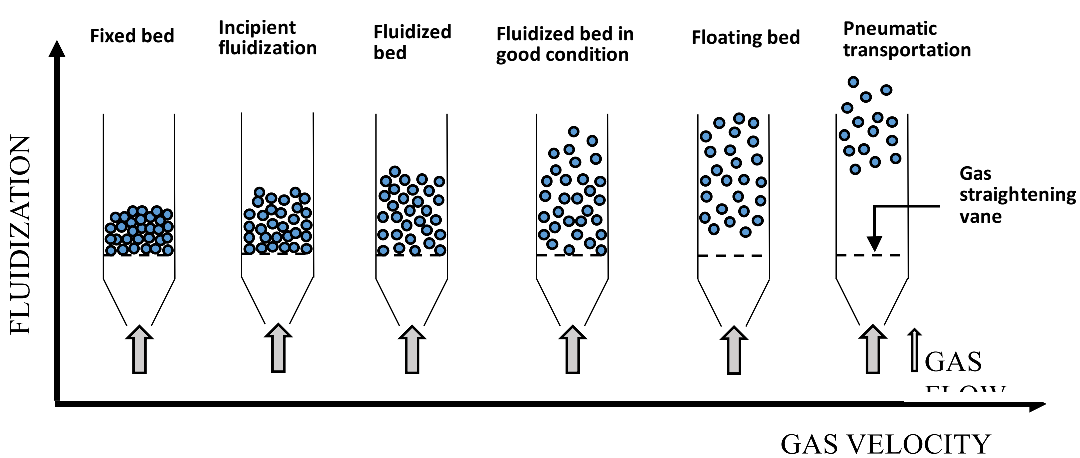

Figure 2. 1: Different stages of fluidization.

2.3.1 Kinetics of Fluidized-Bed Drying

The minimum fluidization velocity, u_{mf}, is the most important factor in designing a fluidization bed (Geldart, 1973). It is dependent on the size and shapes of solid particles and can be calculated using Equations 6 and 7.

For very small particles with $Re_{p,mf} < 20$;

$$u_{mf} = \frac{d_p^2(\rho_s - \rho_g)g}{150\mu} \frac{\varepsilon_{mf}^3 \phi_s^2}{1 - \varepsilon_{mf}} \tag{6}$$

For very large particles with $Re_{p,mf} > 1000$;

$$u_{mf}{}^2 = \frac{d_p(\rho_s - \rho_g)g}{1.75\rho_g} \varepsilon_{mf}^3 \phi_s \tag{7}$$

Where $Re_{p,mf}$ is the particle's Reynolds number, ε_{mf} is the void fraction at minimum fluidization condition, ρ_s and ρ_g are the density of solids and the density of gas respectively, d_p is the particle's diameter, ϕ_s is the sphericity of the particles and μ is the viscosity of gas (kg/m·s) (Kunii and Levenspiel, 2013).

Fluidization occurs when the pressure drop (ΔP) is positive. The ΔP can be calculated using Equation 8.

$$\frac{\Delta P}{L_{mf}} = (1 - \varepsilon_{mf})(\rho_s - \rho_g)\frac{g}{g_c} \tag{8}$$

Where L_{mf} is the height of bed at minimum fluidization and g_c is the conversion factor (Soponronnarit and Prachayawarakorn, 1994).

The diagram of ΔP versus velocity (u) is used for an indication of the quality of fluidization (Chaplin et al., 2004). At the initial stage, the bed remains in a fixed state and the ΔP will be approximately proportional to the air velocity. Increasing the air velocity until ΔP_{max} equals to the gravitational forces will create the incipient-fluidization condition. Further increase in the air velocity will increase the voidage and results in a decrease in the fluid flow resistance. When the air velocity exceeds the minimum fluid velocity, (u_{mf}), the bed expands and a non-homogeneity will occur (Wang and Chen, 2000). However, the ΔP remains at a constant value ($\Delta P_{\max}$). As the air velocity decreases, the ΔP remains constant until the voidage decreases to the fixed bed voidage, (ε_{mf}). Further decreasing the air velocity to zero causes the ΔP to decrease and voidage to increase back to the initial fixed state (ε_m) (Nitz and Taranto, 2007). The reaction between ΔP and air velocity (u) is depicted in Fig 2.2.

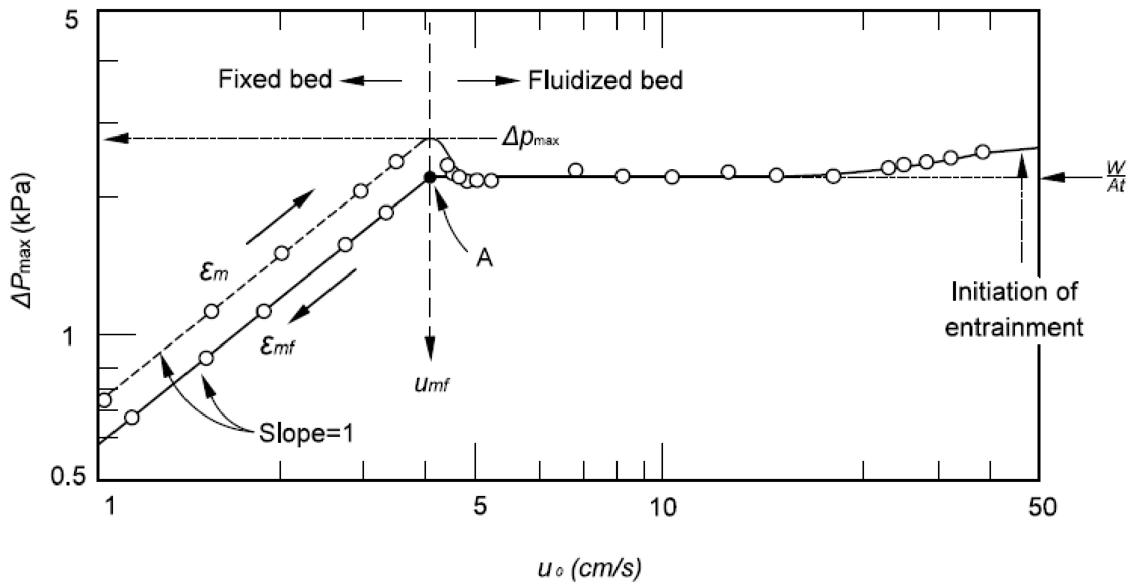

Figure 2. 2: Diagram of pressure drop and air velocity. At is the cross-section area of bed (m^2) and W is the mass of solids (kg) (Kunii and Levenspiel, 2013).

2.3.2 Dynamics of Fluidized-Bed Drying

Fluidized-bed drying has rapid heat and mass transfer properties (Bialobrzewski et al., 2008) and has been considered as an efficient and economical drying technology (Senadeera et al., 2003). In addition, it prevents the materials from being overheated while drying and is a good choice to dry heat sensitive materials (Senadeera et al., 2000).

Fluidized-bed drying is a method of convective drying. At the initial stage of the drying process, the moisture content is very high and the unbound moisture at the surface of particles starts to evaporate as soon as it is exposed to the hot dry air. The rate of water removal is dependent on the temperature, velocity and humidity of the inlet air (Goksu et al., 2005). During this period, the rate of evaporation is very rapid and the critical point of drying process will be reached fast (Geankoplis, 2003).

At lower moisture content levels, the drying process is mainly controlled by the rate of moisture diffusion within the particles and the drying rate decreases significantly (Hovmand, 1995). Ultimately, the surface moisture will evaporate entirely. On further drying, the drying rate continues to decrease with the reduction in internal moisture content. When the moisture content reaches the equilibrium value, the drying process stops. During this period, the drying rate is mainly determined by the physical properties such as the density and porosity of the drying materials (Hlinak and Saleki-Gerhardt, 2000). This decreasing drying rate is one of the drawbacks of the fluidized-bed drying.

Luikov's equations (Equations 9-11) can be used to express the relationships between moisture content *M*, temperature *T* and air pressure *P* for the drying of capillary porous materials.

$$\frac{\partial M}{\partial t} = \nabla^2 k_{11} M + \nabla^2 k_{12} T + \nabla^2 k_{13} P \tag{9}$$

$$\frac{\partial T}{\partial t} = \nabla^2 k_{21} M + \nabla^2 k_{22} T + \nabla^2 k_{23} P \tag{10}$$

$$\frac{\partial P}{\partial t} = \nabla^2 k_{31} M + \nabla^2 k_{32} T + \nabla^2 k_{33} P \tag{11}$$

Where k_{ij} refers to diffusion coefficient and *t* is the drying time (Qin et al., 2006). When the pressure gradient and thermal diffusion are negligible, the Luikov's model can be simplified to a general diffusion equation as in Equation 12:

$$\frac{\partial M}{\partial t} = \nabla^2 k_{11} M \tag{12}$$

The Fick's law of diffusion, which is a linear equation as shown in Equation 13, can be used to simulate numerically the mass transfer in drying systems (Desai, 2015):

$$\ln(MR) = \ln\left(\frac{M_t - M_e}{M_0 - M_e}\right) = lnA - \left(\frac{D_{eff} t}{4L^2}\right) \tag{13}$$

Where the constant A can be determined by using Equation 14:

$$A = \frac{8}{\pi^2} \tag{14}$$

A plot of $\ln(MR)$ versus the drying time (t) gives a straight line with a slope P. The moisture diffusion coefficient can be determined by using the slope value P (Equation 15).

$$P = \frac{D_{eff}}{4L^2} \quad (15)$$

In addition, the activation energy (E_a) of products during drying can be determined by linearizing the Arrhenius equation via taking the natural logarithm of both sides, as shown in Equation 16 (Schwaab and Pinto, 2007).

$$\ln(D_{eff}) = ln(D_0) - (\frac{E_a}{RT})(\frac{1}{T}) \quad (16)$$

By plotting $\ln(D_{eff})$ versus $\frac{1}{T}$, we can find the activation energy (E_a).

2.4 Microwave-Assisted Drying of Materials

2.4.1 Overview of Microwave-Assisted Drying

Microwaves (MW) exist between the infrared (IR) radiation and radio waves of the electromagnetic spectrum, with wavelengths between 1 mm and 1 m and frequencies between 0. 3 and 300 *GHz*. To avoid interference with the telecommunication uses, the main operating frequency is 2.45(±0.050) *GHz* in most of the MW units (Menéndez et al., 2010) and large industrial MW ovens often use 915*MHz* also (Baker and Krajewski, 1966). The invention of magnetron to generates microwaves facilitated the use of microwave for heating of MW-sensitive materials (Metaxas and Meredith, 1983) in industries and kitchens around the world (Kingston and Jassie, 1988).

Microwave drying has several advantages over conventional drying and they include homogenous energy distribution, shortening of drying time by about 50% (Ozkan et al., 2007), nondestructive drying of the materials, requirement of less floor space and handling (Schiffmann, 2001). Microwave penetration to the MW-sensitive materials provides rapid and uniform heating makes it a competitive alternative to the conventional heating methods (Leadbeater and Marco, 2003). It has been used in drying of leather, textiles, paper, and in the extraction compounds from biomaterials. However, food processing industry is the largest consumer of microwave heating technologies (Ayappa et al., 1991). Microwave-assisted drying has been widely used for drying of vegetables and fruits such as onion, potatoes, carrots and cranberries (Nijhuis et al., 1998). Apart from decreasing the drying time, the microwave-dried products are softer than the freeze-dried products (Venkatachalapathy and Raghavan, 1999). Additionally color, shrinkage and rehydration property of final products dried by microwave-assisted process are all superior to conventional drying (Wang and Xi, 2005). However, the drawbacks of the microwave heating include uneven heating within the material and damaging of food texture from the very rapid mass transfer, and the high capital cost (Sumnu et al., 2005).

2.4.2 Mechanism and Kinetics of Microwave-Assisted Heating

There are two main heating mechanisms taking place during the microwave-assisted heating. First one is the ionic conduction in which ions move in the opposite direction of their polarities under an applied electric field (Datta, 1990). While moving the ions collide with non-ionized molecules, and transfer a part of their mechanical energy to stimulate the latter to move fast and collide with other molecules. The ions will accelerate in the opposite direction when the polarity of electric field changes. The electric field changes at millions of times per second that results in a large number of ionic collisions and a significant amount of energy transfer takes place in the system. During the ionic conduction, electric energy converts to kinetic energy to generate the movement of the ions. A part of this kinetic energy will be converted to thermal energy because of the friction and collisions between the ions and non-ions (Janney et al., 1997). The power required for the ionic conduction per unit volume (P_v) can be expressed as Equation 17 (Mujumdar, 2014):

$$P_v = E^2 q n \mu \tag{17}$$

Where, q is the amount of electrical charge on each of the ions, n is the ionic density, and μ is the mobility level of the ions.

Another mechanism takes place during MW-assisted heating is the dipolar rotation. In many dielectric materials, dipolar molecules tend to pull themselves to align themselves in an electric field. The dipoles attempt to realign themselves with the alternating electric field and many continuous collisions will occur in the material under MW irradiation

(Oliveira and Franca, 2002). Heat produced by friction and collision between dipole molecules is released constantly per cycle of alternating electric field (Meredith, 1998). The rapid changing of the electric field from decay to zero results in the dipole molecules aligning and relaxing millions of times per second. This results in the conversion of electrical energy to potential energy and the kinetic energy to thermal energy within the materials under the MW treatment. The power consumption (P_v) required for the dipolar rotation is given in Equation 18 (Mujumdar, 2014):

$$P_v = kE^2 f \epsilon'' \tag{18}$$

Where k is a constant, E is the electric field strength (V/m), f is the microwave frequency, and ϵ'' is the loss factor.

Energy penetration becomes a crucial factor for the bulk heating of materials. There will be uneven heating between the top and the bottom of the drying materials depending on the depth of MW penetration into the material. The depth of the MW penetration can be expressed as shown in Equation 19 (Meredith, 1998):

$$D = \frac{\lambda_0 \sqrt{2}}{2\pi} \left[\epsilon' \left(\sqrt{1 + (\epsilon''/\epsilon')^2} - 1 \right) \right]^{-\frac{1}{2}} \tag{19}$$

Where ϵ' is the dielectric constant of the material and λ_0 is the free space wavelength. If ϵ'' is low, Equation 19 can be simplified to as given in Equation 20:

$$D = \frac{\lambda_0 \sqrt{\epsilon'}}{2\pi \epsilon''} \tag{20}$$

The feasibility of drying of materials using microwave-assisted heating can be evaluated using Equation 21:

$$DE = \frac{m_0 (M_0 - M_f)}{t_{on} P (1 - M_f)} \tag{21}$$

Where, DE is drying performance (kg of evaporated water per J of energy), m_0 is initial mass of drying materials (kg), M_f is final moisture content (a ratio on wet basis), P is MW input power (W), t_{on} is the total time when MW is turned on (Yongsawatdigul and Gunasekaran, 1996).

During microwave-assisted heating, a part of the energy is reflected and a part is absorbed. These energy proportions are defined by the dielectric properties of the materials under MW-heating. The dielectric properties is also known as the relative permittivity (ε^*) (Venkatesh and Raghavan, 2004) and is mathematically expressed as in Equation 22:

$$\varepsilon^* = \varepsilon' - j\varepsilon'' \tag{22}$$

Table 2.3 shows the dielectric properties of some fresh fruits and vegetable at 2.45 MHz.

Table 2. 3: The dielectric properties of fresh fruits and vegetables at room temperature (Nelson et al., 1994).

Fruits/vegetables	**Microwave frequency: 2.45 MHz**	
	ε'	ε''
Apple	54	10
Avocado	45	12
Banana	60	18
Cantaloupe	66	13
Carrot	56	15
Cucumber	69	12
Grape	65	17
Grapefruit	73	15
Honeydew	69	17
Kiwifruit	66	17
Lemon	71	14
Lime	70	15
Mango	61	14
Onion	64	14
Orange	69	16
Papaya	67	14
Peach	67	14
Pear	64	13
Potato	57	17
Radish	67	15
Squash	62	13
Strawberry	71	14
Sweet potato	52	14
Turnip	61	12

The instantaneous energy efficiency ε_{in} can be described as following:

$$\varepsilon_{in} = \frac{energy\ used\ for\ evaporation\ at\ time\ t}{input\ energy\ at\ time\ t} \tag{23}$$

And the cumulative energy efficiency $\bar{\varepsilon}$ among a time interval is:

$$\bar{\varepsilon} = \frac{1}{t}\int_0^t \varepsilon(t)dt \tag{24}$$

The kinetics of microwave-assisted drying are quite different from the kinetics of conventional drying. In the conventional drying system, the falling rate stage is a very slow one due to the limited diffusion of moisture. Therefore, a relatively high external temperature is required to increase the temperature gradient in the system (Bond et al., 1993). Whereas in microwave-assisted drying, diffusion of moisture occurs mainly because of the total pressure gradient created by the rapid moisture evaporation inside the drying materials (Idris et al., 2004). The higher the initial moisture, the greater the influence of the pressure gradient on moisture removal from the materials under MW irradiation (Mujumdar, 2014). Compared to conventional drying, the microwave-assisted heating significantly increases the dying rate, especially at lower moisture contents (Beaudry et al., 2004).

In the initial stages of MW-assisted drying, the effect of moisture content and pressure gradient are the dominating factors and the Luikov's equation can be simplified as shown in Equation 25:

$$\frac{\partial M}{\partial t} = \nabla^2 k_{11} M + \nabla^2 k_{13} P \tag{25}$$

In the latter stages of MW-assisted drying process, the effect of moisture content can be neglected and the Luikov's equation can be shown as in Equation 26:

$$\frac{\partial M}{\partial t} = \nabla^2 k_{12} T + \nabla^2 k_{13} P \tag{26}$$

The effective diffusion coefficient can be estimated by using a simplified Fick's second low of diffusion as shown in Equation 27:

$$MR = \frac{8}{\pi^2}\sum_{n=0}^{\infty}\frac{1}{(2n+1)^2} exp\left[-(2n+1)^2 \frac{\pi^2 D_{eff} t_i}{L^2}\right] \tag{27}$$

Where L is the half thickness of the drying particle.

The Equation 27 can be further simplified as shown in the Equation 28 (Singh et al., 2013):

$$MR = \frac{8}{\pi^2} exp\left[-\frac{\pi^2 D_{eff} t_i}{L^2}\right] \tag{28}$$

Drying efficiency is defined as the ratio of the amount of water evaporated from the drying materials and the amount of MW energy entering the microwave chamber. To achieve the maximum drying efficiency, the power level must be correctly controlled during the microwave-assisted drying (Sunjka et al., 2004). A power control system with thermocouple probe or IR sensor can be used to turn on and off the line power for microwave oven to achieve maximum efficiency (Li et al., 2006).

2.5 Microwave-Assisted Fluidized-Bed Drying of Materials

Combining fluidized-bed drying and microwave-assisted drying compensates for the drawbacks of each method. Drying time can be significantly reduced from the use of microwave energy and the uniformity in temperature distribution can be achieved through the well mixing of materials obtained in the fluidized-bed (Chen et al., 2001).

The capillary flow of fluid in a porous medium taking place in the initial stages of microwave-assisted fluidized-bed drying process can be described by Darcy's law. At first, increasing the temperature of the drying materials to the boiling point of water can cause the pressure gradient to push liquid water from the interior to the surface of the drying particle. As the drying proceeds, internal liquid water transfer cannot exceed the surface evaporation rate and the surface moisture content decreases below the critical moisture content. Darcy's law will not be applicable at this stage, and the Fick's law can be used to describe the drying process when the vapor diffusion is the main mechanism of moisture transfer (Chen et al., 2001; Goksu et al., 2005).

The theoretical analyses of the microwave-assisted fluidized-bed drying process showed that the microwave power affects the magnitude and distribution of moisture content, temperature and pressure distribution in the drying material. Proper fluidization of the material is also important to achieve high drying rate and good product quality in microwave-assisted fluidized-bed drying. However, the high heat-transfer coefficient obtained in the fluidized-bed dryer is disadvantageous as it leads to decreasing microwave heating with drying time (Wang and Chen, 2000b). Studies using porous materials have shown that, intermittent heating during microwave-assisted fluidized-bed drying provides fast drying due to high absorption of microwaves by the drying material (Chen, et al. 2001). Investigation of the heat transfer mechanism in microwave-assisted fluidized bed drying shows higher sample surface temperature than the surrounding air temperature that cools the surface of the drying material (Souraki and Mowla, 2008b).

2.5.1 Applications of Microwave-Assisted Fluidized-Bed Drying

One of the first references to microwave-assisted fluidized-bed drying is a device for microwave-assisted fluidized-bed drying of granular materials patented in 1970 (Smith, 1970). A similar device with improved heating process for the drying of pharmaceutical materials was patented by Doelling in 1990 (Doelling, 1990; Doelling et al. 1992). Microwave-assisted fluidized-bed drying was investigated for the drying of carrots and showed that drying time reduced by 25-90% and the final quality of dried carrots were as good as freeze-dried carrots (Prabhanjan et al., 1995). Moreover, the microwave-assisted fluidized-bed drying was investigated for the drying of materials like apple slices (Feng, 2002), broad beans (Hashemi, et al. 2009), cylindrical carrot (Souraki, et al. 2009), diced carrot (Stanislawski, 2005), garlic (Souraki and Mowla, 2008a), green peas (Mowla, et al. 2012), macaroni beads (Goksu, et al. 2005), paddy (Sangdao, et al. 2010), pepper seeds (Kaensup, et al. 1998), potato slices (Reyes, et al. 2007), shelled corn (Momenzadeh, et al. 2011), short cut macaroni (Altan and Maskan, 2005), soybeans (Ranjbaran and Zare, 2013), turnip seeds (Reyes, et al. 2007), etc., and it was found to be significantly improving the drying rate in comparison to the conventional fluidized-bed drying (Kaensup, et al. 1998). Similarly, microwave assisted vibro-fluidized bed drying of cooked rice was investigated for the preparation of instant rice (Sripinyowanich and Noomhorm, 2011).

Apart from markedly reducing the drying time (usually by half) and energy used, there are environmental and economic advantages of MW-assisted fluidized-bed drying. It has been estimated that about one third of the global food produced is lost or wasted during the preparation for marketing and processing (Gustavsson et al., 2011). Microwave-assisted fluidized-bed drying technology has the potential to allow processors to add value to the vegetables that are usually rejected from packaging lines. It will reduce the amount of food residues to be disposed, generate new revenues for processors and also will create local jobs.

2.6 Quality Measurement of Dried Fruits and Vegetables

Thermal damages, such as change in flavor, color, and nutrients occurred during drying processes are proportional to the inlet air temperature and drying duration (Vadivambal and Jayas, 2007). Quality evaluation of the dried fruits and vegetables includes sensory evaluation (taste and appearance), water activity, color, texture and rehydration ratio (Perera, 2005). Changes in color and texture always occur during thermal treatments including drying (Lau et al., 2000; Nindo et al., 2003). Measurement of color, rehydration capability and firmness can directly express the antioxidant properties and reconstitution abilities of the dehydrated products (Nindo et al., 2003).

2.6.1 Color Measurement

The tri-stimulus color variables are related to the qualities and types of pigments of dried fruits and vegetables and it varies with the chemical composition of the dried products (Özkan et al., 2003). The CIE L^*, a^*, and b^* color variables are measured to define the color of the dried products. These three values are expressed as L^* (whiteness or brightness/darkness), a^* (redness/greenness), and b^* (yellowness/blueness). Color changes are related to browning reactions taking place during drying process. Both enzymatic and non-enzymatic browning reactions result in the browning of fruits and vegetables. The color change (ΔE) can be determined using Equation 29:

$$\Delta E = \sqrt{(L_f - L_d)^2 + (a_f - a_d)^2 + (b_f - b_d)^2} \quad (29)$$

Where, L_f, a_f and b_f are for the fresh materials, L_d, a_d and b_d are for the dried products.

The inlet air temperature and the oxygen level are the main factors to be properly controlled during the drying process to achieve desired color of the dried fruits and vegetables (O'Neill et al., 1998).

2.6.2 Rehydration Capability and Firmness

Rehydration aims at restoration of the properties of the dried products to that of the fresh materials through the contact with water. Rehydration capability has been considered as one of the measurements of injuries caused by the drying process (Lewicki, 1998). Final dried products with high rehydration capability are considered as in good quality. The rehydration capability can be calculated using the Equation 30 (Askari et al., 2006):

$$\%RC = \frac{W_r}{W_d} \times 100 \quad (30)$$

Where, RC is the rehydration capability, W_r is the total mass after rehydration (g), and W_d is the mass of the dried materials (g).

Firmness or texture strength correlates with porosity and bulk density of materials and is one of the most important properties that determines the quality of the dried fruits and vegetables (Rahimi et al., 2013). The dried products with slow rehydration capability will be firm in structure and causes undesirable chewiness for the consumers (Perera, 2005). However, during microwave-assisted fluidized-bed drying, the rehydration properties, which indicate the physical and chemical changes take place during drying process, are found to be improved due to the fast drying of the materials and the minimal shrinkage of the products (Krokida and Maroulis, 2000).

2.7 Conclusion

With the increasing utilization of drying technology in various fields, an optimal method for drying is required to achieve; shorter drying duration, higher efficiency, better final quality and flavor, and lower energy consumption and capital expenses. This article described the aerodynamic properties of the particles and drying kinetics of the fluidized-bed drying, microwave-assisted drying and microwave-assisted fluidized-bed drying methods. Improvements in the current drying technologies are required, while optimizing the microwave-assisted fluidized-bed drying, to add value to the vegetable residues and to make it ready for the markets.

Acknowledgements

The authors are grateful to the Natural Sciences and Engineering Research Council of Canada (NSERC) and ministère de l'Agriculture, des Pêcheries et de l'Alimentation du Québec (MAPAQ) for the financial support (Grant No. IA113076).

References

Akpinar, E.K., Bicer, Y., Yildiz, C. 2003. Thin layer drying of red pepper. *Journal of food engineering*, **59**(1), 99-104.

Altan, A., Maskan, M. 2005. Microwave assisted drying of short-cut (datalini) macaroni: Drying characteristics and effect of drying processes on starch properties. *Food research international*, **38**(7), 787-796.

Askari, G., Emam-Djomeh, Z., Mousavi, S. 2006. Effects of combined coating and microwave assisted hot-air drying on the texture, microstructure and rehydration characteristics of apple slices. *Food Science and Technology International*, **12**(1), 39-46.

Ayappa, K., Davis, H., Crapiste, G., Davis, E., Gordon, J. 1991. Microwave heating: an evaluation of power formulations. *Chemical engineering science*, **46**(4), 1005-1016.

Babalis, S.J., Belessiotis, V.G. 2004. Influence of the drying conditions on the drying constants and moisture diffusivity during the thin-layer drying of figs. *Journal of Food Engineering*, **65**(3), 449-458.

Baker, B.J., Krajewski, E.Z. 1966. Food package for microwave heating, Google Patents.

Batchelor, W., Kibblewhite, R., He, J. 2008. A new method for measuring RBA applied to the Page equation for the tensile strength of paper. *Appita Journal*, **61**(4), 302.

Beaudry, C., Raghavan, G., Ratti, C., Rennie, T. 2004. Effect of four drying methods on the quality of osmotically dehydrated cranberries. *Drying Technology*, **22**(3), 521-539.

Białobrzewski, I., Zielińska, M., Mujumdar, A.S., Markowski, M. 2008. Heat and mass transfer during drying of a bed of shrinking particles–Simulation for carrot cubes dried in a spout-fluidized-bed drier. *International Journal of Heat and Mass Transfer*, **51**(19), 4704-4716.

Bond, G., Moyes, R.B., Whan, D.A. 1993. Recent applications of microwave heating in catalysis. *Catalysis today*, **17**(3), 427-437.

Brenner, H. 2013. *Gas-liquid-solid fluidization engineering*. Butterworth-Heinemann.

Chaplin, G., Pugsley, T., Winters, C. 2004. Application of chaos analysis to pressure fluctuation data from a fluidized bed dryer containing pharmaceutical granule. *Powder Technology*, **142**(2), 110-120.

Chen, G., Wang, W., Mujumdar, A.S. 2001. Theoretical study of microwave heating patterns on batch fluidized bed drying of porous material. *Chemical Engineering Science*, **56**(24), 6823-6835.

Datta, A. 1990. Heat and mass transfer in the microwave processing of food. *Chemical Engineering Progress*, **86**(6), 47-53.

De la Fuente-Blanco, S., De Sarabia, E.R.-F., Acosta-Aparicio, V., Blanco-Blanco, A., Gallego-Juárez, J. 2006. Food drying process by power ultrasound. *Ultrasonics*, **44**, e523-e527.

Desai, R. 2015. Fick's law of diffusion.

Dincer, I. 2002. On energetic, exergetic and environmental aspects of drying systems. *International Journal of Energy Research*, **26**(8), 717-727.

Dincer, I., Hussain, M., Sahin, A., Yilbas, B. 2002. Development of a new moisture transfer (Bi–Re) correlation for food drying applications. *International Journal of Heat and Mass Transfer*, **45**(8), 1749-1755.

Dincer, I., Sahin, A. 2004. A new model for thermodynamic analysis of a drying process. *International Journal of Heat and Mass Transfer*, **47**(4), 645-652.

Doelling, M.K. 1990. Microwave assisted fluidized bed processor. US Patent US4967486. U.S. Patent and Trademark Office, Washington, DC.

Doelling, M. K., Jones, D. M., Smith, R. A., Nash, R.A. 1992. The Development of a Microwave Fluid-Bed Processor. I. Construction and Qualification of a Prototype Laboratory Unit. Pharmaceutical Research 9(11): 1487-1492.

Doelling, M. K., Nash, R.A. 1992. The Development of a Microwave Fluid-Bed Processor. II. Drying Performance and Physical Characteristics of Typical Pharmaceutical Granulations. Pharmaceutical Research 9(11): 1493-1501.

Drouzas, A., Schubert, H. 1996. Microwave application in vacuum drying of fruits. *Journal of Food Engineering*, **28**(2), 203-209.

Dufour, P. 2006. Control engineering in drying technology: review and trends. *Drying technology*, **24**(7), 889-904.

Dwivedi, P.N., Upadhyay, S. 1977. Particle-fluid mass transfer in fixed and fluidized beds. *Industrial and Engineering Chemistry Process Design and Development*, **16**(2), 157-165.

Ertekin, C., Yaldiz, O. 2004. Drying of eggplant and selection of a suitable thin layer drying model. *Journal of food engineering*, **63**(3), 349-359.

Feng, H. 2002. Analysis of microwave assisted fluidized-bed drying of particulate product with a simplified heat and mass transfer model. *International Communications in heat and mass transfer*, **29**(8), 1021-1028.

Galwey, A.K., Brown, M.E. 2002. Application of the Arrhenius equation to solid state kinetics: can this be justified? *Thermochimica Acta*, **386**(1), 91-98.

Gayot, S., Santarelli, X., Coulon, D. 2003. Modification of flavonoid using lipase in non-conventional media: effect of the water content. *Journal of biotechnology*, **101**(1), 29-36.

Geankoplis, C. 2003. *Transport processes and separation process principles (includes unit operations)*. Prentice Hall Press.

Geldart, D. 1973. Types of gas fluidization. *Powder technology*, **7**(5), 285-292.

Giri, S., Prasad, S. 2007. Drying kinetics and rehydration characteristics of microwave-vacuum and convective hot-air dried mushrooms. *Journal of food engineering*, **78**(2), 512-521.

Goksu, E.I., Sumnu, G., Esin, A. 2005. Effect of microwave on fluidized bed drying of macaroni beads. *Journal of Food Engineering*, **66**(4), 463-468.

Goodenough, T.I., Goodenough, P.W., Goodenough, S.M. 2007. The efficiency of corona wind drying and its application to the food industry. *Journal of food Engineering*, **80**(4), 1233-1238.

Gustavsson, J., Cederberg, C., Sonesson, U., Van Otterdijk, R., Meybeck, A. 2011. Global food losses and food waste. *Food and Agriculture Organization of the United Nations, Rom*.

Gutoff, E.B., Cohen, E.D., Mujumdar, A. 1995. Coating and drying defects. *Drying Technology*, **13**(8), 2251-2252.

Hashemi, G., Mowla, D., Kazemeini, M. 2009. Moisture diffusivity and shrinkage of broad beans during bulk drying in an inert medium fluidized bed dryer assisted by dielectric heating. *Journal of food engineering*, **92**(3), 331-338.

Hlinak, A.J., Saleki-Gerhardt, A. 2000. An evaluation of fluid bed drying of aqueous granulations. *Pharmaceutical development and technology*, **5**(1), 11-17.

Hovmand, S. 1995. Fluidized bed drying. *Handbook of Industrial Drying*, **1**, 195-248.

Idris, A., Khalid, K., Omar, W. 2004. Drying of silica sludge using microwave heating. *Applied thermal engineering*, **24**(5), 905-918.

Janney, M., D KIMREY, H., Allen, W., Kiggans, J. 1997. Enhanced diffusion in sapphire during microwave heating. *Journal of materials science*, **32**(5), 1347-1355.

Kaensup, W., Wongwises, S., Chutima, S. 1998. Drying of pepper seeds using a combined microwave/fluidized bed dryer. *Drying Technology*, **16(**3-5), 853-862.

Kingston, H.M., Jassie, L.B. 1988. *Introduction to microwave sample preparation: theory and practice*. American Chemical Society.

Kowalski, S. 2010. Control of mechanical processes in drying. Theory and experiment. *Chemical Engineering Science*, **65**(2), 890-899.

Krokida, M., Maroulis, Z. 2000. Quality changes during drying of food materials. *Drying technology in agriculture and food sciences*, 61-106.

Krokida, M.K., Karathanos, V., Maroulis, Z., Marinos-Kouris, D. 2003. Drying kinetics of some vegetables. *Journal of Food engineering*, **59**(4), 391-403.

Kunii, D., Levenspiel, O. 2013. *Fluidization engineering*. Elsevier.

Laidler, K.J. 1984. The development of the Arrhenius equation. *Journal of Chemical Education*, **61**(6), 494.

Lakshmi, B., Vimala, V. 2000. Nutritive value of dehydrated green leafy vegetable powders. *Journal of food science and technology*, **37**(5), 465-471.

Lau, M., Tang, J., Swanson, B. 2000. Kinetics of textural and color changes in green asparagus during thermal treatments. *Journal of Food Engineering*, **45**(4), 231-236.

Laufenberg, G., Kunz, B., Nystroem, M. 2003. Transformation of vegetable waste into value added products::(A) the upgrading concept;(B) practical implementations. *Bioresource Technology*, **87**(2), 167-198.

Leadbeater, N.E., Marco, M. 2003. Rapid and amenable Suzuki coupling reaction in water using microwave and conventional heating. *The Journal of organic chemistry*, **68**(3), 888-892.

Lewicki, P.P. 1998. Some remarks on rehydration of dried foods. *Journal of Food Engineering*, **36**(1), 81-87.

Li, Z., Wang, N., Raghavan, G., Cheng, W. 2006. A microcontroller-based, feedback power control system for microwave drying processes. *Applied engineering in agriculture*, **22**(2), 309-314.

Lopez, A., Iguaz, A., Esnoz, A., Virseda, P. 2000. Thin-layer drying behaviour of vegetable wastes from wholesale market. *Drying technology*, **18**(4-5), 995-1006.

Marques, L.G., Silveira, A.M., Freire, J.T. 2006. Freeze-drying characteristics of tropical fruits. *Drying technology*, **24**(4), 457-463.

May, B., Perré, P. 2002. The importance of considering exchange surface area reduction to exhibit a constant drying flux period in foodstuffs. *Journal of Food Engineering*, **54**(4), 271-282.

Menéndez, J., Arenillas, A., Fidalgo, B., Fernández, Y., Zubizarreta, L., Calvo, E., Bermúdez, J. 2010. Microwave heating processes involving carbon materials. *Fuel Processing Technology*, **91**(1), 1-8.

Meredith, R.J. 1998. *Engineers' handbook of industrial microwave heating*. IET.

Metaxas, A.a., Meredith, R.J. 1983. *Industrial microwave heating*. IET.

Midilli, A., Kucuk, H. 2003. Mathematical modeling of thin layer drying of pistachio by using solar energy. *Energy conversion and Management*, **44**(7), 1111-1122.

Midilli, A., Kucuk, H., Yapar, Z. 2002. A new model for single-layer drying. *Drying technology*, **20**(7), 1503-1513.

Mohapatra, D., Rao, P.S. 2005. A thin layer drying model of parboiled wheat. *Journal of food engineering*, **66**(4), 513-518.

Momenzadeh, L., Zomorodian, A., Mowla, D. 2011. Experimental and theoretical investigation of shelled corn drying in a microwave-assisted fluidized bed dryer using Artificial Neural Network. *Food and bioproducts processing*, **89**(1), 15-21.

Mowla, D., Zomorodian, A., Momenzadeh, L. 2012. Applying Artificial Neural Network for Drying Time Prediction of Green Pea in a Microwave Assisted Fluidized Bed Dryer. *Journal of agricultural science and technology*, **14**(3), 513-522.

Mujumdar, A.S. 2014. *Handbook of industrial drying*. CRC Press.

Nelson, S., Forbus, W., Lawrence, K. 1994. Microwave permittivities of fresh fruits and vegetables from 0.2 to 20 GHz. *Transactions of the ASAE*, **37**(1), 183-189.

Nijhuis, H., Torringa, H., Muresan, S., Yuksel, D., Leguijt, C., Kloek, W. 1998. Approaches to improving the quality of dried fruit and vegetables. *Trends in Food Science and Technology*, **9**(1), 13-20.

Nindo, C.I., Sun, T., Wang, S.W., Tang, J., Powers, J.R. 2003. Evaluation of drying technologies for retention of physical quality and antioxidants in asparagus (Asparagus officinalis, L.). *LWT - Food Science and Technology*, **36**(5), 507-516.

Nitz, M., Taranto, O.P. 2007. Drying of beans in a pulsed fluid bed dryer: Drying kinetics, fluid-dynamic study and comparisons with conventional fluidization. *Journal of food engineering*, **80**(1), 249-256.

O'Neill, M.B., Rahman, M.S., Perera, C.O., Smith, B., Melton, L.D. 1998. Color and density of apple cubes dried in air and modified atmosphere. *International Journal of Food Properties*, **1**(3), 197-205.

Oliveira, M., Franca, A. 2002. Microwave heating of foodstuffs. *Journal of Food Engineering*, **53**(4), 347-359.

Overhults, D., White, G., Hamilton, H., Ross, I. 1973. Drying soybeans with heated air. *Amer Soc Agr Eng Trans ASAE*.

Ozkan, I.A., Akbudak, B., Akbudak, N. 2007. Microwave drying characteristics of spinach. *Journal of Food Engineering*, **78**(2), 577-583.

Özkan, M., Kirca, A., Cemeroğlu, B. 2003. Effect of moisture content on CIE color values in dried apricots. *European Food Research and Technology*, **216**(3), 217-219.

Perera, C.O. 2005. Selected quality attributes of dried foods. *Drying Technology*, **23**(4), 717-730.

Prabhanjan, D., Ramaswamy, H., Raghavan, G. 1995. Microwave-assisted convective air drying of thin layer carrots. *Journal of Food engineering*, **25**(2), 283-293.

Qin, M., Belarbi, R., Aït-Mokhtar, A., Seigneurin, A. 2006. An analytical method to calculate the coupled heat and moisture transfer in building materials. *International Communications in Heat and Mass Transfer*, **33**(1), 39-48.

Raghavan, G., Orsat, V. 2007. Recent advances in drying of biomaterials for superior quality bioproducts. *Asia-Pacific Journal of Chemical Engineering*, **2**(1), 20-29.

Rahimi, J., Singh, A., Adewale, P.O., Adedeji, A.A., Ngadi, M.O., Raghavan, V. 2013. Effect of Carboxylmethyl Cellulose Coating and Osmotic Dehydration on Freeze Drying Kinetics of Apple Slices. *Foods*, **2**(2), 170-182.

Ranjbaran, M., Zare, D. Simulation of energetic- and exergetic performance of microwave-assisted fluidized bed drying of soybeans. *Energy*, **59**, 484-493.

Reyes, A., Campos, C., Vega, R. 2007. Drying of Turnip Seeds with Microwaves in Fixed and Pulsed Fluidized Beds. *Drying technology: an international journal*, **24**(11), 1469-1480.

Reyes, A., Ceron, S., Zuniga, R., Moyano, P. 2007. A comparative study of microwave-assisted air drying of potato slices. *Biosystems engineering*, **98**(3), 310-318.

Rockstrom, E.I. 2000. Process for preparing dehydrated vegetable products, Google Patents.

Sangdao, C., Songsermpong, S., Krairish, M. 2010. A Continuous Fluidized Bed Microwave Paddy Drying System Using Applicators with Perpendicular Slots on a Concentric Cylindrical Cavity. *Drying technology: an international journal*, **29**(1), 35-46.

Scherer, G.W. 1990. Theory of drying. *Journal of the American Ceramic Society*, **73**(1), 3-14.

Schiffmann, R.F. 2001. Microwave processes for the food industry. *Food science and technology* New York Marcel Dekker-, 299-338.

Schwaab, M., Pinto, J.C. 2007. Optimum reference temperature for reparameterization of the Arrhenius equation. Part 1: Problems involving one kinetic constant. *Chemical Engineering Science*, **62**(10), 2750-2764.

Senadeera, W., Bhandari, B.R., Young, G., Wijesinghe, B. 2003. Influence of shapes of selected vegetable materials on drying kinetics during fluidized bed drying. *Journal of Food Engineering*, **58**(3), 277-283.

Senadeera, W., Bhandari, B.R., Young, G., Wijesinghe, B. 2000. Methods for effective fluidization of particulate food materials. *Drying technology*, **18**(7), 1537-1557.

Singh, A., Nair, G.R., Rahimi, J., Gariepy, Y., Raghavan, V. 2013. Effect of static high electric field pre-treatment on microwave-assisted drying of potato slices. *Drying Technology*, **31**(16), 1960-1968.

Smith, F.J. 1970. Microwave fluidized bed dryer. US Patent US3528179. U.S. Patent and Trademark Office, Washington, DC.

Soponronnarit, S., Prachayawarakorn, S. 1994. Optimum strategy for fluidized bed paddy drying. *Drying Technology*, **12**(7), 1667-1686.

Souraki, B.A., Mowla, D. 2008a. Experimental and theoretical investigation of drying behaviour of garlic in an inert medium fluidized bed assisted by microwave. *Journal of food engineering*, **88**(4), 438-449.

Souraki, B.A., Mowla, D. 2008b. Simulation of drying behaviour of a small spherical foodstuff in a microwave assisted fluidized bed of inert particles. *Food research international*, **41**(3), 255-265.

Sripinyowanich, J., Noomhorn, A. 2011. A New Model and Quality of Unfrozen and Frozen Cooked Rice Dried in a Microwave Vibro-Fluidized Bed Dryer. *Drying technology:an international journal*, **29**(7), 735-748.

Stanislawski, J. 2005. Drying of diced carrot in a combined microwave-fluidized bed dryer. *Drying technology: An international journal*, 23(8), 1711-1721.

Sumnu, G., Turabi, E., Oztop, M. 2005. Drying of carrots in microwave and halogen lamp–microwave combination ovens. *LWT-Food Science and Technology*, **38**(5), 549-553.

Sunjka, P., Rennie, T., Beaudry, C., Raghavan, G. 2004. Microwave-convective and microwave-vacuum drying of cranberries: A comparative study. *Drying Technology*, **22**(5), 1217-1231.

Thompson, T., Peart, R., Foster, G. 1968. Matllematical Simulation of Corn Drying A New Model. *Transaction of the ASAE*, **11**(4), 582-586.

Toğrul, İ.T., Pehlivan, D. 2002. Mathematical modelling of solar drying of apricots in thin layers. *Journal of Food Engineering*, **55**(3), 209-216.

Toğrul, İ.T., Pehlivan, D. 2003. Modelling of drying kinetics of single apricot. *Journal of Food Engineering*, **58**(1), 23-32.

Vadivambal, R., Jayas, D. 2007. Changes in quality of microwave-treated agricultural products—a review. *Biosystems engineering*, **98**(1), 1-16.

Van Arsdel, W.B., Copley, M.J., Morgan Jr, A. 1973. *Food dehydration. Vol. 1. Drying methods and phenomena*.

Venkatachalapathy, K., Raghavan, G. 1999. Combined osmotic and microwave drying of strawberries. *Drying Technology*, **17**(4-5), 837-853.

Venkatesh, M., Raghavan, G. 2004. An overview of microwave processing and dielectric properties of agri-food materials. *Biosystems Engineering*, **88**(1), 1-18.

Villagran, M.D.M.-S., Achanta, S., Boyle, E.M., Li, J., Patton, D.R. 2003. Method for preparing dehydrated food products, Google Patents.

Wang, J., Xi, Y. 2005. Drying characteristics and drying quality of carrot using a two-stage microwave process. *Journal of food Engineering*, **68**(4), 505-511.

Wang, Z.H., Chen, G. 2000. Heat and mass transfer in batch fluidized-bed drying of porous particles. *Chemical Engineering Science*, **55**(10), 1857-1869.

Wang, Z.H., Chen, G. 2000b. Theoretical study of fluidized-bed drying with microwave heating. *Industrial and Engineering Chemistry Research*, **39**(3), 775-782.

Xanthopoulos, G., Oikonomou, N., Lambrinos, G. 2007. Applicability of a single-layer drying model to predict the drying rate of whole figs. *Journal of Food Engineering*, **81**(3), 553-559.

Yaldiz, O., Ertekin, C., Uzun, H.I. 2001. Mathematical modeling of thin layer solar drying of sultana grapes. *Energy*, **26**(5), 457-465.

Yongsawatdigul, J., Gunasekaran, S. 1996. Microwave-vacuum drying of cranberries: Part I. Energy use and efficiency. *Journal of Food Processing and Preservation*, **20**(2), 121-143.

CONNECTING TEXT

In the following chapter, an experimental study of fluidized-bed drying of carrot slices at controlled temperatures was conducted. The quality of final dried carrot slices was compared. The drying performance of pre-treated carrot slices at the inlet air temperature of 60 ºC was analyzed.

CHAPTER 3

FLUIDIZED-BED DRYING OF CARROT SLICES AT CONTROLLED TEMPERATURES**

Xue Hu*, Jiby Kurian, Yvan Gariépy, Vijaya Raghavan

Department of Bioresource Engineering, McGill University, 21111 Lakeshore Rd., Ste-Anne-de-Bellevue, QC, H9X 3V9, Canada

* Correspondence author:
Xue Hu, Department of Bioresource Engineering, McGill University, QC, H9X 3V9, Canada.
Phone: (438)-881-0425, Email: xue.hu@mail.mcgill.ca

**Submitted to Food Science and Technology (LWT).

Abstract

Different drying technologies have different impacts on the physical and biochemical properties of the dried vegetables and fruits. In this study, the fluidized-bed drying of carrot slices without any pre-treatment at controlled temperatures (40°C, 50°C and 60°C) and with pre-treatment methods (water blanching, sugar solution and citric acid) at 60°C were conducted. Increase in inlet air temperature and the application of pre-treatments decreased the drying duration. The application of pre-treatments retained the natural color of carrot in the dried carrot slices. Texture strength of the dried carrot slices increased with drying temperature and the dried carrot slices with pre-treatment were harder than the dried carrot slices without any pre-treatments.

Key words: Fluidized-bed drying, carrot slices, drying kinetics, pre-treatments.

3.1 Introduction

Fluidized-bed dryers are commonly used in various food industries. Rapid transfer of surface heat and mass could be realized during the fluidized-bed drying due to fast mixing between food particles and inlet hot air (Doymaz, 2004). Compared with other drying techniques, fluidized-bed drying has been considered to be one of the most economical drying methods with faster and more uniform drying, higher thermal efficiency, lower final moisture content and better dried product quality (Hovmad, 1995). In addition, fluidized-bed drying technology is applicable to heat sensitive foods such as broccoli and garlic due to the fluidization during drying process which prevents food particles from overheating (Mulet et al., 1993).

Essential nutrients such as minerals and vitamins and fibre are mainly obtained from vegetables and fruits. Vegetables and fruits are defined as highly perishable commodities due to high moisture content which is over 80 % (Orsat et al., 2007). Carrot is one of the most widely consumed perishable commodities and is high in vitamins and fibre content (Doymaz, 2004). Since the high moisture content of carrots leads to deformation and decay, dehydrated carrots can be produced using various drying methods to store carrots for a long time (Ketelaars, 1994).

The acceptance of dehydrated vegetables and fruits in market is raising and the demand for a large quantity of dried foods with longer shelf-life and better final quality has been increased (Krokida et al., 1998). Different drying methods have been investigated for the production of dried carrots. Sun drying of carrots was investigated by Mulet et al. (1993) and freeze drying of carrots was conducted by Krokida et al. (1998). Combination of microwave heating and freeze drying of carrots was investigated by Lin et al. (1998) and Cui et al. (2008). Hot air drying method was investigated for the drying of carrots (Amami et al., 2008). Generally, convective drying method is more efficient than conductive and radiation drying methods to remove water from the material with high moisture content. Therefore, drying of vegetables and fruits is mostly conducted by convective drying methods such as fluidized-bed drying (Lin et al., 1998).

The effect of different drying conditions such as the inlet air temperature and air velocity on the quality of dried carrots during fluidized-bed drying was investigated by Sereno et al. (2001). Earlier, Lewicki (1998) has concluded that the energy utilization of fluidized-bed drying decreased with decrease in inlet air temperature and bed depth. Recently, Singh et al. (2013) have developed a thermodynamic model of the fluidized-bed dryer to predict and improve the drying efficiency. The objective of this study are:

1) To design and optimize a new fluidized-bed dryer with lower energy consumption and drying duration for better quality and longer shelf-life of the dried products,

2) To compare the drying results under different drying temperatures,

3) To study the effect of different pre-treatment methods for carrot slices on the drying efficiency and quality of dried carrot slices, and

4) To measure the color and texture strength of the dried carrot slices.

3.2 Materials and Methods

3.2.1 Materials

The carrots used for fluidized-bed drying were obtained from a local supermarket in Montreal, Quebec, Canada. The initial moisture content of the carrot was 89.4 % on wet basis. Moisture content (M.C.) was determined by keeping 20 g carrots slices at 105 °C in a hot air chamber (Model 6528, Thermo Electron Corporation, USA) for 24 hours. The moisture content was calculated based on Equation (1):

$$M.C.(w.b.) = \frac{M_w}{M_w + M_s} \quad (1)$$

Where M_w is the mass of water in the sample (g); M_s is the mass of solid in the sample (g).

The carrots were cut into quadrant slices (radius: 9.85–10.15 mm, thickness: 2.35–2.65 mm) with a food processor (DLC-2009CHB 9-Cup Prep Plus Food Processor, Cuisinart, USA).

3.2.2 Equipment and Apparatus

The fluidized-bed dryer system was set up in the Machine Shop, Macdonald Campus, McGill University (Fig. 3.1). The cylindrical drying chamber with the diameter of 10 cm and the height of 35 cm was made of Polycarbonate plastic and was equipped with a metal screen to hold the carrot slices. A blower (Lesson Electric, Wisconsin, USA) was used to maintain the air velocity in the range of 6.8 m/s to 15.5 m/s. The heaters (Ceramic heater, Cranbury, USA) were controlled by a PID controller to adjust the inlet air temperature between 20 °C and 90 °C. Thermocouples (Type K) and humidity sensors (Mamac Systems, Minneapolis, USA) were installed at the top and the bottom of the drying chamber to monitor the inlet and outlet air temperature and humidity. A data acquisition system (Agilent, 34970A) was used to track the drying performance.

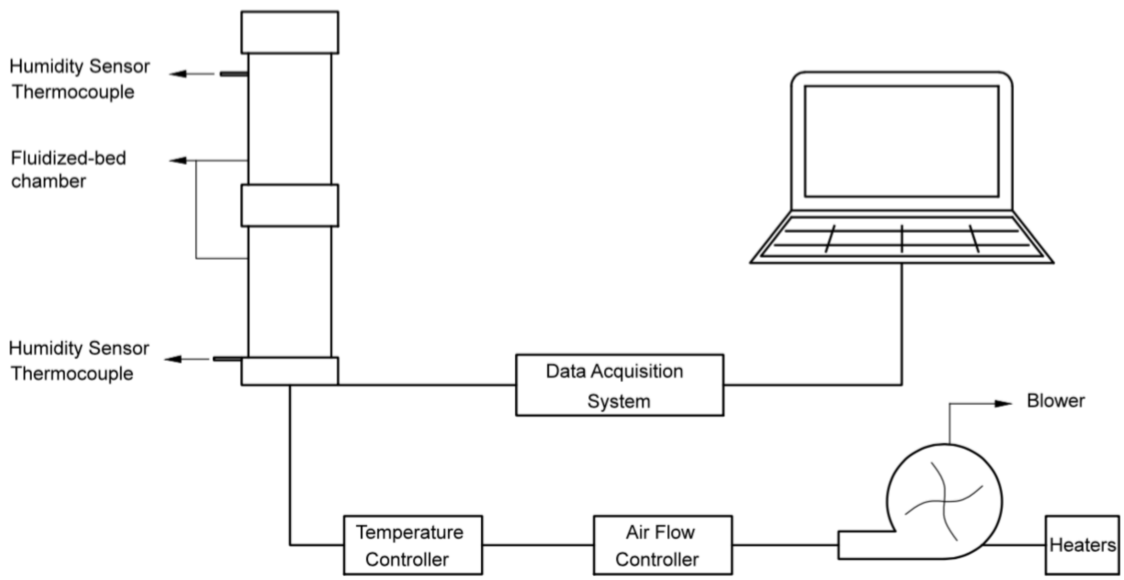

Figure 3. 1: Schematic of Fluidized-bed dryer apparatus.

3.2.3 Experimental Design

The carrot slices (400 g) were dried in the fluidized-bed chamber under the inlet air temperature of 40°C, 50 °C and 60 °C respectively. In a separate experiment, the pre-treatment of carrot slices with methods like (1) water blanching (WB), (2) 20% (w/w) sugar solution (SS), and (3) 1% (w/w) citric acid solution (CAS) was investigated. The pre-treatment of carrot slices was investigated with fluidized-bed drying at 60°C. The air velocity applied was at 6.7 ± 0.5 m/s.

3.2.4 Fluidized-Bed Drying of Carrot Slices

The drying process was stopped when the moisture content of the carrot slices reached 15% on wet basis. The relevant characteristics of fluidized-bed drying (mass of carrots slices, air velocity) were recorded and analyzed. The color and textural strength of dried carrot slices were measured. Each experiment was conducted in triplicate.

3.2.5 Pre-treatment of Carrot Slices

In order to improve the quality of final product and to increase the drying efficiency, different pre-treatment methods were applied on carrots slices (Sereno et al., 2001).

(1) Water blanching (WB): The carrot slices (400 g) were blanched in boiling water at 100℃ for 5 min and then chilled in ice water for 10 seconds. Paper towel was used to remove water until no droplet left on the surface of the blanched carrot slices.

(2) Osmotic dehydration in 20% (w/w) sugar solution (SS): The sugar solution was prepared by dissolving 250 g sugar (granulated sugar, Lantic Inc.) in 1 kg distilled water at ambient temperature of 22 °C. The carrot slices (400 g) were immersed in sugar solution for 10 min at the room temperature of 22 °C. Paper towel was used to remove the excess sugar solution from the surface of the carrot slices.

(3) Osmotic dehydration in 1% (w/w) citric acid solution (CAS): The citric acid solution was prepared in the same way by solving 10 g citric acid powder (Sigma

Aldrich, Canada) in 1kg distilled water at ambient temperature of 22 °C. The carrot slices (400 g) were immersed in citric acid solution for 10 min at the room temperature of 22 °C. Paper towel was used to remove the excess citric acid solution from the surface of the carrot slices.

3.2.6 Rehydration of Dried Carrot Slices

Rehydration capability has been defined as one of the criterion of injuries in the dried products caused by the drying process. The higher the rehydration capability, the better the final dried product's quality (Lewicki, 1998). Dried carrot slices samples (5 g per treatment) were submerged in boiling water for 10 min. The rehydration capability was calculated using Equation (2):

$$\%RC = \frac{W_r}{W_d} \times 100 \tag{2}$$

Where RC is the rehydration capability, W_r is the total mass after rehydration (g), and W_d is the mass of the dried materials (g).

3.2.7 Mathematical Models

Various mathematic models, namely Page, Newton, Wang and Singh, Modified Page, Henderson & Pabis, Logarithmic (Table 3.1), were used to describe the kinetics of fluidized-bed drying process.

The moisture ratio (*MR*) is defined as Equation (3):

$$MR = \frac{M_t - M_e}{M_o - M_e} \tag{3}$$

Where, M_t, M_o and M_e are the moisture content at time *t*, initial moisture content and equilibrium moisture content, respectively. Since the equilibrium moisture content M_e is negligible both in microwave and convective drying (Singh et al., 2013), the Equation (3) reduces to Equation (4):

$$MR = \frac{M_t}{M_o} \tag{4}$$

Table 3. 1: Mathematic models of the kinetics of fluidized bed drying.

Model name	Model equation	Reference	Equation No.
Newton	$MR = e^{-kt}$	(Midilli and Kucuk, 2003)	5
Page	$MR = e^{-kt^n}$	(Batchelor et al., 2008)	6
Modified Page	$MR = e^{(-kt)^n}$	(Overhults et al., 1973)	7
Henderson & Pabis	$MR = a\, e^{-kt}$	(Yaldiz et al., 2001)	8
Logarithmic	$MR = a\, e^{-kt^n} + c$	(Xanthopoulos et al., 2007)	9
Wang and Singh	$MR = 1 + at + bt^2$	(Mohapatra and Rao, 2005)	10

The *k* in the models in Table 3.1 is the drying rate constant (min^{-1}), a, b, c and n are the drying coefficients (unit-less) that have different values depending on the equation and drying curve and *t* is the time (min).

3.2.8 Correlation Coefficients and Error Analysis

The quality of fit of drying models to the observed values was determined by the reduced chi-square (χ^2), root mean square error (RMSE), correlation coefficient (R^2) and reduced sum square error (SSE) (Ertekin and Yaldiz, 2004). The reduced chi-square (χ^2) and root mean square error (RMSE) can be calculated using Equation (11) and Equation (12) respectively.

$$\chi^2 = \frac{\sum_{i=1}^{N}\left(MR_{exp,i} - MR_{pre,i}\right)^2}{N - n} \tag{11}$$

$$RMSE = \left[\frac{1}{N}\sum_{i=1}^{N}\left(MR_{pre,i} - MR_{exp,i}\right)^2\right]^{1/2} \tag{12}$$

Where $MR_{exp,i}$ is the experimental moisture ratio at time *t*; $MR_{pre,i}$ is the predicted moisture ratio at time *t*; *N* and *n* are the observations number and the constants number respectively.

The R^2 can be calculated using the Equation (13).

$$R^2 = 1 - \frac{\sum_{i=1}^{N}\left(MR_{pre,i} - MR_{exp,i}\right)^2}{\sum_{i=1}^{N}\left(MR_{exp,i} - \overline{MR}_{exp}\right)^2} \tag{13}$$

Where $\overline{MR}_{exp}$ is the mean experimentally measured value of MR. The reduced sum square error (SSE) could also be used as criteria of goodness of fit by using the Equation (14).

$$SSE = \frac{1}{N}\sum_{i=1}^{N}\left(MR_{pre,i} - MR_{exp,i}\right)^2 \tag{14}$$

3.2.9 Color Measurement

The color changes of dried carrots after the fluidized-bed drying process were measured by using a Chroma-meter with d/0 diffuse illumination/0° viewing system (Model CR-300X, Minolta Co. Ltd., Japan). The CIE 1976 (L^*, a^*, b^*) color space was used to determine the color values of all the samples, expressed as L^* (whiteness or brightness/darkness), a^* (redness/greenness) and b^* (yellowness/blueness) (Billmeyer, 1981).

The carrot slices were placed on a table, and the color values were measured by perpendicularly illuminating the samples with the measuring head of the instrument from all directions. Three measurements of each sample were taken. The color values differences (ΔL^*, Δa^* and Δb^*) were calculated with respect to the color values of fresh carrots. The total color difference (ΔE) is defined as Equation (15):

$$\Delta E = \sqrt{(L_f - L_d)^2 + (a_f - a_d)^2 + (b_f - b_d)^2} \tag{15}$$

Where, L_f, a_f and b_f are for the fresh materials, L_d, a_d and b_d are for the dried products.

3.2.10 Textural Strength Analysis

The textural strength of carrot slices was measured using the Universal Testing Machine (Instron–4502, Instron Corporation, USA) equipped with a cylindrical probe (diameter: 1.5 mm) (Fig. 3.2). The whole process was controlled and the data was collected by the computer software (Instron series IX, version 8.25). A piece of carrot slice was placed on the platform with a 2 mm hole in the center. And the hole on the platform was aligned with the center of carrot slice, and the crosshead was set speed at 10 mm/min. The load and the energy to break the point were recorded.

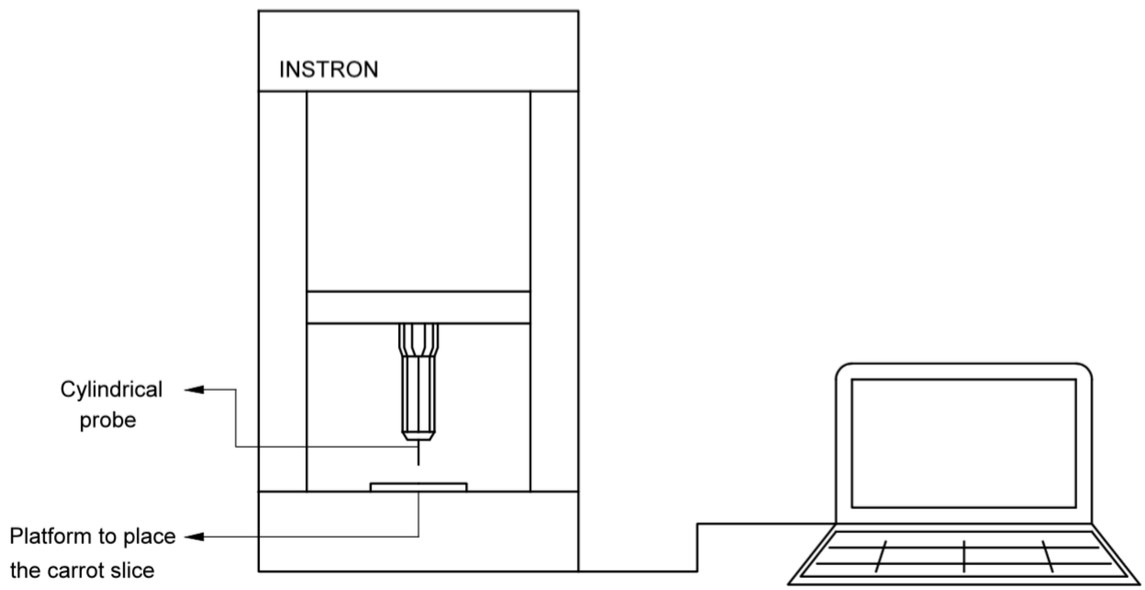

Figure 3. 2: Universal Testing machine equipped with a probe for the textural analysis.

3.2.11 Statistical Analysis

The statistical analysis of variance (ANOVA) of each experiment was performed using the Statistical Analysis Software (SAS 9.2 SAS Institute Inc., Cary, NC, USA) with a confidence level ($p \leq 0.05$) of 95%. The mathematical models of drying kinetics were fitted and analyses were done by using MATLAB R2015a (Mathworks Inc., USA).

3.3 Results and Discussion

3.3.1 Analysis of Drying Kinetics

The results of fluidized-bed drying of carrot slices at different temperatures (40 °C, 50 °C and 60 °C) are shown to assess where the drying was faster with the increase in the inlet air temperature (Fig. 3.3). It took about 80 min to reach the required final moisture content of 15% (w.b.) from the initial moisture content of 89.4% (w.b.) at 60 °C inlet- air temperature. This was 18.8% and 75% less time than the time taken to dry the carrot slices at 50 °C and 40 °C respectively. The carrot slices dried at 60 °C with pre-treatment reached the required final moisture content in 50 min, with a reduction of 60% in drying time compared to drying of carrot slices without any pre-treatment (Fig. 3.4). In 50 min, the water blanched carrot slices reached the final moisture content of 10.19% (w.b.), sugar solution treated carrot slices reached 14.41% (w.b.) moisture content and citric acid solution treated carrot slices reached a moisture content of 12.88% (w.b.).

Thus fluidized-bed drying of carrot slices at 60 °C showed a significant reduction of drying time among all the temperature condition investigated. The fluidized-bed drying of water blanched carrot slices at 60 °C had the maximum drying efficiency due to the partial cell wall destruction during boiling water blanching. Soponronnarit and Prachayawarakorn (1994) and Kim and Toledo (1987) have reported similar observations.

(a)

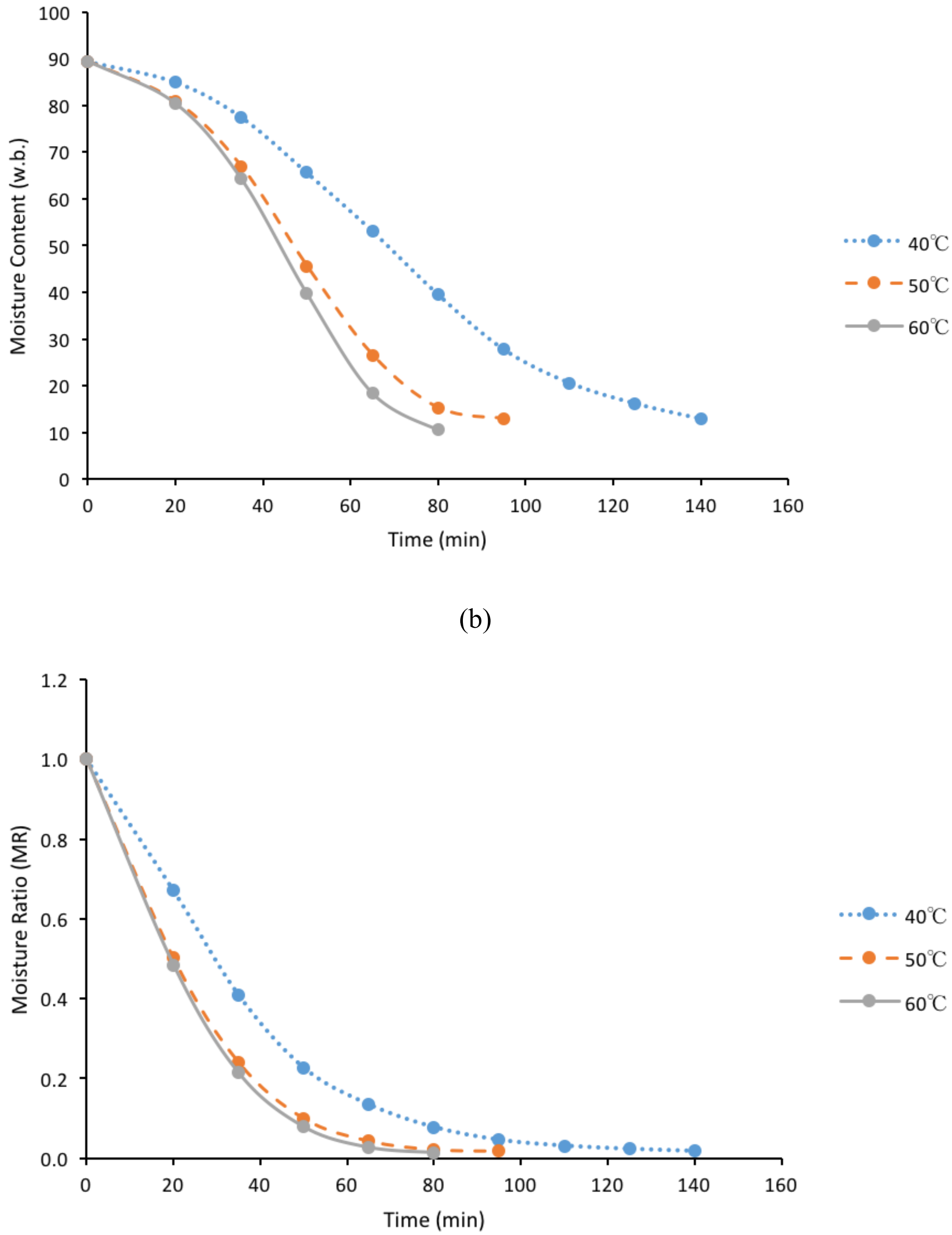

Figure 3. 3: (a) The moisture content (%) and (b) moisture ratio over time in fluidized-bed drying of carrot slices at 40 °C, 50 °C and 60 °C.

(a)

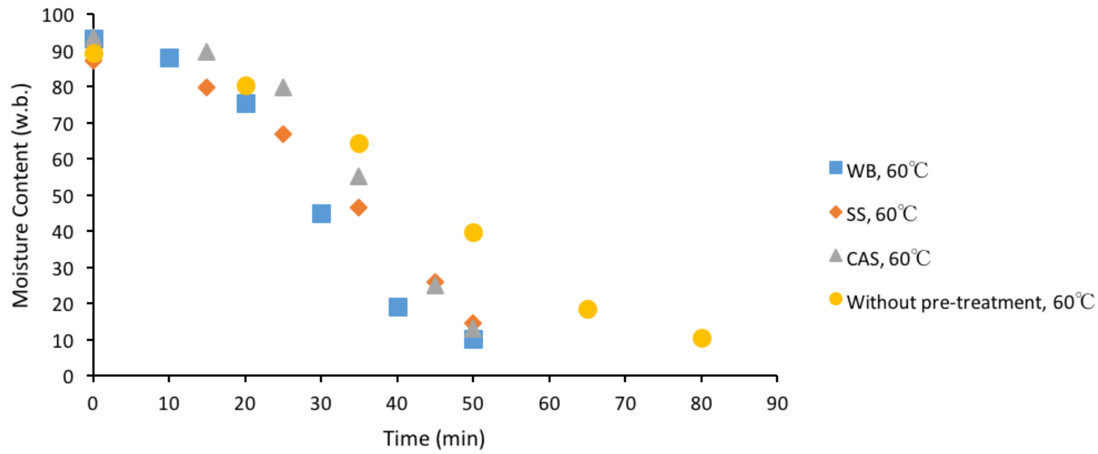

(b)

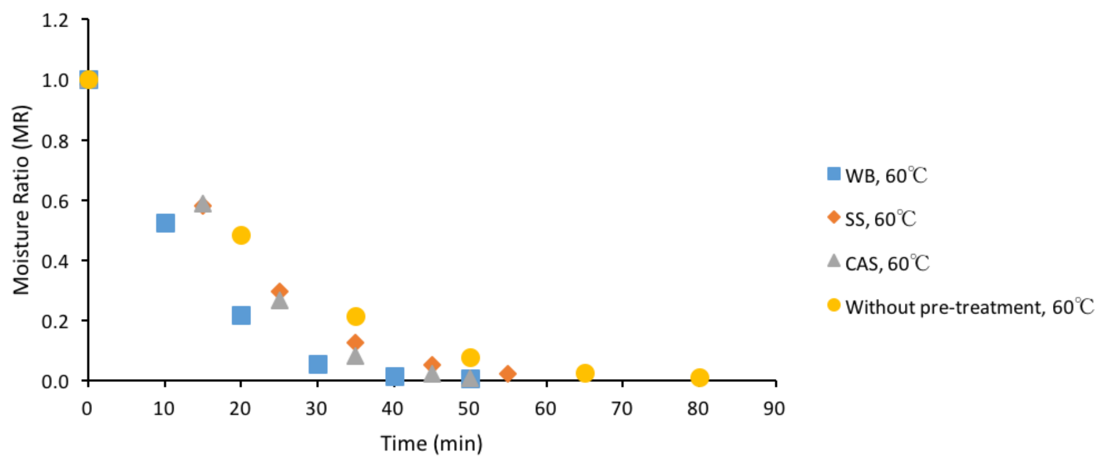

Figure 3. 4: (a) The variation of moisture content and (b) moisture ratio in carrot slices, with and without the pre-treatment, in fluidized-bed drying at 60 °C.

3.3.2 Mathematical Models

The mathematical models from Table 3.1 (Eq. 5-10) were fitted to the observed responses of carrot slices drying and the statistical significance was calculated for reflecting the fitness of the models (Table 3.2). The best fitting models for describing the drying kinetics were selected according to the highest R^2, the lowest RMSE, SSE, and χ^2 (Senadeera et al., 2003). From Table 3.2 we could observe that the values of correlation coefficient (R^2) exceed 0.95 for all drying conditions and mathematical models. The drying constant k increased with the temperature when the carrot slices were dried without any pre-treatment. While comparing the models of the fluidized-bed drying of the carrot slices with different pre-treatment methods, the drying constant, k, of the drying process with the pre-treatment using citric acid solution (CAS) was smaller than the k value of others.

The Logarithmic model fitted the best for fluidized-bed drying without pre-treatment at all temperatures investigated (Fig. 3.5). The R^2 values were 0.9998, 0.9999 and 0.9999; the χ^2 values were 0.00003, 0.00001 and 0.00001; the RMSE values were 0.005278, 0.003529 and 0.003572; the SSE values were 0.0001672, 0.000037 and 0.0000255 for 40 °C, 50 °C and 60 °C respectively. The Logarithmic model is also considered to be the most appropriate model to estimate the drying kinetics for drying with water blanching (WB) and sugar solution pre-treatments. For drying with citric acid solution (CAS) pre-treatment, the Page model was found as the best fitting drying model (Fig. 3.6). From Fig. 3.5 and Fig. 3.6 we could determine that the Wang & Singh model only fitted well with the fluidized-bed drying of carrot slices pretreated with sugar solution (SS). There were negative values of moisture ratio (MR) in Wang and Singh model for other drying conditions. For all thin layer drying of vegetables and fruits, these models are thus applicable to describe the drying kinetics.

Table 3. 2: Estimated statistical values of drying constants, chi- square (χ^2), root mean square error (RMSE), correlation coefficient (R^2) and reduced sum square error (SSE) in Fluidized-bed drying of carrot slices.

Methods	Temp ℃	Statistics /Coefficient	Models											
			Newton	Page		Modified Page		Henderson & Pabis		Logarithmic			Wang &Singh	
			k	k	n	k	n	k	a	k	a	c	a	b
Drying without Pre-treatment	40℃	Coeffi.	0.02735	0.007899	1.326	0.01431	1.911	0.02815	1.036	0.006048	0.98	0.02115	1.413	-0.01866
		χ^2	0.00152	0.00015		0.00171		0.00152		0.00003			0.00157	
		RMSE	0.03892	0.01213		0.04128		0.03886		0.005278			0.03947	
		SSE	0.01363	0.001177		0.01363		0.01208		0.0001672			0.01247	
		R^2	0.9864	0.9988		0.9864		0.9879		0.9998			0.9876	
	50℃	Coeffi.	0.04021	0.01227	1.292	0.1483	0.201	0.04064	1.015	0.01235	0.99	0.01168	1.347	-0.02699
		χ^2	0.00091	0.00180		0.01453		0.00105		0.00001			0.00122	
		RMSE	0.03032	0.006506		0.03321		0.03252		0.003529			0.03487	
		SSE	0.005514	0.0002117		0.005514		0.005288		0.000037			0.006078	
		R^2	0.9931	0.9997		0.9917		0.9933		0.9999			0.9923	
	60℃	Coeffi.	0.04273	0.01444	1.361	0.2005	0.309	0.04319	1.015	0.01262	0.99	0.00424	1.38	-0.02957
		χ^2	0.00136	0.00177		0.01229		0.00164		0.00001			0.00040	
		RMSE	0.037	0.003182		0.04137		0.04067		0.003572			0.01998	
		SSE	0.006845	0.0000405		0.006845		0.006615		0.0000255			0.001597	
		R^2	0.9907	0.9999		0.9907		0.991		0.9999			0.9978	
WB	60℃	Coeffi.	0.07497	0.03084	1.313	0.3633	0.206	0.07593	1.016	0.03164	1.00	-0.0036	1.3	-0.05061
		χ^2	0.00132	0.00007		0.00165		0.00158		0.00013			0.00093	
		RMSE	0.03626	0.008023		0.04054		0.03964		0.01104			0.03054	
		SSE	0.006574	0.0002575		0.006574		0.006286		0.0002438			0.003731	
		R^2	0.9915	0.9996		0.9915		0.9919		0.9997			0.9952	
20% (w/w) SS	60℃	Coeffi.	0.05814	0.006	1.723	0.5753	0.101	0.05913	1.025	0.007235	0.99	0.01222	1.6	-0.04064
		χ^2	0.00626	0.00383		0.00784		0.00762		0.000002			0.00381	
		RMSE	0.06576	0.004646		0.07352		0.07235		0.001232			0.02821	
		SSE	0.02162	0.000086		0.02162		0.02094		0.0000304			0.003184	
		R^2	0.972	0.9999		0.972		0.9729		0.9999			0.9948	
1% (w/w) CAS	60℃	Coeffi.	0.05273	0.003902	1.811	0.4018	0.131	0.05402	1.036	0.003862	1.00	0.00071	1.815	-0.03662
		χ^2	0.00655	0.000004		0.00819		0.00784		0.00001			0.00163	
		RMSE	0.08105	0.002019		0.09062		0.08865		0.002814			0.04045	
		SSE	0.03285	0.0000163		0.03285		0.03144		0.0000158			0.006544	
		R^2	0.9578	1		0.9578		0.9596		0.9999			0.9916	

(a)

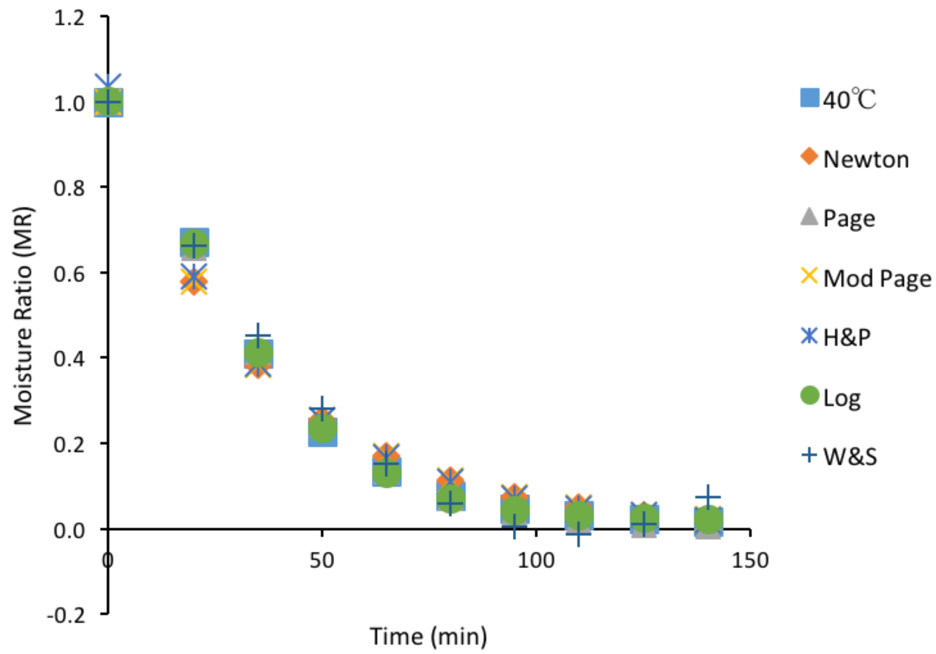
1.2
1.0
0.8
0.6
0.4
0.2
0.0
-0.2
Moisture Ratio (MR)
0
50
100
150
Time (min)
40℃
Newton
Page
Mod Page
H&P
Log
W&S

(b)

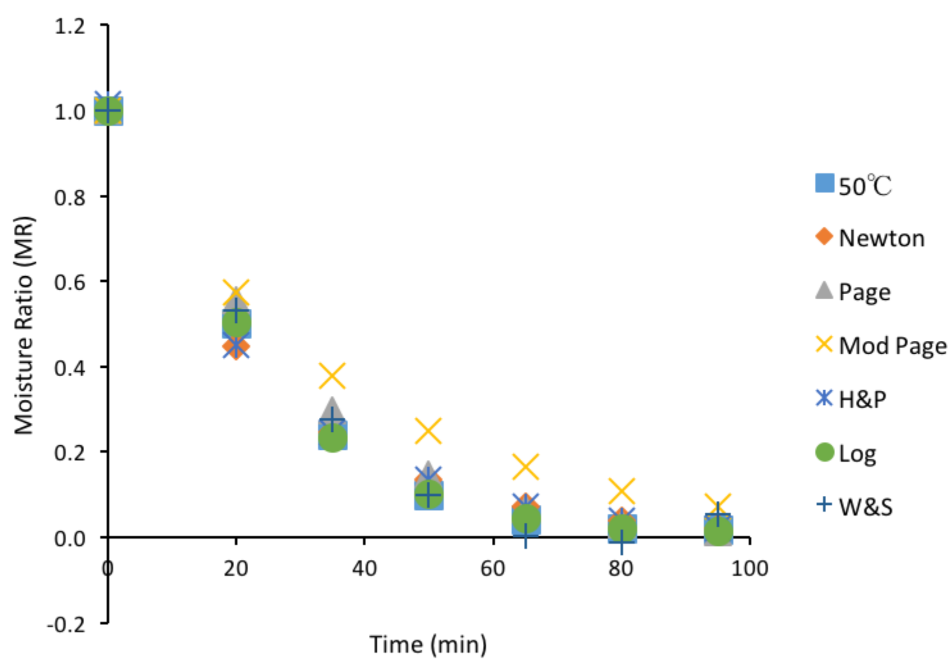
1.2
1.0
0.8
0.6
0.4
0.2
0.0
-0.2
Moisture Ratio (MR)
0
20
40
60
80
100
Time (min)
50℃
Newton
Page
Mod Page
H&P
Log
W&S

(c)

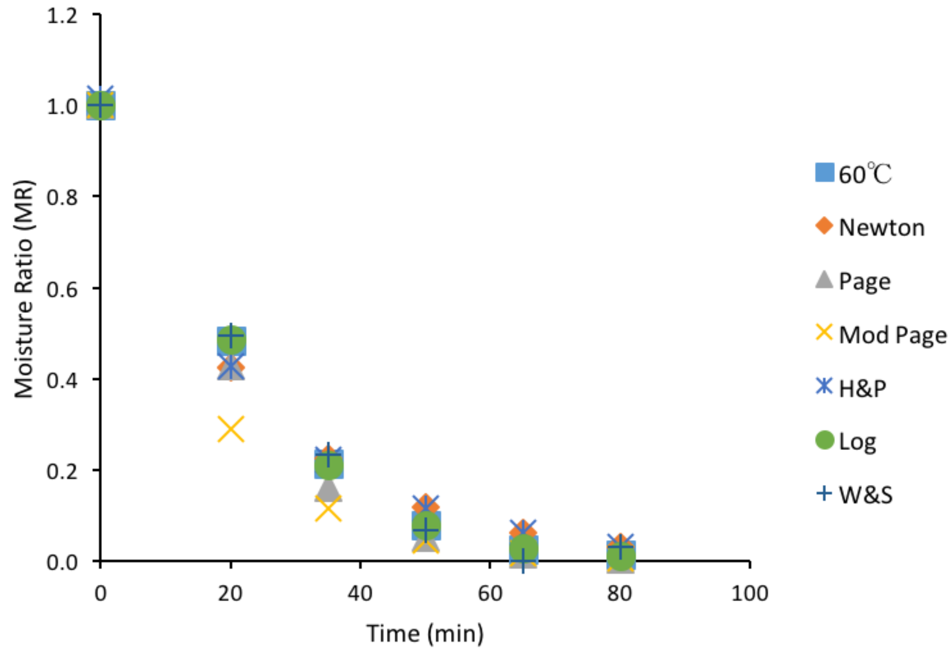

Figure 3. 5: The mathematic models fitting to the drying curve of (a) carrot slices dried without pre-treatment at 40 °C; (b) carrot slices dried without pre-treatment at 50 °C and (c) carrot slices dried without pre-treatment at 60 °C. Mod Page: Modified Page model; H&P: Henderson & Pabis model; Log: Logarithmic model; W&S: Wang and Singh model.

(a)

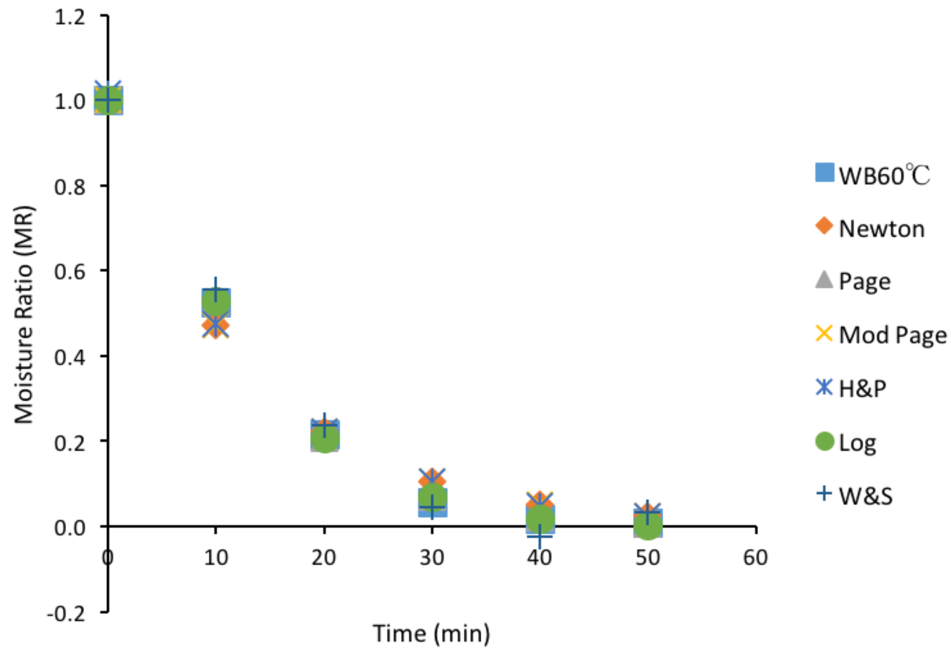
1.2
1.0
0.8
0.6
0.4
0.2
0.0
-0.2
Moisture Ratio (MR)
0
10
20
30
40
50
60
Time (min)
WB60℃
Newton
Page
Mod Page
H&P
Log
W&S

(b)

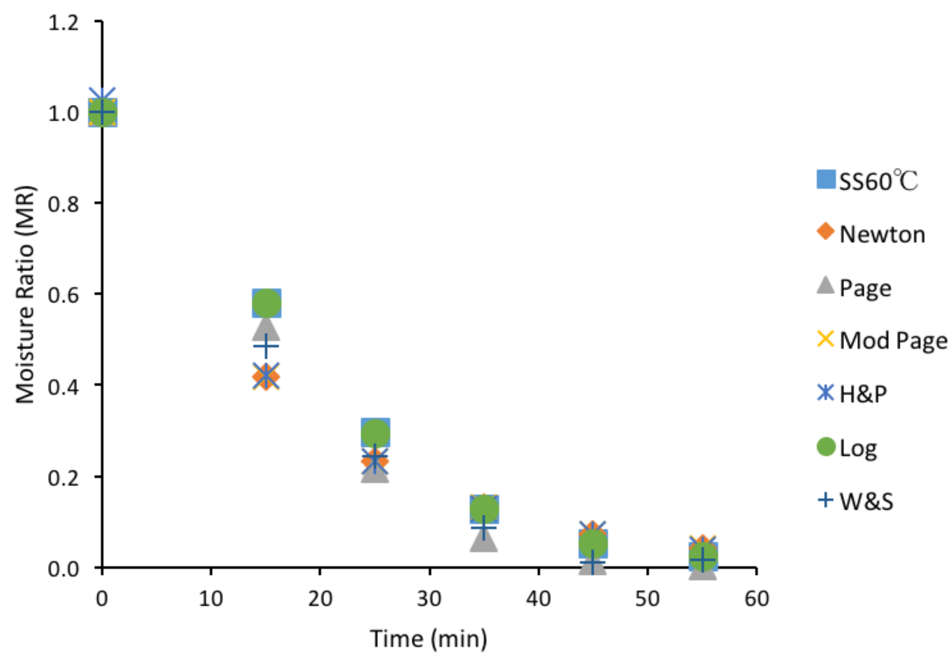
1.2
1.0
0.8
0.6
0.4
0.2
0.0
Moisture Ratio (MR)
0
10
20
30
40
50
60
Time (min)
SS60℃
Newton
Page
Mod Page
H&P
Log
W&S

(c)

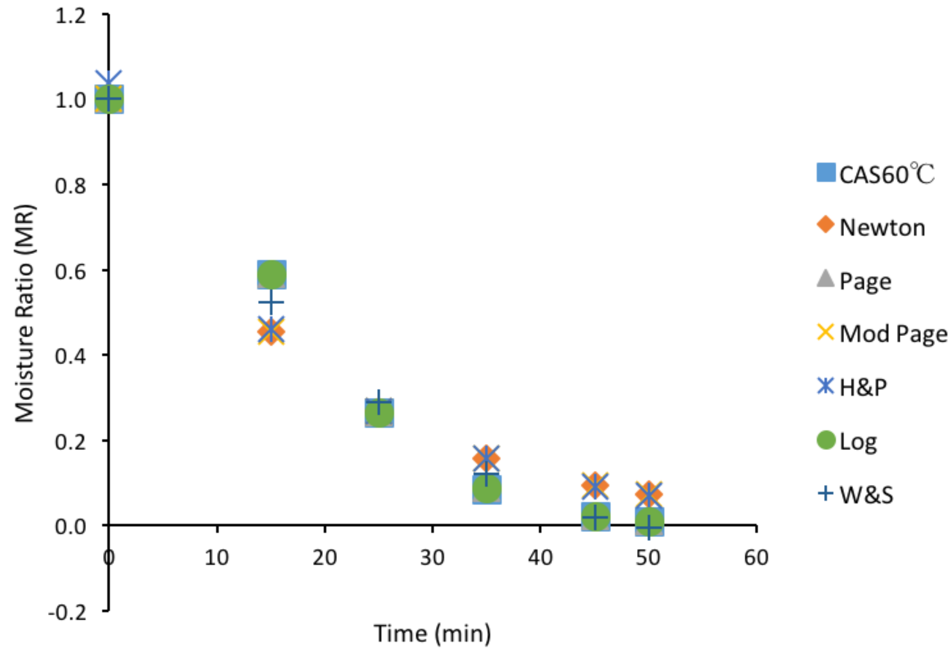

Figure 3. 6: The mathematic model fitting to the drying curve of (a) carrot slices dried at 60 °C with pre-treatment of water blanching (WB); (b) carrot slices dried at 60 °C with pre-treatment of sugar solution (SS) and (c) carrot slices dried at 60 °C with pre-treatment of citric acid solution (CAS). Mod Page: Modified Page model; H&P: Henderson & Pabis model; Log: Logarithmic model; W&S: Wang and Singh model.

3.3.3 Rehydration Capability Analysis

Table 3.3 shows the rehydration capability (RC) of dried carrot slices at different drying conditions in fluidized-bed drying. Although the rehydration capability of the dried carrot slices was found to increase with increase in inlet air temperature, there were no significant differences among rehydration capabilities of dried carrot slices due to different inlet air temperature applied. Different pre-treatments obviously affected the rehydration capability of the dried carrot slices. The rehydration capability of dried carrot slices pre-treated with water blanching increased 28% compared with carrot slices dried without any pre-treatment. On the contrary, the rehydration capability decreased 13.5% when sugar solution was applied. It can be attributed to the change in porosity in the pre-treated carrot slices.

Table 3. 3: Rehydration capability (RC) of dried carrot slices in different drying condition.

Treatment	RC (g g^{-1})
40 °C	4.23
50 °C	4.26
60 °C	4.38
WB, 60 °C	6.08
SS, 60 °C	3.86
CAS, 60 °C	4.68

3.3.4 Color Analysis

The Table 3.4 and Table 3.5 present the influence of drying conditions and rehydration on the color of dried carrot slices. There was no significant difference in the L^* value (ranged from +50.19 to +43.08) and rehydration under all drying conditions investigated. Both the a^* value and b^* value were increased significantly with the application of different pre-treatments (Table 3.4). The ΔE value which shows the total color change was decreased when carrot slices were pre-treated (Fig. 3.7). After rehydration, the a^* value didn't have an important change compared with carrot slices before rehydration. The b^* value increased and the ΔE value significantly decreased after rehydration (Fig. 3.8).

Table 3. 4: Color values of carrot slices in all drying conditions.

Drying Method	Temperature °C	Color values			
		L^*	a^*	b^*	ΔE
Fresh	Ambient	51.95	25.46	47.97	
Without pre-treatment	40	42.67	18.67	28.47	22.64
	50	44.77	20.34	31.46	18.72
	60	46.03	19.78	30.97	18.88
WB	60	43.68	25.24	37.53	13.32
SS	60	43.08	25.64	34.53	16.10
CAS	60	43.14	27.55	37.17	14.10

Table 3. 5: Color values of dried carrot slices after rehydration.

Drying Method	Temperature °C	Color values			
		L^*	a^*	b^*	ΔE
Without pre-treatment	40	44.14	20.59	39.54	12.48
	50	44.54	20.57	40.06	11.89
	60	45.01	31.22	39.21	12.58
WB	60	48.50	24.93	51.46	4.94
SS	60	44.62	24.15	43.12	8.89
CAS	60	50.19	27.48	50.94	4.00

(a)

(b)

(c)

(d)

Figure 3. 7: The color of (a) carrot slices dried at 60 °C; (b) carrot slices with pre-treatment of water blanching (WB) dried at 60 °C; (c) carrot slices with pre-treatment of sugar solution (SS) dried at 60 °C; (d) carrot slices with pre-treatment of citric acid solution (CAS) dried at 60 °C.

(a) (b)

(c) (d)

Figure 3. 8: Carrot slices after rehydration, (a) carrot slices dried at 60 °C; (b) carrot slices with pre-treatment of water blanching (WB) dried at 60 °C; (c) carrot slices with pre-treatment of sugar solution (SS) dried at 60 °C; (d) carrot slices with pre-treatment of citric acid solution (CAS) dried at 60 °C.

3.3.5 Textural Strength Analysis

Textural strength analysis of rehydrated carrot slices was measured using the Universal Testing Machine (Instron–4502, Instron Corporation, USA). Fig. 3.9 and Fig. 3.10 show that the dried carrot required less force and energy to be broken than fresh carrot slices. When the carrot slices were dried without pre-treatment, the maximum load and energy to break the rehydrated carrots increased with the drying temperature and rehydration capability. Carrot slices pre-treated with water blanching got the highest rehydration capability, the difference was not significant in comparison with carrot slices without pre-treatment. Citric acid solution had a significant influence on the maximum load and energy to break the rehydrated carrot slices. It was increased 60.5% and 11.11% more for the maximum load and the energy to break respectively than for the carrot slices dried at 60°C without pre-treatment. The slope of the displacement and load (Fig. 3.11) presents that the higher the slope value is, the harder the carrot slices are. The dried carrot slices with pre-treatments (WB, SS and CAS) were harder than dried carrot slices without pre-treatment.

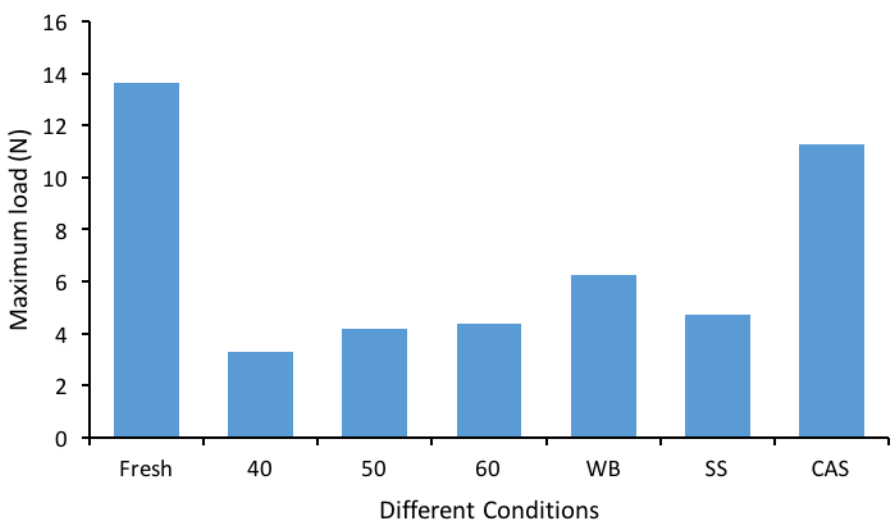

Figure 3. 9: Comparison of maximum load (N) of rehydrated carrot slices from different drying conditions.

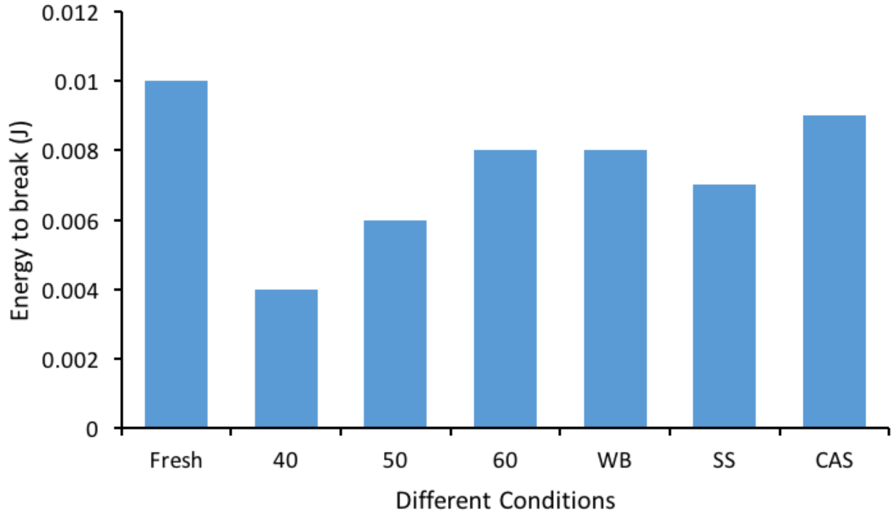

Figure 3. 10: Comparison of the energy to break (J) the rehydrated carrot slices from different drying conditions.

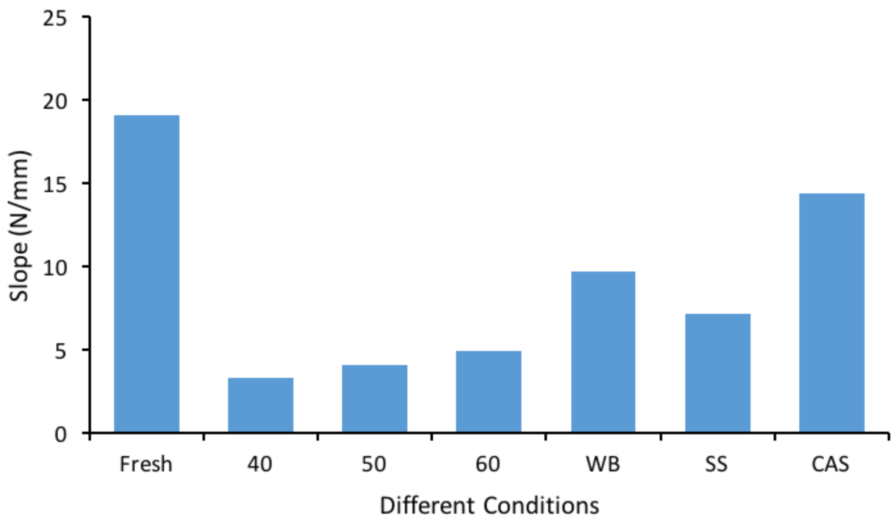

Figure 3. 11: Comparison of Slope (N/mm) of rehydrated carrot slices from different drying conditions.

3.4 Conclusion

The fluidized-bed drying of carrot slices was conducted without pre-treatment at controlled temperature of 40 °C, 50 °C and 60 °C, and with different pre-treatment methods (WB, SS, CAS) at 60 °C. The drying kinetics and the quality of the final dried carrot slices were analyzed. The inlet air temperature and the application of pre-treatment had a significant effect on moisture ratio (MR). The color difference decreased after rehydration of the dried carrot slices with pre-treatments, which means that the color of pre-treated carrot slices was highly protected. Moreover, the textural strength of the dried carrot slices was affected by both the inlet air temperature and the application of pre-treatments.

Acknowledgements

The authors are grateful to the Natural Sciences and Engineering Research Council of Canada (NSERC) and ministère de l'Agriculture, des Pêcheries et de l'Alimentation du Québec (MAPAQ) for the financial support (Grant No. IA113076).

References

Amami, E., Khezami, L., Vorobiev, E., Kechaou, N. 2008. Effect of pulsed electric field and osmotic dehydration pretreatment on the convective drying of carrot tissue. *Drying technology*, **26**(2), 231-238.

Batchelor, W., Kibblewhite, R., He, J. 2008. A new method for measuring RBA applied to the Page equation for the tensile strength of paper. *Appita Journal*, **61**(4), 302.

Billmeyer FW, Saltzman M. 1981. Principles of color technology. J. Wiley & sons.

Cui, Z.-W., Li, C.-Y., Song, C.-F., Song, Y. 2008. Combined microwave-vacuum and freeze drying of carrot and apple chips. *Drying Technology*, **26**(12), 1517-1523.

Doymaz, I. 2004. Convective air drying characteristics of thin layer carrots. *Journal of Food Engineering*, **61**(3), 359-364.

Ertekin, C., Yaldiz, O. 2004. Drying of eggplant and selection of a suitable thin layer drying model. *Journal of food engineering*, **63**(3), 349-359.

Hovmand, Svend. 1995. Fluidized bed drying. *Handbook of Industrial Drying*, **22** (1), 195-248.

Ketelaars, Antonius Adrianus Josephus. 1994. Drying deformable media kinetics, shrinkage and stresses. *Drying Technology*, **12**(4), 983-987.

Kim, M., Toledo, R. 1987. Effect of osmotic dehydration and high temperature fluidized bed drying on properties of dehydrated rabbiteye blueberries. *Journal of Food Science*, **52**(4), 980-984.

Krokida, M., Karathanos, V., Maroulis, Z. 1998. Effect of freeze-drying conditions on shrinkage and porosity of dehydrated agricultural products. *Journal of Food Engineering*, **35**(4), 369-380.

Lewicki, P.P. 1998. Some remarks on rehydration of dried foods. *Journal of Food Engineering*, **36**(1), 81-87.

Lin, T.M., Durance, T.D., Scaman, C.H. 1998. Characterization of vacuum microwave, air and freeze dried carrot slices. *Food Research International*, **31**(2), 111-117.

Midilli, A., Kucuk, H. 2003. Mathematical modeling of thin layer drying of pistachio by using solar energy. *Energy conversion and Management*, **44**(7), 1111-1122.

Mohapatra, D., Rao, P.S. 2005. A thin layer drying model of parboiled wheat. *Journal of food engineering*, **66**(4), 513-518.

Mulet, A., Berna, A., Rossello, C., Canellas, J. 1993. Analysis of open sun drying experiments. *Drying technology*, **11**(6), 1385-1400.

Nair, G.R., Li, Z., Gariepy, Y., Raghavan, V. 2011. Microwave drying of corn (Zea mays L. ssp.) for the seed industry. *Drying Technology*, **29**(11), 1291-1296.

Orsat, V., Yang, W., Changrue, V., & Raghavan, G. S. V. 2007. Microwave-assisted drying of biomaterials. *Food and Bioproducts Processing*, **85**(3), 255-263.

Overhults, D., White, G., Hamilton, H., Ross, I. 1973. Drying soybeans with heated air. *Amer Soc Agr Eng Trans ASAE*.

Senadeera, W., Bhandari, B.R., Young, G., Wijesinghe, B. 2003. Influence of shapes of selected vegetable materials on drying kinetics during fluidized bed drying. *Journal of Food Engineering*, **58**(3), 277-283.

Sereno, A., Hubinger, M., Comesana, J., Correa, A. 2001. Prediction of water activity of osmotic solutions. *Journal of Food Engineering*, **49**(2), 103-114.

Singh, A., Nair, G.R., Rahimi, J., Gariepy, Y., Raghavan, V. 2013. Effect of static high electric field pre-treatment on microwave-assisted drying of potato slices. *Drying Technology*, **31**(16), 1960-1968.

Soponronnarit, S., Prachayawarakorn, S. 1994. Optimum strategy for fluidized bed paddy drying. *Drying Technology*, **12**(7), 1667-1686.

Xanthopoulos, G., Oikonomou, N., Lambrinos, G. 2007. Applicability of a single-layer drying model to predict the drying rate of whole figs. *Journal of Food Engineering*, **81**(3), 553-559.

Yaldiz, O., Ertekin, C., Uzun, H.I. 2001. Mathematical modeling of thin layer solar drying of sultana grapes. *Energy*, **26**(5), 457-465.

CONNECTING TEXT

After studying the fluidized-bed drying of carrot slices at controlled temperatures, in the following chapter, the optimization of microwave-assisted fluidized-bed drying of carrot slices was carried out. The drying conditions such as microwave power density and inlet air temperature were optimized. The drying performance of pre-treated carrot slices in the optimized drying conditions was analyzed.

CHAPTER 4

OPTIMIZATION OF MICROWAVE-ASSISTED FLUIDIZED BED DRYING OF CARROT SLICES**

Xue Hu*, Jiby Kurian, Yvan Gariépy, Vijaya Raghavan

Department of Bioresource Engineering, McGill University, 21111 Lakeshore Rd., Ste-Anne-de-Bellevue, QC, H9X 3V9, Canada

* Correspondence author:
Xue Hu, Department of Bioresource Engineering, McGill University, QC, H9X 3V9, Canada.
Phone: (438)-881-0425, Email: xue.hu@mail.mcgill.ca

**Submitted to Drying Technology, An International Journal.

Abstract

The drying of carrot slices in a microwave-assisted fluidized-bed drying (MWFBD) system was investigated. The drying conditions such as the initial microwave power density and the inlet air temperature were optimized. The effects of different pre-treatment processes such as water blanching (WB), osmotic drying with 20% sugar solution (SS) and 1% citric acid solution (CAS) on the drying of carrot slices were investigated under the optimized drying conditions. The drying kinetics and the physical properties of the dried carrot slices were analysed. Different mathematical models of the drying process were explored and fitted to the drying of carrot slices in MWFBD. The pre-treatment of the carrot slices reduced the drying time required and improved the quality such as color and textural strength of the dried carrot slices.

Key words: Microwave-assisted fluidized-bed drying, carrot slices, drying kinetics, mathematical models, dried carrot slices

4.1 Introduction

One third of the global food produced is wasted or lost (Gustavsson et al., 2011) that includes the residues produced during the processing and marketing of the fresh fruits and vegetables. Even though these residues should be disposed-off to prevent environmental problems, drying of it to by-products is one of the best way to reclaim the value in them. Drying processes are used to produce good quality dried products at minimum cost by the efficient supply of thermal energy (Mujumdar, 2014). There are conventional and advanced drying methods available to produce dried products from food residues. In the conventional drying methods, heated air acts as the heat and moisture carrier. Moisture diffused from the interior to the surface of the material and the rate of which is higher at the first falling rate period of the drying process. The diffusion of moisture decreases with decrease in drying rate as the moisture content of the product becomes lowered (Maskan, 2001). The conduction of heat from the surface to the interior of the drying material results in hardness of the products. There are physical and chemical changes taking place during the drying process that can affect the final quality of the dried products. In addition, drying with higher temperatures causes poor appearance and wilt of the product, resulting in higher-energy consumption (Sanga et al., 2002).

For over a century, carrots are the most widely consumed vegetable for high vitamin and fibre content, which are usually pre-cooked to be used in instant soups (Sumnu et al., 2005). Many different drying methods have been investigated to dry carrots. For example, Wang and Xi (2005) studied two-stage microwave drying of carrots; Mayor and Sereno (2004) dried carrots by hot air drying; solar drying was investigated by Ratti and Mujumdar (1997), combined microwave-vacuum and freeze drying of carrot slices was conducted by Cui et al. (2008) and Prabhanjan et al. (1995) did research on microwave-assisted convective air drying of carrots.

In recent years, microwave-assisted drying method became one of the ways to improve the quality of the dried products due to the homogenous energy distribution and shortening of drying time. But this method is most effective when the moisture content of the material is lower than 20% (Giese, 1992). Thus the drying process usually takes place in a combination of microwave heating and convective drying. Compared with traditional convective drying such as hot air drying, fluidized-bed drying is known for its uniform and faster drying and higher thermal efficiency, because the surface area for heat and mass transfer is increased in the fluidized-bed drying by suspending the material in the air by fluidization (Hovmand, 1995). In microwave-assisted fluidized-bed drying, drying time can be significantly reduced with the application of microwave energy, and the uniformity in temperature distribution can be achieved by the fluidization (Chen et al., 2001).

The objectives of this study were:

1) Design and build a microwave-assisted fluidized-bed dryer and test the system.
2) To establish an optimal microwave-assisted fluidized-bed drying conditions.
3) To reclaim the value of food residues by drying them into useful by-products.

4.2 Materials and Methods

4.2.1 Preparation of Carrot Slices

Carrots used for microwave-assisted fluidized-bed drying (MWFBD) were obtained from a local supermarket in Montreal, Quebec, Canada. A food processor (DLC-2009CHB 9-Cup Prep Plus Food Processor, Cuisinart, USA) was used to slice the carrots into quadrant chips of 2.35–2.65 mm thickness, with a radius of 9.85–10.15 mm.

4.2.2 The Moisture Content of Carrot Samples

The moisture content of fresh and dried carrots on wet basis (w.b.) was determined in triplicate by drying carrot slices (10 g) in a hot air chamber (Model 6528, Thermo Electron Corporation, USA) at 105 °C for 24 hours. The moisture content (*M.C.*) was calculated based on Equation (1):

$$M.C.(w.b.) = \frac{M_w}{M_w + M_s} \quad (1)$$

Where, M_w is the mass of water in the sample (g); M_s is the mass of solid in the sample (g). For analytical purposes, it is preferable to express the moisture content as a function of the mass of solid. The moisture content on dry basis (d.b.) was calculated by Equation (2):

$$M.C.(d.b.) = \frac{M_w}{M_s} \quad (2)$$

The initial moisture content of the carrots was 89.8% (w.b.).

4.2.3 Microwave-Assisted Fluidized-Bed Drying of Carrot Slices

A sample of (200 ± 0.5 g) carrot slices was dried in the microwave-assisted fluidized-bed drying (MWFBD) system designed and built at the machine shop of Bioresource Engineering department of McGill University (Fig. 4.1). A counter top microwave oven (Panassonic NN-SN733B, 2450 MHz, 45 litre capacity) with a maximum power output of 700 W was modified to fit a fluidization chamber inside it. A fluidized-bed chamber (a 30 cm long glass tube with 10 cm internal diameter and 2.5 mm thickness) was placed in the middle of the microwave oven. The magnetron of the microwave oven was situated above the fluidization chamber. Grounding strips were used to prevent the microwave leakage from the unit. The control unit of the microwave oven was used to set the microwave power and duration of treatment. An air blower (Lesson Electric, Wisconsin, USA) connected with ceramic heaters (Comfort Zone, Cranbury, USA) was used to provide inlet air at different temperatures to the fluidization chamber. The heaters were controlled by a PID controller to maintain the temperature at 40 °C, 50 °C and 60 °C.

Air flow was controlled manually by using a gate system and the inlet air velocity was controlled to be between 2.5 and 15.5 m/s. An anemometer was used to monitor the inlet air velocity. A flexible aluminum pipe and polyvinyl chloride (PVC) connectors were used to connect the air blower to the fluidization chamber. Polypropylene flanges were used to connect the glass fluidization chamber to the PVC connector at the bottom and to the filter cap at the top. The filter cap was used to load and take samples as well as to prevent the vegetable residues flown away from the fluidization chamber during drying. Polypropylene mesh was used to make the filter cap of the fluidization chamber. A humidity/temperature sensor system (Mamac Systems, Minneapolis, USA) was used to monitor the inlet air temperature and humidity. The Agilent 34970A data acquisition system was installed to track the drying performance. A hand held infra-red thermometer is used to monitor the product temperature during drying. A microwave leak detector is used to check leakage of microwave during the drying process and to take corrective measures. The mass of carrot slices was measured and recorded at 5 min intervals with an Electronic scale (APX-1502, Denver Instrument). The drying stopped when the final moisture content of carrot slices reached ~15% (w.b.).

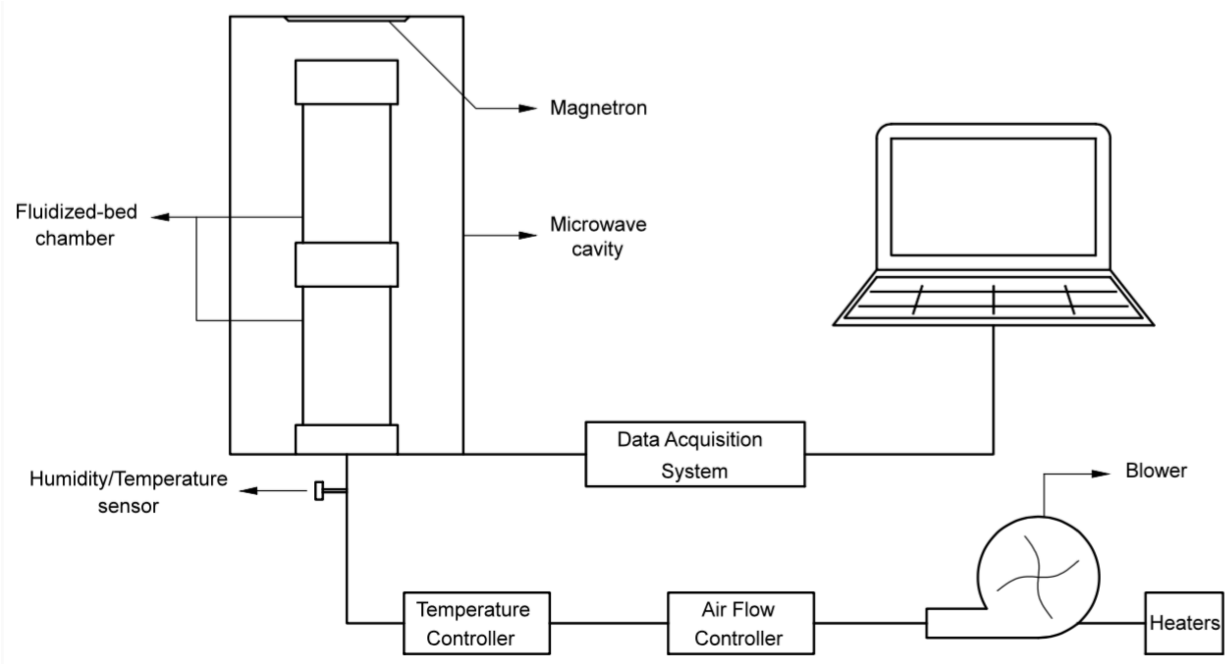

Figure 4. 1: Schematic of Microwave-assisted fluidized-bed dryer apparatus.

4.2.4 Experimental Design

The central composite design (CCD) of experiment with two factors (microwave power density and inlet air temperature) at three levels was followed for the investigation of drying of carrot slices in the MWFBD. The fresh carrot slices were dried in the MWFBD at the initial power density of 0.44 W/g, 0.77 W/g and 1.21 W/g, and at inlet air temperatures of 40 °C, 50 °C and 60 °C. The drying conditions (inlet air temperature and the initial microwave power density) were optimized to minimize drying duration and change in color of the dried carrot slices. The effect of pre-treatments viz. (1) water blanching (WB), (2) osmotic drying with 20% (w/w) sugar solution (SS), and (3) 1% (w/w) citric acid solution (CAS) on the drying of carrot slices at the optimized conditions were also investigated. The inlet air velocity applied was optimized to 6.7 ± 0.5 m/s to get good fluidization of the carrot slices. The color properties and texture strength of the dried carrot slices were measured and analyzed.

4.2.5 Pre-treatment of Carrot Slices

The application of different pre-treatments can prevent the loss of color by inactivating enzymes on the surface of the carrot slices and shortening the drying time by partially breaking tissue structure and produce good quality dried product (Kingsly et al., 2007). Blanching is one of the pre-treatment methods widely treated on vegetables and fruits before drying them with steam and hot water (Doymaz, 2010). In this study, the carrot slices were pre-treated with the following three different methods before dring under the optimized drying conditions;

(1) Water blanching (WB): Boiling water (100 °C) was applied on the carrot slices (180 g) for 5 min. Water blanched carrot slices were chilled by ice water for 10 seconds. The droplets on the surface of the blanched carrot slices were wiped off with a paper towel.

(2) Sugar solution (SS) 20% (w/w): The 20% (w/w) sugar solution was prepared by dissolving 175 g granulated sugar, (Lantic Inc., Canada) in 700 g distilled water at the room temperature of 22 °C. The carrot slices (180 g) were blanched in boiling water for 3 min and then soaked in the prepared sugar solution for 10 min before drying. The sugar solution on the surface of the treated carrot slices were wiped off with a paper towel.

(3) Citric acid solution (CAS) 1% (w/w): The 1% (w/w) citric acid solution was prepared by dissolving 7 g citric acid powder (Sigma Aldrich, Canada) in 700 g distilled water at the room temperature of 22 °C. The carrot slices (180 g) were blanched in boiling water for 3 min and then immersed in the prepared citric acid solution for 10 min before drying. The citric acid solution on the surface of the treated carrot slices were wiped off with a paper towel.

4.2.6 Mathematical Models

The data on the drying of carrot slices in MWFBD was used to study the drying kinetics and to analyze the fit of mathematical models on thin layer drying, including Page, Newton, Wang and Singh, Modified Page, Henderson & Pabis, andthe Logarithmic model (Table 4.1) to the observed data (Singh et al., 2013).

Table 4. 1: Mathematic models of the kinetics of fluidized bed drying.

Model name	Model equation	Reference	Equation No.
Newton	$MR = e^{-kt}$	(Midilli and Kucuk, 2003)	3
Page	$MR = e^{-kt^n}$	(Batchelor et al., 2008)	4
Modified Page	$MR = e^{(-kt)^n}$	(Overhults et al., 1973)	5
Henderson & Pabis	$MR = a\, e^{-kt}$	(Midilli et al., 2002)	6
Logarithmic	$MR = a\, e^{-kt^n} + c$	(Xanthopoulos et al., 2007)	7
Wang and Singh	$MR = 1 + at + bt^2$	(Mohapatra and Rao, 2005)	8

In Table 4.1, the *MR* in the equations (3-8) is the moisture ratio which is defined as in Equation (9):

$$MR = \frac{M_t - M_e}{M_o - M_e} \tag{9}$$

Where M_t, M_o and M_e are the moisture content (d.b.) at time *t*, initial moisture content (d.b.) and equilibrium moisture content (d.b.), respectively. The *k* is the drying rate constant (min^{-1}); n, a, b and c are the drying coefficients (unit-less) that have different values depending on the equation and the drying curve; *t* is time (min).

When the difference between the moisture content at time *t* and the equilibrium moisture content is negligible (Midilli and Kucuk, 2003), the Equation (9) reduces to Equation (10):

$$MR = \frac{M_t}{M_o} \tag{10}$$

4.2.7 Optimization of Drying Conditions

The drying time to reach the desired final moisture content of 15% (w.b.) was predicted by analyzing different mathematical models using Curve Expert Professional® ver. 2.0.3 (Daniel G. Hyams, USA). The models had the general form of a rational function which can be written as:

$$MR = \frac{a+b*T}{1+c*T+d*T^2} \tag{11}$$

Where, *MR* is the moisture ratio, *T* is the drying time in minutes, and a, b, c and d are the regression parameters.

The predicted drying times were compared in order to assess the effects of inlet air temperature and initial microwave power density on drying of carrot slices in MWFBD. The total color difference of the dried carrot slices from all drying treatments were measured and analysed for the optimization of the drying process. The Design-Expert® Software Version 9 (Stat-Ease Inc., USA) was used to select the optimal drying temperature and initial microwave power density according to the predicted drying time and color difference. The mass of fresh carrot slices was revised based on the optimized initial microwave power density. The initial microwave power density was selected using Equation (12):

$$D = \frac{P}{m} \tag{12}$$

Where, *D* is the microwave power density (W/g); *P* is the chosen microwave power level (W); *m* is the total initial mass of carrot slices (g).

4.2.8 Correlation Coefficients and Error Analysis

Statistical parameters such as the root mean square error (RMSE) (Equation (13)), the chi-square (χ^2) (Equation (14)), and the correlation coefficient (R^2) (Equation (15)) were used to estimate the quality of fit of drying models to the observed values (Nair et al., 2011).

$$RMSE = \left[\frac{1}{N}\sum_{i=1}^{N}\left(MR_{pre,i} - MR_{exp,i}\right)^2\right]^{1/2}$$

(13)

Where, $MR_{exp,i}$ is the experimental moisture ratio at time *t*, $MR_{pre,i}$ is the predicted moisture ratio at time *t* and *N* is the observations number.

$$\chi^2 = \frac{\sum_{i=1}^{N}\left(MR_{exp,i} - MR_{pre,i}\right)^2}{N - n}$$

(14)

Where, *n* is the constant number in drying models.

$$R^2 = 1 - \frac{\sum_{i=1}^{N}\left(MR_{pre,i} - MR_{exp,i}\right)^2}{\sum_{i=1}^{N}\left(MR_{exp,i} - \overline{MR}_{exp}\right)^2}$$

(15)

Where, $\overline{MR}_{exp}$ is the mean experimentally measured value of *MR*.

In addition to the parameters mentioned above, the reduced sum square error (SSE) is also used as a criterion to analyze the closeness of fit.

$$SSE = \frac{1}{N}\sum_{i=1}^{N}\left(MR_{pre,i} - MR_{exp,i}\right)^2$$

(16)

4.2.9 Effective Diffusion Coefficient

One of the simplifications of Fick's second law of moisture diffusion given by Crank (Crank, 1979) was used to determine the effective diffusion coefficient of drying (Equation (17)).

$$MR = \frac{8}{\pi^2}\sum_{n=0}^{\infty}\frac{1}{(2n+1)^2} exp\left[-(2n+1)^2\frac{\pi^2 D_{eff} t_i}{L^2}\right] \tag{17}$$

Where, D_{eff} is the effective diffusion coefficient of moisture diffusivity (m^2/s) and L is the half-thickness of carrot slices.

Equation (17) can be simplified to a one-term exponential model to determine the effective diffusion coefficient of drying of food samples (Gekas and Lamberg, 1991). Thus Equation (17) is written in a logarithmic form as in Equation (18):

$$\ln(MR) = ln\frac{8}{\pi^2} - \frac{\pi^2 D_{eff} t_i}{L^2} \tag{18}$$

The effective diffusion coefficient was determined by plotting the drying data in terms of *ln(MR)* versus drying time, t_i. The plot gave a straight line with a slope as in Equation (19):

$$Slope = \frac{\pi^2 D_{eff}}{L^2} \tag{19}$$

4.2.10 Rehydration of the Dried Carrot Slices

During drying process, structural changes influence the renewed absorption of water by the dried product. Rehydration is a reverse process to drying, reflects the degree of structural change of dried food samples (Doymaz et al., 2015). The rehydration capability (RC) was measured by soaking the dried carrot slices (5 g) in boiling water for 10 min. The weight of the carrot slices before and after soaking was used to calculate the RC. The RC was calculated according to Equation (20):

$$\%RC = \frac{W_r}{W_d}\times 100 \tag{20}$$

Where, W_r is the total weight after rehydration (g) and W_d is the weight of the dried material (g).

4.2.11 Color Measurement

The color change is one of the quality criteria for dried products. The color parameters (L^*, a^*, b^*) were measured directly on the surface of fresh, dried and rehydrated carrot slices by using a Chroma-meter with d/0 diffuse illumination/0° viewing system (Model CR-300X, Minolta Co. Ltd., Japan). The CIE 1976 (L^*, a^*, b^*) color space was used to estimate the color values of carrot slice samples. Color values, expressed as L^* (whiteness or brightness/darkness), a^* (redness/greenness) and b^* (yellowness/blueness), were determined for sample in all drying conditions (Billmeyer and Saltzman, 1981). The total color difference (ΔE) was calculated based on color values of fresh (L_f, a_f and b_f) and dried carrot slices (L_d, a_d and b_d) based on Equation (21):

$$\Delta E = \sqrt{(L_f - L_d)^2 + (a_f - a_d)^2 + (b_f - b_d)^2} \tag{21}$$

4.2.12 Texture Strength Analysis

The Instron-4502 Universal Testing Machine (Instron Corporation, USA), equipped with a cylindrical probe with a diameter of 1.5 mm, was used to measure the texture strength of fresh and rehydrated carrot slices. The probe was aligned to the center of the sample of a rehydrated carrot slices and to the hole (diameter: 2 mm) on the platform (Fig. 4.2). The crosshead speed of the probe was set at 10 mm/min. The testing process was controlled and the data was collected by using the computer software (Instron series IX, version 8.25). The maximum force, energy to break the point and the slope were recorded and analyzed.

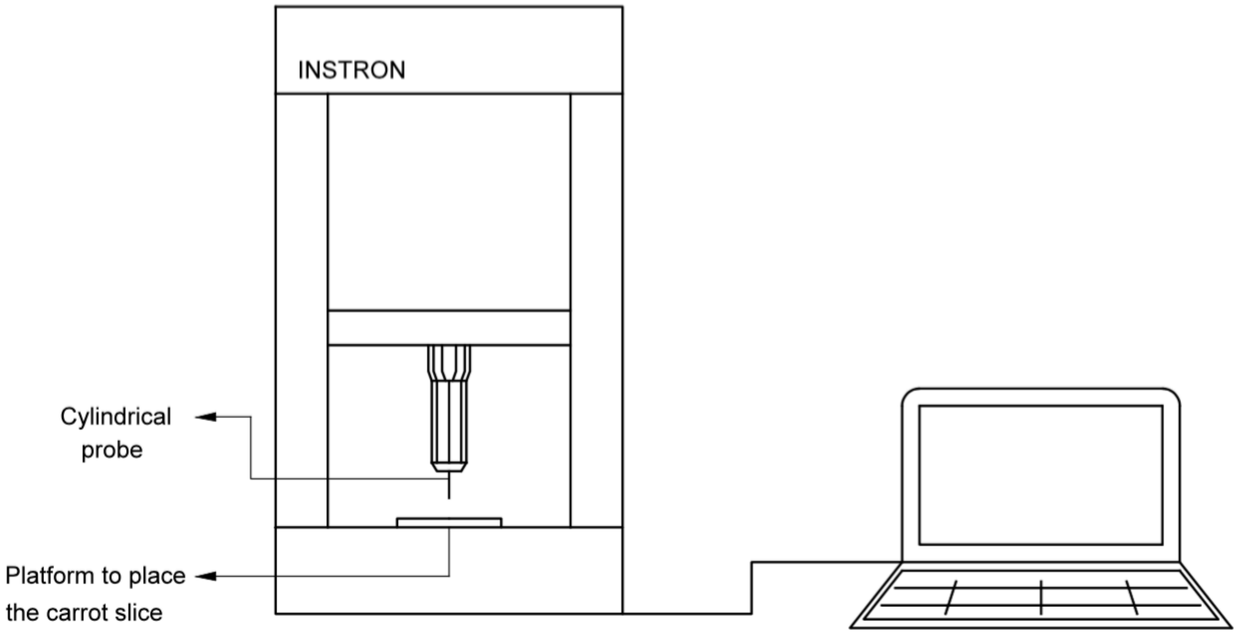

Figure 4. 2: Universal Testing machine equipped with a probe for the texture analysis.

4.2.13 Statistical Analysis

The statistical analysis of variance (ANOVA) of the experiment results was conducted using the Statistical Analysis Software (SAS 9.2 SAS Institute Inc., Cary, NC, USA) with a confidence level ($p \leq 0.05$) of 95%. The Curve Expert Professional® ver. 2.0.3 (Daniel G. Hyams) and the Design-Expert® Software Version 9 (Stat-Ease Inc., USA) were used to analyze and optimize the drying conditions. The mathematical models of drying of the drying of carrot slices in MWFBD were fitted and analyses by using MATLAB R2015a (Mathworks Inc., USA).

4.3 Results and Discussion

4.3.1 Drying Curves

The curves of the drying of carrot slices during microwave-assisted fluidized-bed drying at different initial microwave power density and inlet air temperatures are shown in Figure 4.3 and Figure 4.4. At the initial microwave power density of 0.44 W/g, it took only 35 min at 60 ºC to reach the desired final moisture content of 15% (w. b.) in the carrot slices. This was a reduction of 30% and 41.7% when compared with the drying of carrot slices at 50 ºC and 40 ºC respectively. Similar results were obtained at the initial microwave power density of 0.77 W/g and 1.21 W/g. At 0.77 W/g with 60 ºC inlet air temperature, the drying time was reduced by 12.5% and 36.4% in comparison to the drying of carrot slices at 50 ºC and 40 ºC respectively. Similarly, at 1.21 W/g with 60 ºC inlet air temperature, the drying time reduction of 14.3% and 40% was achieved in comparison to the drying of carrot slices at 50 ºC and 40 ºC respectively. At inlet air temperature of 60 ºC, different initial microwave power densities did not make significant difference in terms of drying time, which were all between 30 and 35 min. However, at 40 ºC, the drying time required to reach the targeted moisture content in the carrot slices at the initial microwave power density of 1.21 W/g was 9.0% and 16.7% less than that of drying at the initial microwave power density of 0.77 W/g and 0.44 W/g. At 50 ºC, the drying time was reduced by 12.5% and 30% when compared to the drying of carrot slices at an initial power density of 1.21 W/g with 0.77 W/g and 0.44 W/g respectively. High initial microwave power density had high moisture transfer driving force that resulted in short drying time. Similar observations were reported by Balbay and Şahin (2012) and Murthy et al. (2012). Even though the initial microwave power density helped to shorten the drying time, the inlet air temperature influenced the drying time very much.

(a)

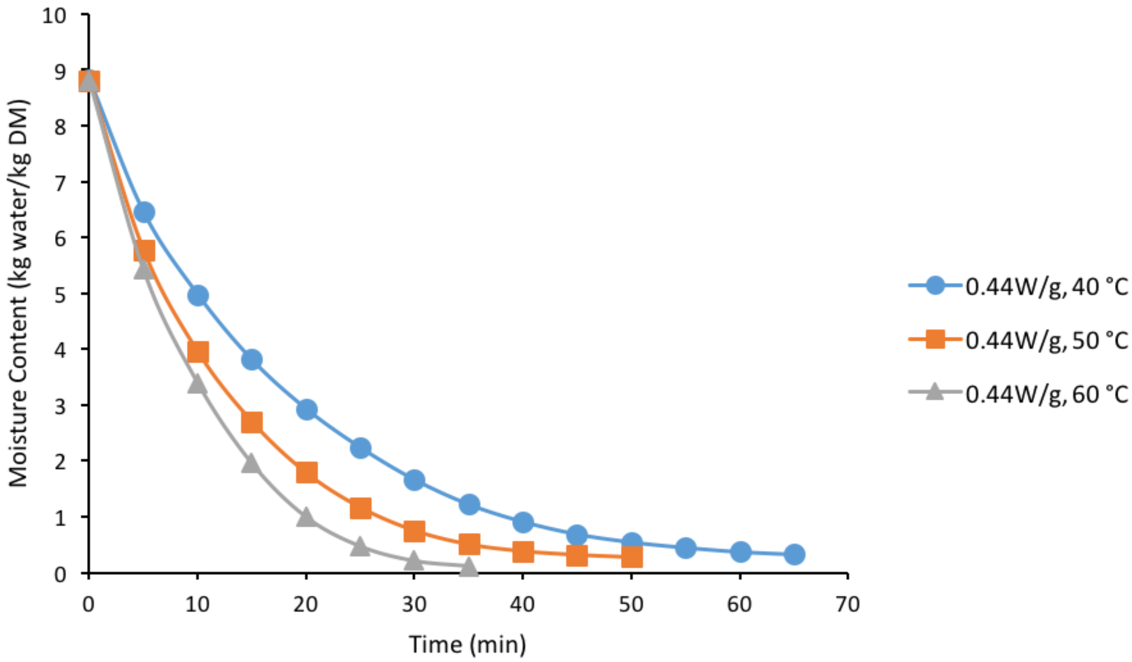

Moisture Content (kg water/kg DM)
Time (min)
0.44W/g, 40 °C
0.44W/g, 50 °C
0.44W/g, 60 °C

(b)

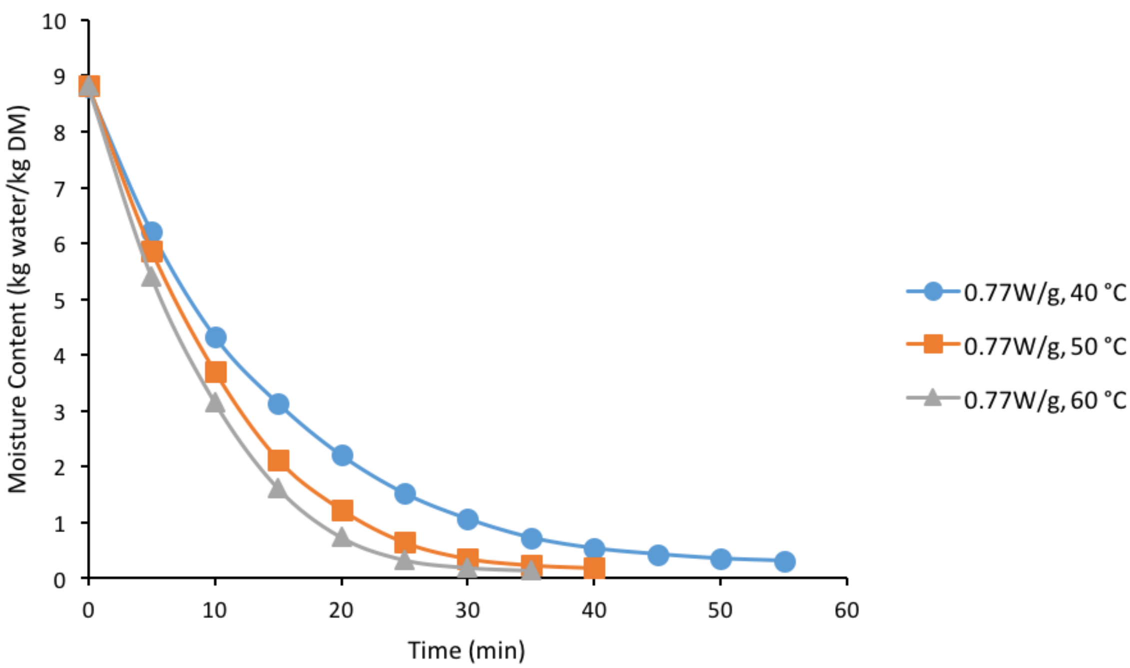

Moisture Content (kg water/kg DM)
Time (min)
0.77W/g, 40 °C
0.77W/g, 50 °C
0.77W/g, 60 °C

(c)

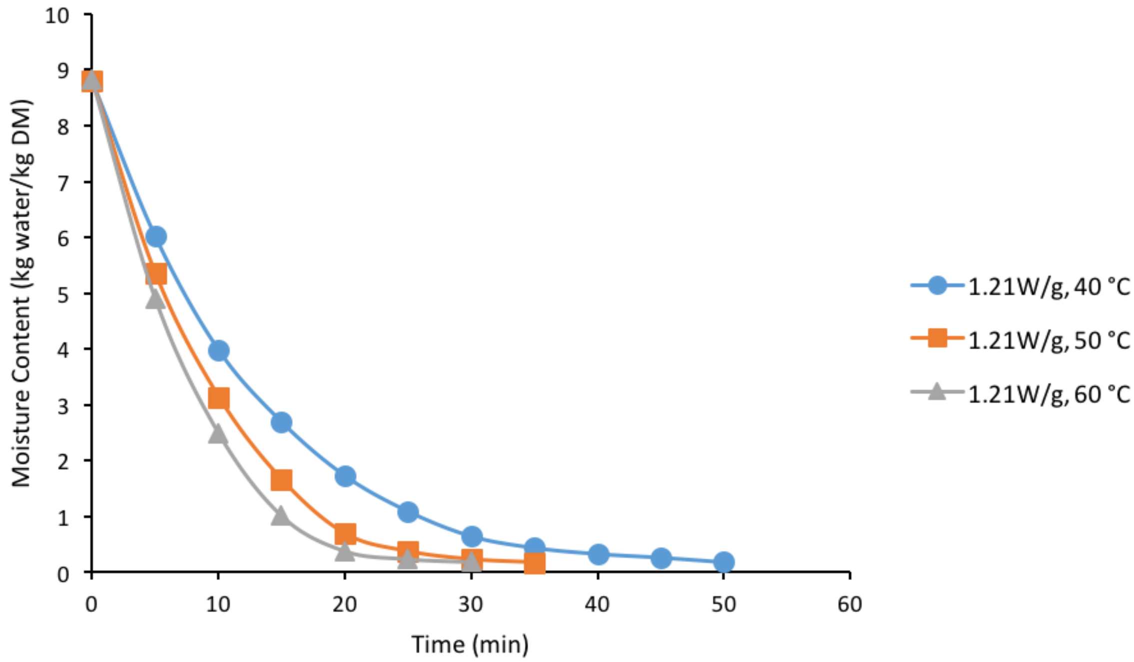

Figure 4. 3: Moisture content (d.b.) curves of carrot slices at (a) initial microwave power density of 0.44 W/g at inlet air temperature of 40 ºC, 50 ºC and 60 ºC; (b) initial microwave power density of 0.77 W/g at inlet air temperature of 40 ºC, 50 ºC and 60 ºC; (c) initial microwave power density of 1.21 W/g at inlet air temperature of 40 ºC, 50 ºC and 60 ºC.

(a)

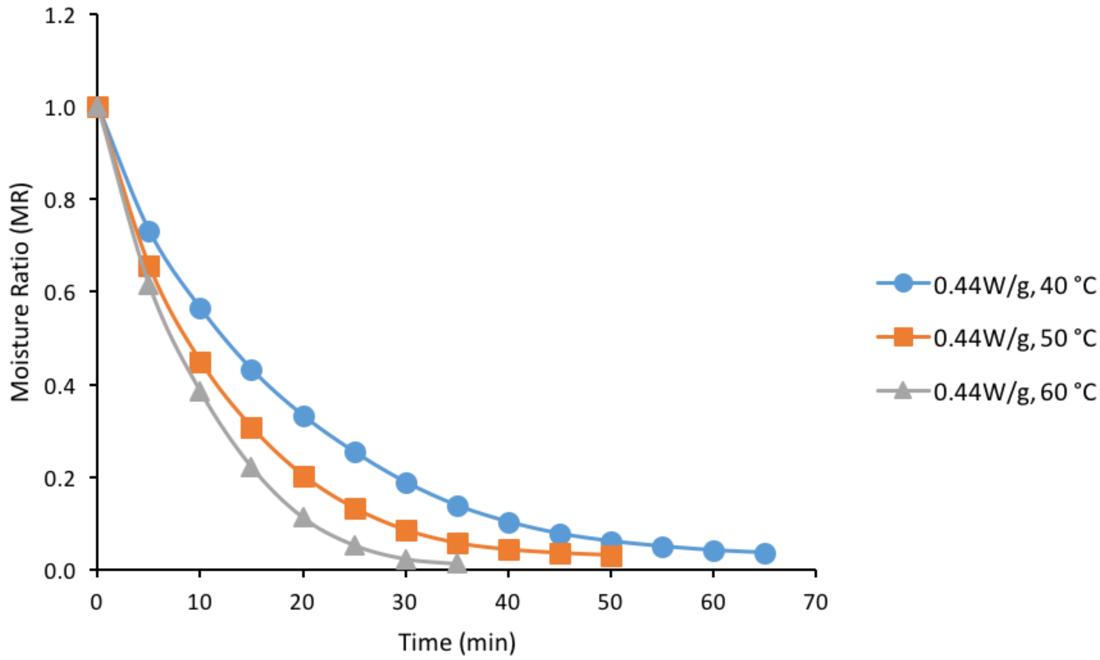

Moisture Ratio (MR)
1.2
1.0
0.8
0.6
0.4
0.2
0.0
0
10
20
30
40
50
60
70
Time (min)
0.44W/g, 40 °C
0.44W/g, 50 °C
0.44W/g, 60 °C

(b)

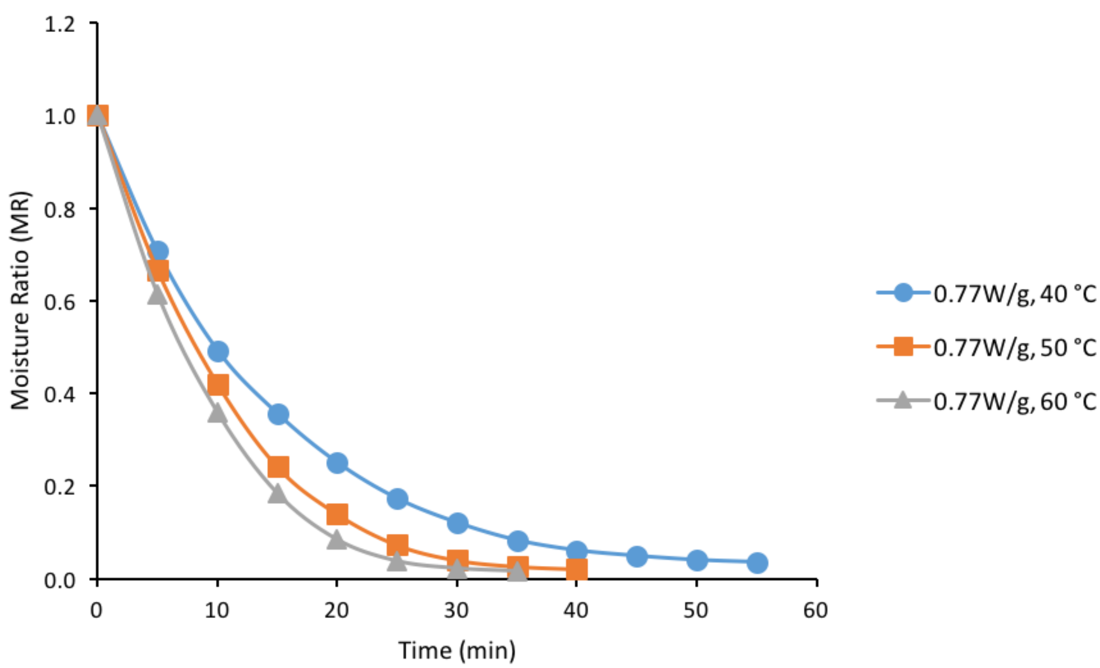

Moisture Ratio (MR)
1.2
1.0
0.8
0.6
0.4
0.2
0.0
0
10
20
30
40
50
60
Time (min)
0.77W/g, 40 °C
0.77W/g, 50 °C
0.77W/g, 60 °C

(c)

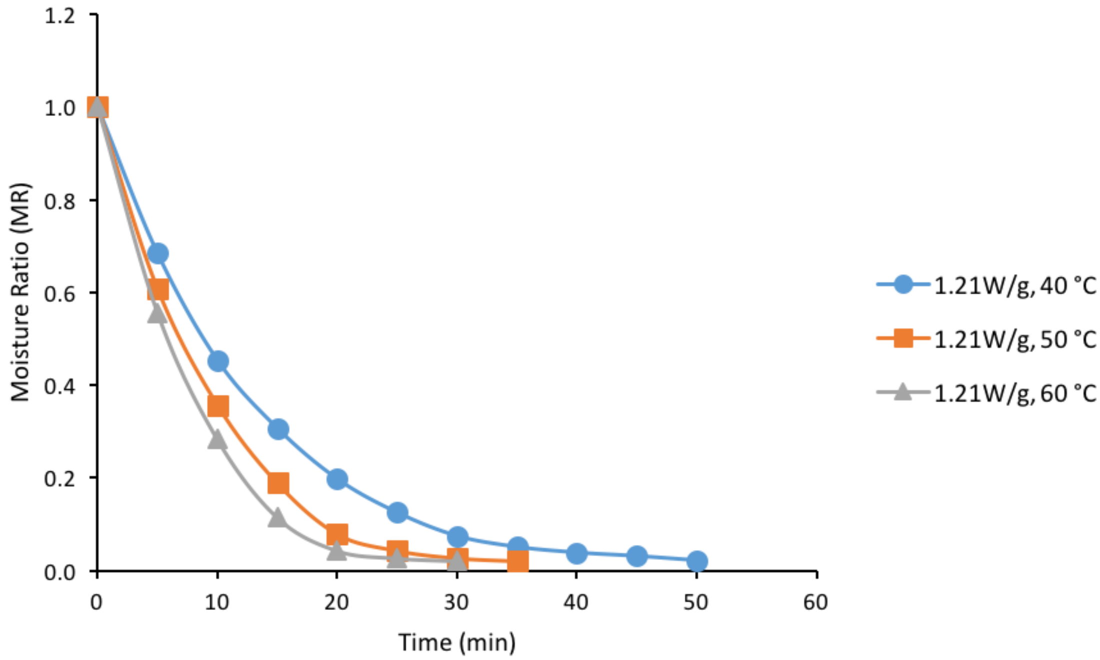

Figure 4. 4: Drying rate of carrot slices at (a) initial microwave power density of 0.44 W/g at inlet air temperature of 40 ºC, 50 ºC and 60 ºC; (b) initial microwave power density of 0.77 W/g at inlet air temperature of 40 ºC, 50 ºC and 60 ºC; ; (c) initial microwave power density of 1.21 W/g at inlet air temperature of 40 ºC, 50 ºC and 60 ºC.

4.3.2 Color Values

The results of color parameters of dried carrot slices in microwave-assisted fluidized-bed drying (MWFBD) are presented in Table 4.2. The L^* and b^* values of all the dried carrot slices decreased significantly in comparison with the fresh carrot slices. However, a^* values were almost stayed the same in all drying conditions, which shows the redness of carrot slices, and were ranged from 22.64 to 27.33. The total color difference (ΔE) of the dried carrot slices from all the drying conditions was between 12.13 and 17.88, which may be due to lack of pre-treatment before drying for color protection.

Table 4. 2: Color values of carrot slices in all drying conditions.

Drying Method	Power Density (W/g)	Temperature (ºC)	Color values			
			L^*	a^*	b^*	ΔE
Fresh	-	Ambient	53.86	26.46	50.51	-
MWFBD	0.44	40	50.09	27.33	38.59	12.53
		50	44.37	24.22	35.53	17.88
		60	46.39	27.50	38.44	14.23
MWFBD	0.77	40	47.16	22.64	35.38	16.98
		50	45.19	26.07	35.34	17.48
		60	48.57	26.31	37.65	13.91
MWFBD	1.21	40	46.51	24.56	34.38	17.83
		50	45.57	26.16	36.77	17.76
		60	50.32	25.10	38.99	12.13

4.3.3 Optimization of the Drying Conditions

The optimal drying conditions was determined by using the predicted drying time and the total color difference of the dried carrot slices from all the drying conditions. The predicted drying time (Table 4.3 and Figure 4.5) required to reach the target moisture content in the dried carrot slices during MWFBD in all conditions was calculated using Equation (11) using Curve Expert Professional® ver. 2.0.3. Figure 4.5 shows that, with high initial microwave power density and inlet air temperature, the predicted drying time are shorter. At the same initial microwave power density, the predicted drying time increased with the increase in the inlet air temperature (Table 4.3). The shortest predicted drying time was obtained at the power density of 1.21 W/g with the inlet air temperature of 60 ºC. It reflected that higher power density and inlet air temperature had a positive effect in accelerating the mass transfer and shortening the drying duration. Similar observations were made by Goksu et al. (2005).

Table 4. 3: Drying time predicted with different initial microwave power density and inlet air temperature based on the drying model.

Power Density (W/g)	Temperature (ºC)	Predicted Time (min)
0.44	40	67.50
	50	49.19
	60	30.92
0.77	40	57.50
	50	35.96
	60	29.86
1.21	40	46.46
	50	30.60
	60	25.97

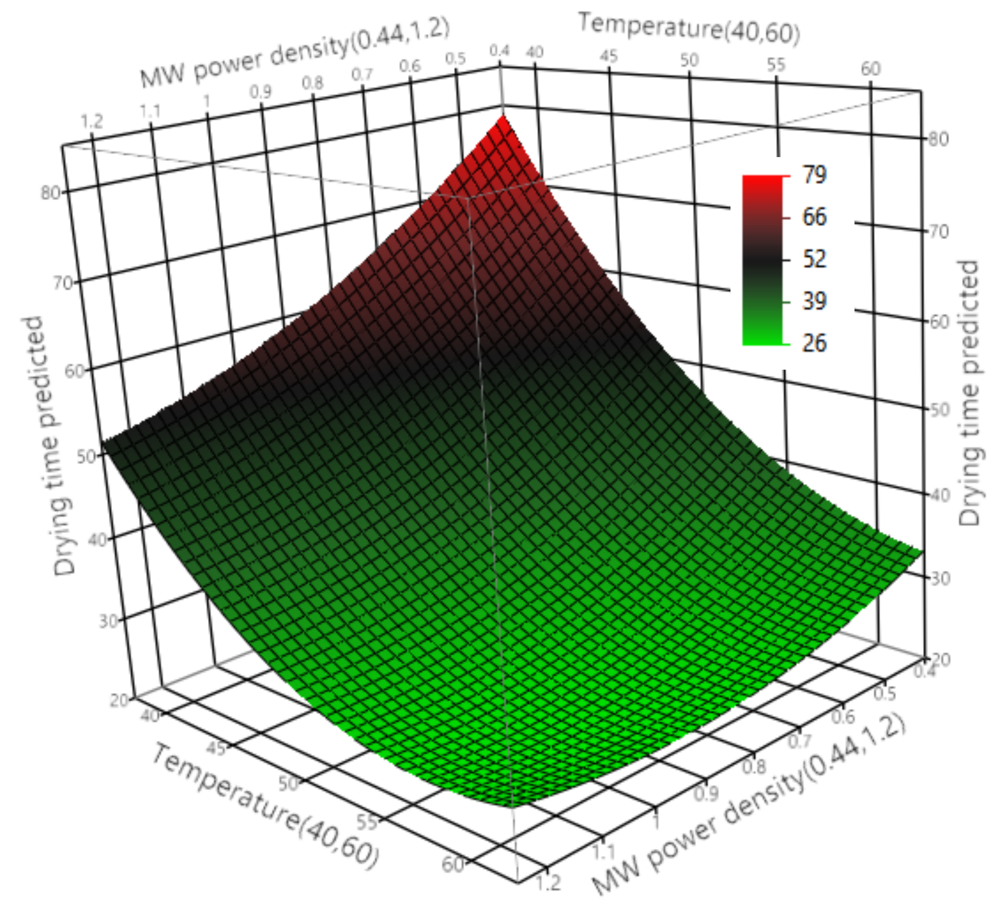

Figure 4. 5: Response surface of the effect of initial microwave power density and inlet air temperature on the predicted time in all drying conditions.

Combined with the total color difference shown in Table 4.2, the drying conditions were optimized using the Design-Expert® Software Version 9. The initial mass of carrot slices for drying was revised based on Equation (12) and the final results are presented in Table 4.4.

Table 4. 4: The optimized conditions for drying of carrot slices in MWFBD.

	Optimal condition	Optimal condition after revising the initial mass of the carrot slices for drying
Initial microwave power density (W/g)	0.48	0.44
Temperature (ºC)	55	55
Mass (g)	200	180

The carrot slices were pre-treated and dried at the optimized drying conditions with an initial microwave power density of 0.44 W/g and inlet air temperature of 55 ºC for further studies on microwave-assisted fluidized bed drying.

4.3.4 Mathematical Models and Statistical Analysis

The drying curves of carrot slices were fitted to the mathematical models (Equations (3) – (8)) and are shown in Figures 4.6–4.9. The statistical values to estimate the accuracy of closeness of fit were calculated and shown in Tables 4.5–4.8. The best fitting model was determined according to the lowest χ^2, RMSE and SSE, and the highest R^2 values. The drying coefficient, k, increased with the increase in inlet air temperature in all the drying conditions for all the initial microwave power densities (Table 4.5–4.7). The R^2 values ranged from 0.9712 to 0.9996, 0.9687 to 0.9998 and 0.9740 to 0.9998, and the SSE values ranged from 0.000344 to 0.03324, 0.0001839 to 0.02977 and 0.0002129 to 0.02664 for power density of 0.44 W/g, 0.77 W/g and 1.21 W/g respectively. The Logarithmic model was the best fitting mathematical model for the initial microwave power density of 0.44 W/g at 40 ºC and 60 ºC, 0.77 W/g at 40 ºC, and 1.21 W/g at 40 ºC and 50 ºC. The Page model was the best fitting model for the initial microwave power density of 0.44 W/g at 50 ºC, 0.77 W/g at 50 ºC and 60 ºC, and 1.21 W/g at 60 ºC (Tables 4.5–4.7, Figures 4.6–4.8).

The Logarithmic model was found as the best fitting with the highest R^2 values of 0.9999 and 0.9993, the lowest SSE values of 0.000043 and 0.0005445, and the lowest χ^2 values of 0.00001 and 0.000187 for the drying of the carrot slices pre-treated with 20% sugar solution and 1% citric acid solution respectively at the optimized drying conditions in MWFBD. The Page model was best, to reflect the drying kinetics for carrot slices pre-treated with water blanching, with the highest R^2 values of 0.9998, lowest SSE value and χ^2 value of 0.00018 and 0.000038(Table 4.8 and Figure 4.9). These models can be used to scale-up the microwave-assisted fluidized-bed dryer to a commercial scale.

Table 4. 5: Estimated chi-square (χ^2), correlation coefficient (R^2), root mean square error (RMSE) and reduced sum square error (SSE) for drying of carrot slices in MWFBD at the power density of 0.44 W/g.

Power Density (W/g)	Temp °C	Statistics /Coefficient	Models: Newton	Page		Modified Page		Henderson & Pabis		Logarithmic			Wang &Singh	
			k	k	n	k	n	k	a	k	a	c	a	b
0.44	40°C	Coeffi.	0.05605	0.06267	0.964	0.1199	0.4673	0.0554	0.9885	0.06166	0.9963	0.000110	-0.0391	0.00039
		χ^2	0.000073	0.000044		0.000079		0.000062		0.000052			0.002750	
		RMSE	0.008449	0.006539		0.008794		0.007809		0.007073			0.0524	
		SSE	0.000928	0.0005131		0.000928		0.0007318		0.0005003			0.03295	
		R^2	0.9992	0.9996		0.9992		0.9994		0.9996			0.9712	
	50°C	Coeffi.	0.08019	0.08606	0.974	0.6725	0.1192	0.07977	0.995	0.08349	0.9924	0.005909	-0.0533	0.000707
		χ^2	0.000054	0.000045		0.00006		0.000056		0.000053			0.003658	
		RMSE	0.007204	0.006473		0.007594		0.007325		0.00701			0.06077	
		SSE	0.000519	0.0003771		0.000519		0.0004829		0.000344			0.03324	
		R^2	0.9995	0.9996		0.9995		0.9995		0.9996			0.9923	
	60°C	Coeffi.	0.1018	0.07777	1.107	0.1692	0.6018	0.1028	1.01	0.08519	1.027	-0.0287	-0.0701	0.00123
		χ^2	0.000358	0.00147		0.000417		0.000396		0.000106			0.001584	
		RMSE	0.01892	0.01218		0.02044		0.01991		0.01035			0.03985	
		SSE	0.002507	0.0008901		0.002507		0.002379		0.0004289			0.009527	
		R^2	0.9971	0.999		0.9971		0.9972		0.9995			0.9889	

Table 4. 6: Estimated chi-square (χ^2), correlation coefficient (R^2), root mean square error (RMSE) and reduced sum square error (SSE) for drying of carrot slices in MWFBD at the power density of 0.77 W/g.

Power Density (W/g)	Temp °C	Statistics /Coefficient	Models											
			Newton	Page		Modified Page		Henderson & Pabis		Logarithmic			Wang &Singh	
			k	k	n	k	n	k	a	k	a	c	a	b
0.77	40°C	Coeffi.	0.06956	0.07135	0.991	0.3437	0.2023	0.06949	0.999	0.06721	0.986	0.01322	-0.0475	0.000567
		χ^2	0.000036	0.000037		0.000039		0.000039		0.000026			0.002965	
		RMSE	0.005831	0.005957		0.006116		0.006106		0.004794			0.05457	
		SSE	0.000374	0.0003548		0.0003741		0.0003729		0.0001839			0.02977	
		R^2	0.9996	0.9997		0.9996		0.9996		0.9998			0.9687	
	50°C	Coeffi.	0.09248	0.06263	1.15	0.108	0.856	0.09408	1.019	0.06116	0.9948	0.003804	-0.0636	0.001006
		χ^2	0.000449	0.000032		0.000513		0.00049		0.000042			0.00144	
		RMSE	0.02125	0.005678		0.02272		0.02126		0.006472			0.03781	
		SSE	0.003613	0.0002257		0.003613		0.003164		0.0002094			0.01001	
		R^2	0.9962	0.9998		0.9962		0.9966		0.9998			0.9893	
	60°C	Coeffi.	0.1087	0.0728	1.164	0.3069	0.354	0.1102	1.016	0.07313	1.001	-0.002219	-0.074	0.001334
		χ^2	0.000521	0.00007		0.000608		0.000559		0.000102			0.001557	
		RMSE	0.02295	0.008442		0.02479		0.02376		0.01024			0.0393	
		SSE	0.003687	0.0004276		0.003687		0.003388		0.0004197			0.009268	
		R^2	0.9958	0.9995		0.9958		0.9961		0.9995			0.9894	

Table 4. 7: Estimated chi-square (χ^2), correlation coefficient (R^2), root mean square error (RMSE) and reduced sum square error (SSE) for drying of carrot slices in MWFBD at the power density of 1.21 W/g.

Power Density (W/g)	Temp °C	Statistics /Coefficient	Models Newton	Page		Modified Page		Henderson & Pabis		Logarithmic			Wang &Singh	
			k	k	n	k	n	k	a	k	a	c	a	b
1.21	40℃	Coeffi.	0.08017	0.07039	1.047	0.1533	0.5228	0.08077	1.008	0.06764	0.9914	0.007643	-0.0533	0.000703
		χ^2	0.000075	0.000032		0.000084		0.000074		0.000031			0.00297	
		RMSE	0.008576	0.005621		0.00904		0.008524		0.005515			0.0544	
		SSE	0.000736	0.0002843		0.0007355		0.0006539		0.0002129			0.02664	
		R^2	0.9993	0.9997		0.9993		0.9994		0.9998			0.974	
	50℃	Coeffi.	0.07718	1.14	0.762	0.1429	0.1101	1.014	0.076	0.9976	0.00083	0.07718	-0.0737	0.001342
		χ^2	0.000438	0.000107		0.000511		0.000475		0.00016			0.001706	
		RMSE	0.02088	0.01026		0.02255		0.02173		0.01254			0.04136	
		SSE	0.003052	0.0006313		0.003052		0.002834		0.0006286			0.01026	
		R^2	0.9965	0.9993		0.9965		0.9967		0.9993			0.9882	
	60℃	Coeffi.	0.088	1.171	0.127	1.024	0.1313	1.013	0.085	0.9924	0.00665	0.088	-0.087	0.001858
		χ^2	0.000517	0.000097		0.000621		0.000587		0.000147			0.001825	
		RMSE	0.02282	0.009867		0.02499		0.02429		0.0212			0.04265	
		SSE	0.003123	0.0004868		0.003124		0.00295		0.0004396			0.009096	
		R^2	0.9961	0.9994		0.9961		0.9963		0.9995			0.9887	

Table 4. 8: Estimated chi-square (χ^2), correlation coefficient (R^2), root mean square error (RMSE) and reduced sum square error (SSE) for drying of pretreated carrot slices at the optimized drying conditions in MWFBD.

Drying Conditions	Pre-treat Methods	Statistics /Coefficient	Models: Newton	Page		Modified Page		Henderson & Pabis		Logarithmic			Wang &Singh	
			k	k	n	k	n	k	a	k	a	c	a	b
0.44	WB	Coeffi.	0.1363	0.09405	1.165	1.029	0.1324	0.1375	1.011	0.09737	1.007	-0.00761	-0.0884	0.001895
(W/g)		χ^2	0.000424	0.000038		0.000509		0.000482		0.010961			0.002558	
		RMSE	0.02076	0.006		0.02274		0.02213		0.006326			0.05042	
55℃		SSE	0.002587	0.00018		0.002587		0.00245		0.0001201			0.01271	
		R^2	0.9968	0.9998		0.9968		0.997		0.9999			0.9845	
	SS	Coeffi.	0.1271	0.1161	1.039	0.3095	0.4107	0.1275	1.003	0.1122	0.993	0.00669	-0.0793	0.001518
		χ^2	0.000037	0.000014		0.000043		0.000041		0.00001			0.004925	
		RMSE	0.006067	0.003944		0.006553		0.006388		0.003269			0.07012	
		SSE	0.000258	0.000093		0.0002577		0.0002448		0.000043			0.0295	
		R^2	0.9997	0.9999		0.9997		0.9997		0.9999			0.9649	
	CAS	Coeffi.	0.1311	0.09424	1.144	0.888	0.1476	0.1322	1.01	0.09954	1.013	-0.01366	-0.0866	0.001832
		χ^2	0.000442	0.00019		0.000531		0.000509		0.000187			0.002148	
		RMSE	0.02124	0.01186		0.02327		0.02278		0.01347			0.04603	
		SSE	0.002707	0.0007031		0.002707		0.002595		0.0005445			0.01059	
		R^2	0.9967	0.9991		0.9967		0.9968		0.9993			0.9843	

(a)

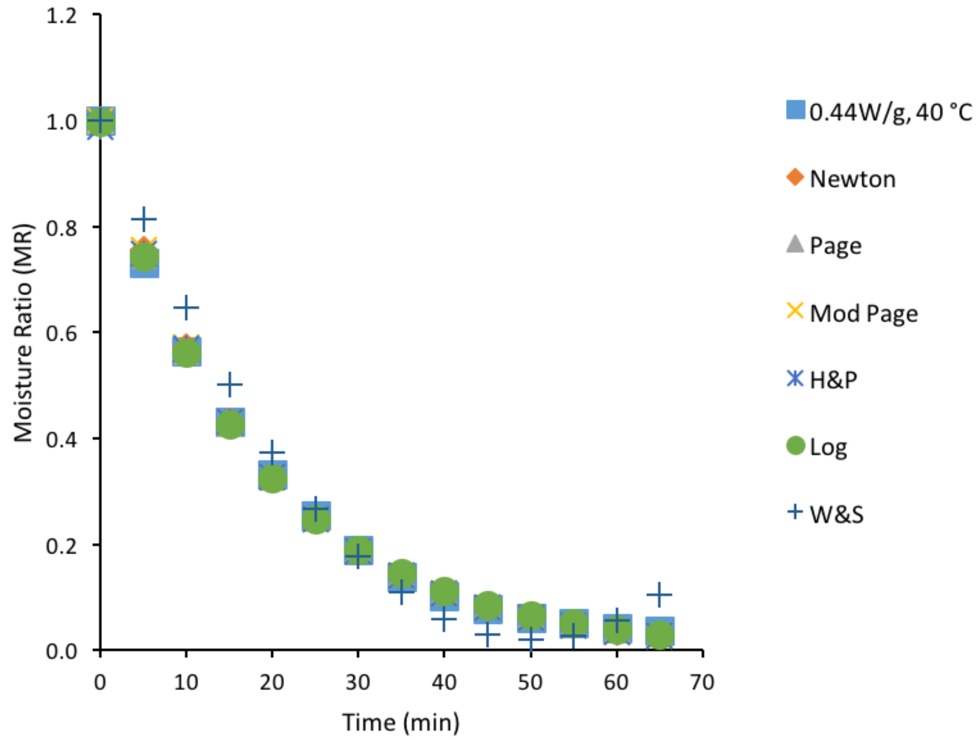
1.2
1.0
0.8
0.6
0.4
0.2
0.0
Moisture Ratio (MR)
0
10
20
30
40
50
60
70
Time (min)
0.44W/g, 40 °C
Newton
Page
Mod Page
H&P
Log
W&S

(b)

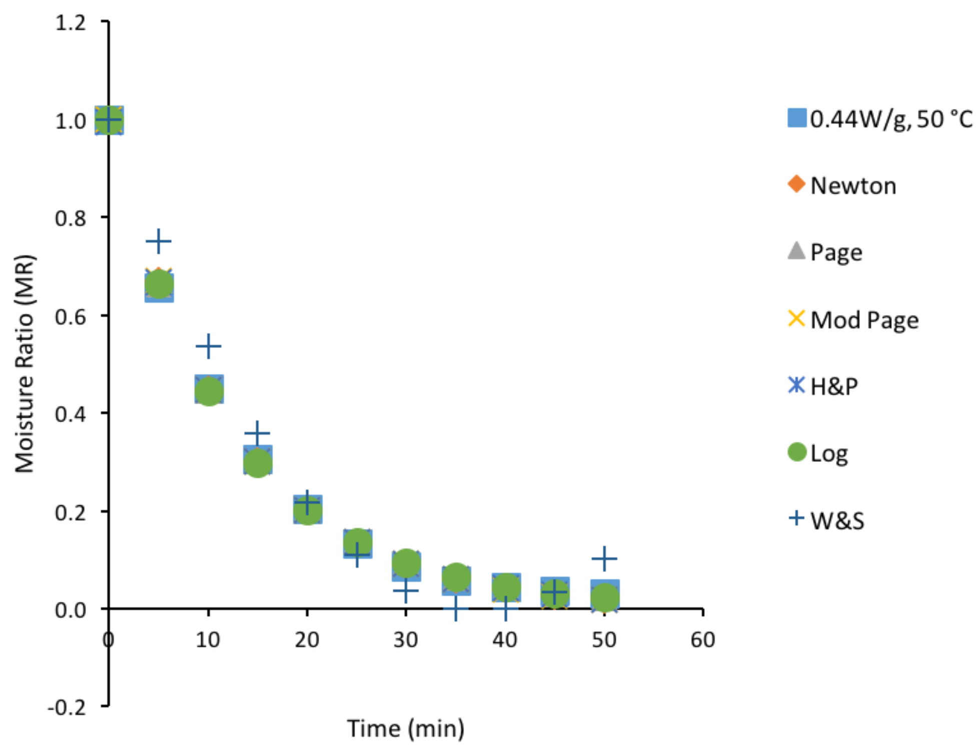
1.2
1.0
0.8
0.6
0.4
0.2
0.0
-0.2
Moisture Ratio (MR)
0
10
20
30
40
50
60
Time (min)
0.44W/g, 50 °C
Newton
Page
Mod Page
H&P
Log
W&S

(c)

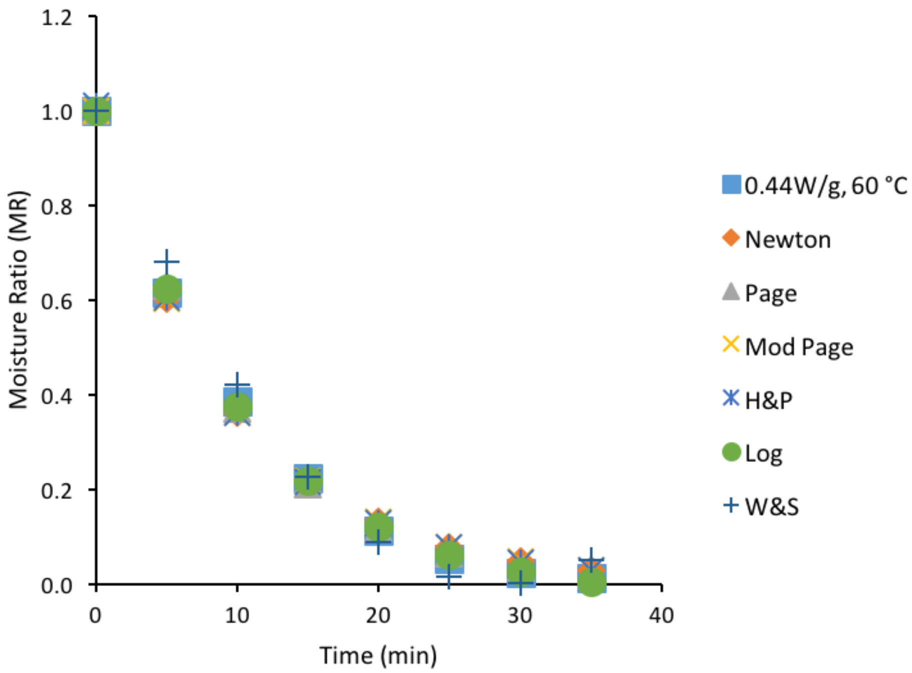

Figure 4. 6: The mathematical models fitting to the drying curve of (a) carrot slices dried at the initial microwave power density of 0.44 W/g, inlet air temperature of 40 °C; (b) carrot slices dried at the initial microwave power density of 0.44 W/g, inlet air temperature of 50 °C and (c) carrot slices dried at the initial microwave power density of 0.44 W/g, inlet air temperature of 60 °C. Mod Page: Modified Page model; H&P: Henderson & Pabis model; Log: Logarithmic model; W&S: Wang and Singh model.

(a)

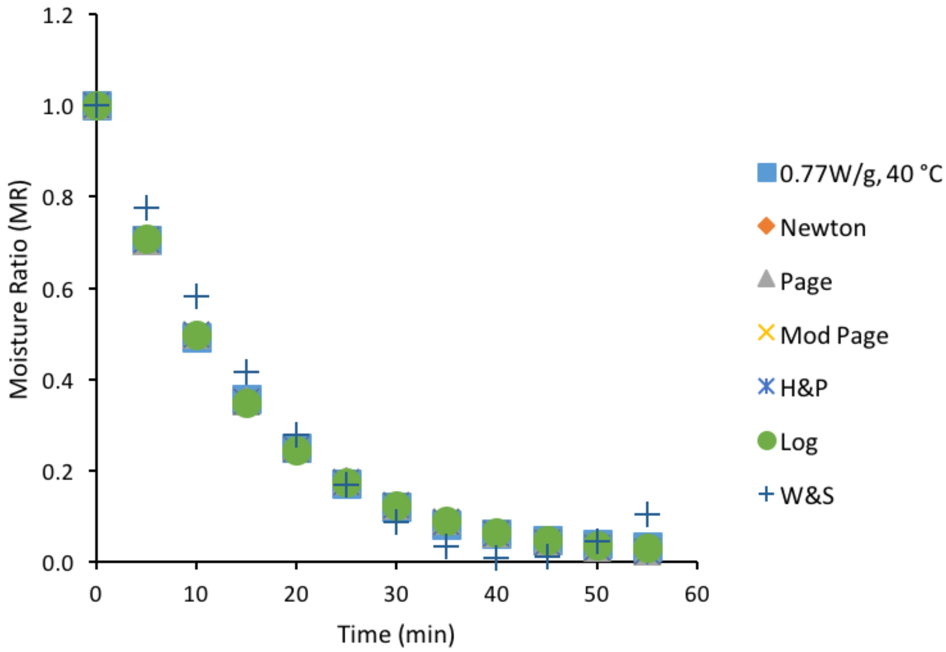

1.2
1.0
0.8
0.6
0.4
0.2
0.0
Moisture Ratio (MR)
0
10
20
30
40
50
60
Time (min)
0.77W/g, 40 °C
Newton
Page
Mod Page
H&P
Log
W&S

(b)

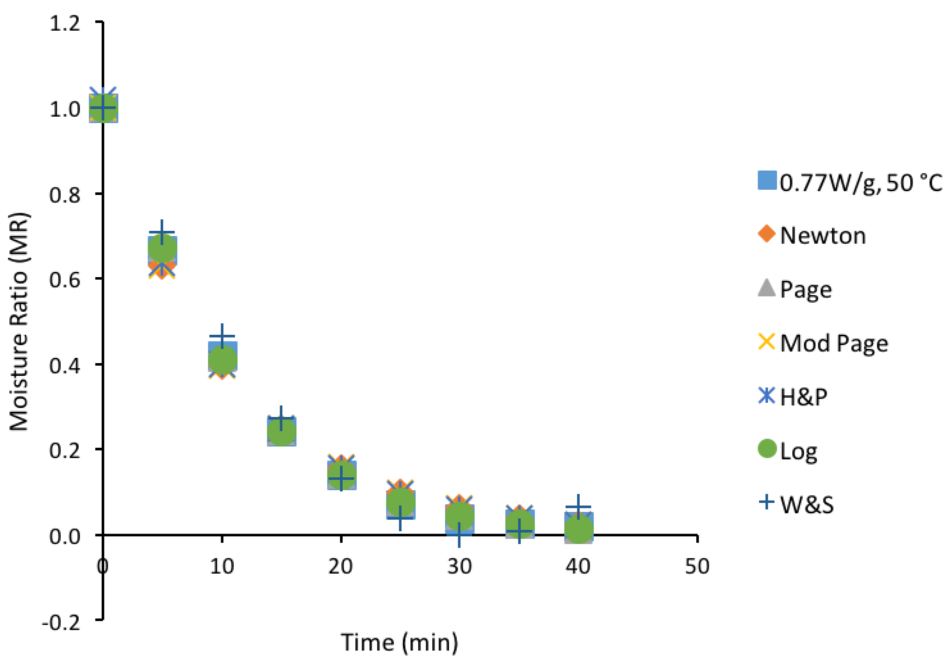

1.2
1.0
0.8
0.6
0.4
0.2
0.0
-0.2
Moisture Ratio (MR)
0
10
20
30
40
50
Time (min)
0.77W/g, 50 °C
Newton
Page
Mod Page
H&P
Log
W&S

(c)

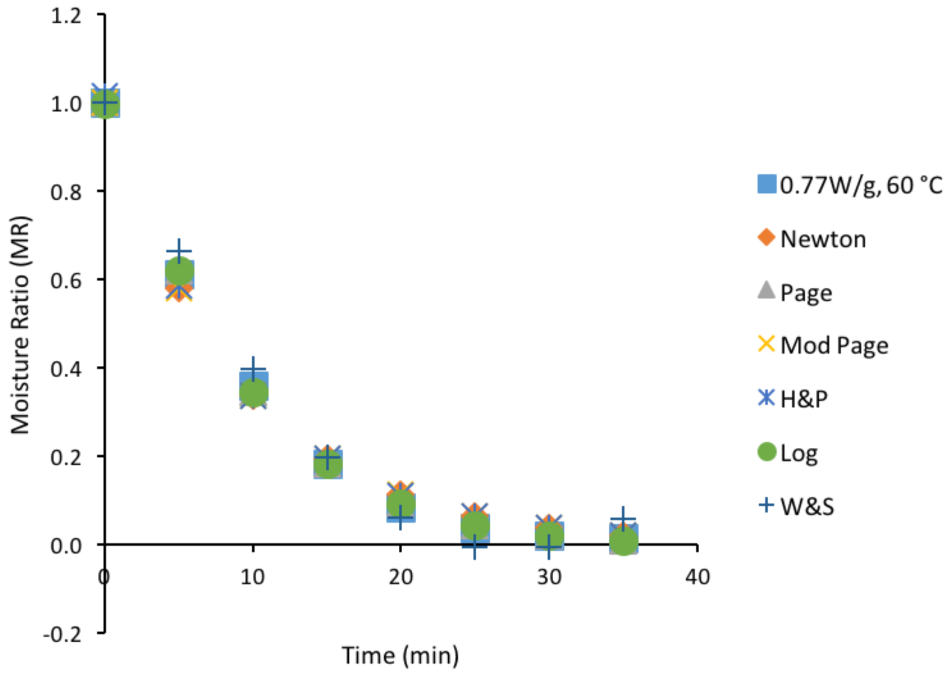

Figure 4. 7: The mathematical models fitting to the drying curve of (a) carrot slices dried at the initial microwave power density of 0.77 W/g, inlet air temperature of 40 °C; (b) carrot slices dried at the initial microwave power density of 0.77 W/g, inlet air temperature of 50 °C and (c) carrot slices dried at the initial microwave power density of 0.77 W/g, inlet air temperature of 60 °C. Mod Page: Modified Page model; H&P: Henderson & Pabis model; Log: Logarithmic model; W&S: Wang and Singh model.

(a)

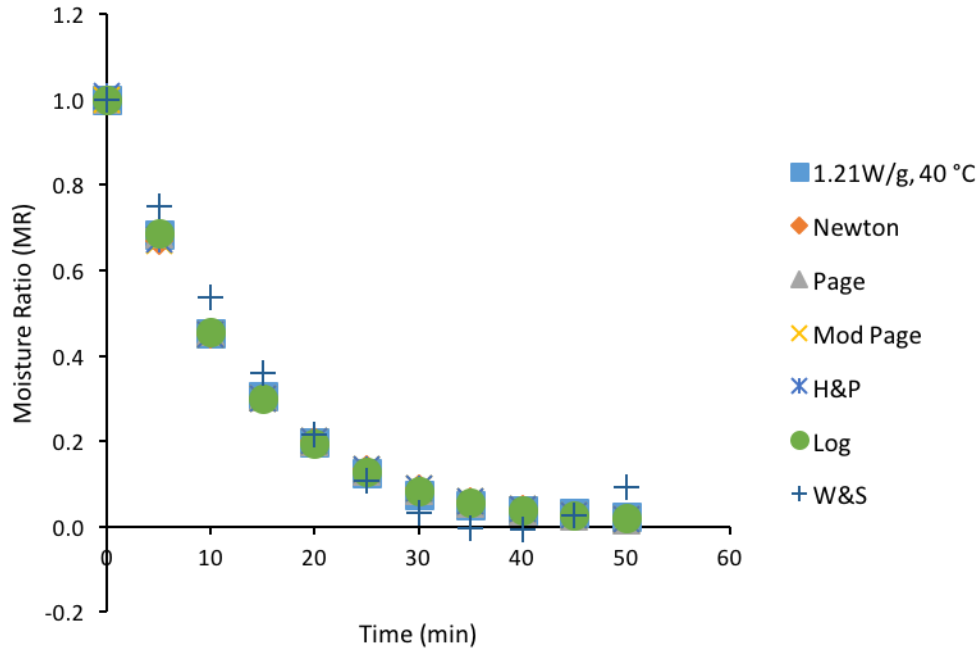

Moisture Ratio (MR)
1.2
1.0
0.8
0.6
0.4
0.2
0.0
-0.2
0
10
20
30
40
50
60
Time (min)
1.21W/g, 40 °C
Newton
Page
Mod Page
H&P
Log
W&S

(b)

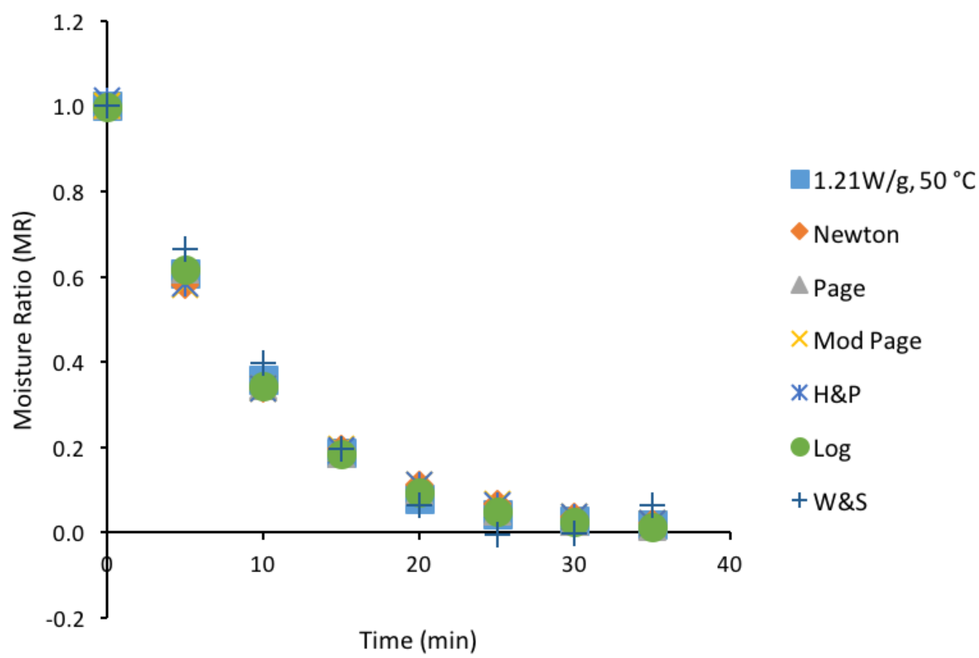

Moisture Ratio (MR)
1.2
1.0
0.8
0.6
0.4
0.2
0.0
-0.2
0
10
20
30
40
Time (min)
1.21W/g, 50 °C
Newton
Page
Mod Page
H&P
Log
W&S

(c)

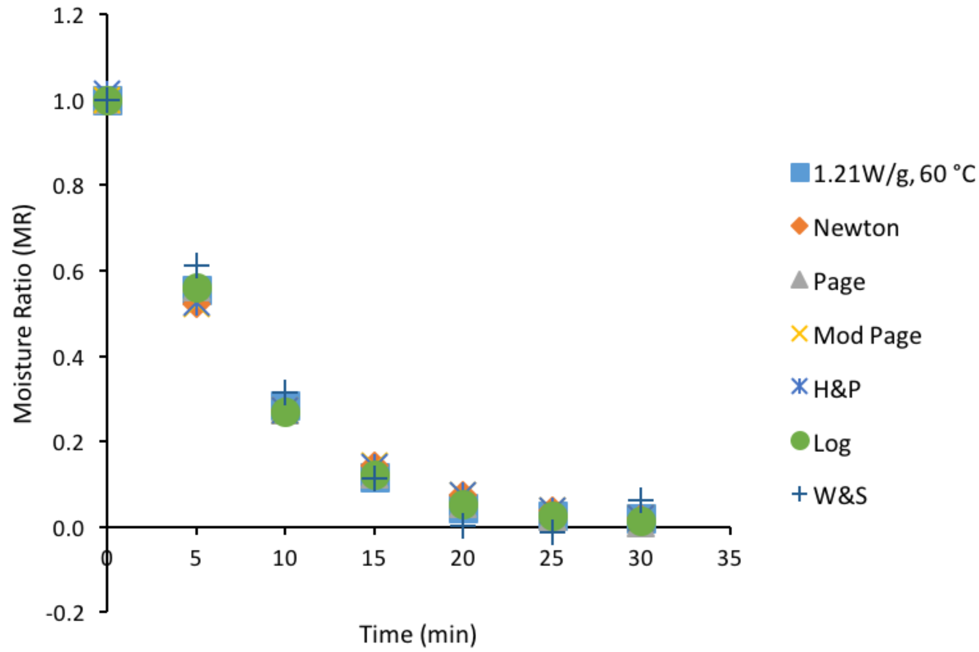

Figure 4. 8: The mathematical models fitting to the drying curve of (a) carrot slices dried at the initial microwave power density of 1.21 W/g, inlet air temperature of 40 °C; (b) carrot slices dried at the initial microwave power density of 1.21 W/g, inlet air temperature of 50 °C and (c) carrot slices dried at the initial microwave power density of 1.21 W/g, inlet air temperature of 60 °C. Mod Page: Modified Page model; H&P: Henderson & Pabis model; Log: Logarithmic model; W&S: Wang and Singh model.

(a)

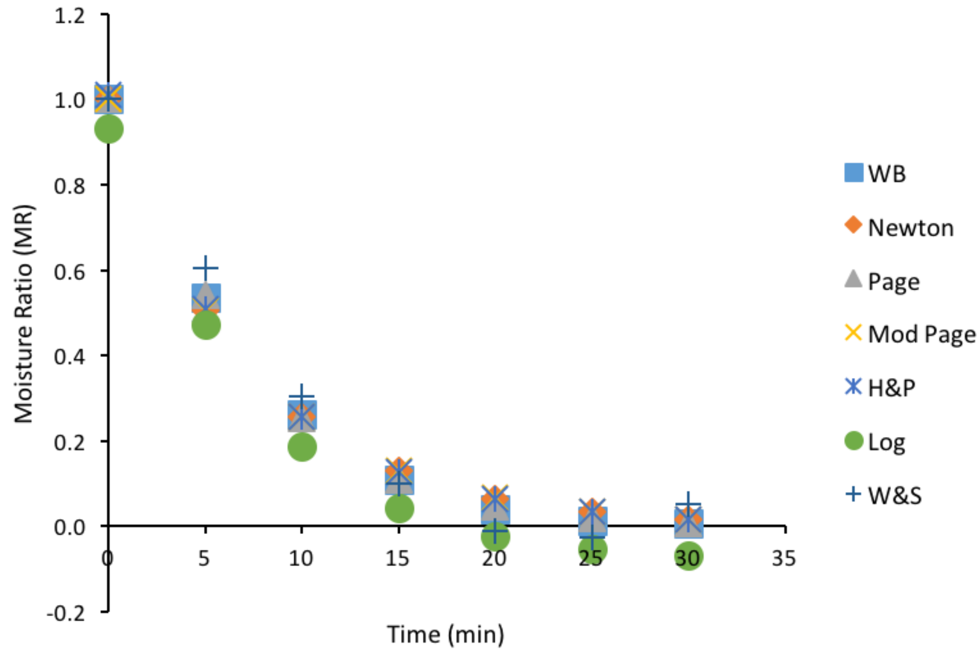

1.2
1.0
0.8
0.6
0.4
0.2
0.0
-0.2
Moisture Ratio (MR)
0
5
10
15
20
25
30
35
Time (min)
WB
Newton
Page
Mod Page
H&P
Log
W&S

(b)

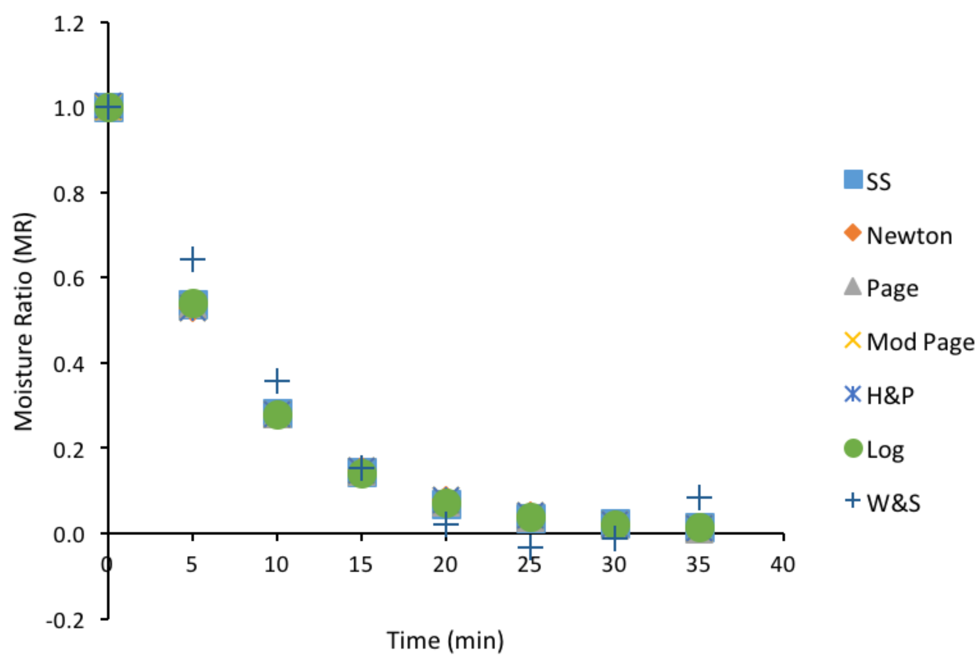

1.2
1.0
0.8
0.6
0.4
0.2
0.0
-0.2
Moisture Ratio (MR)
0
5
10
15
20
25
30
35
40
Time (min)
SS
Newton
Page
Mod Page
H&P
Log
W&S

(c)

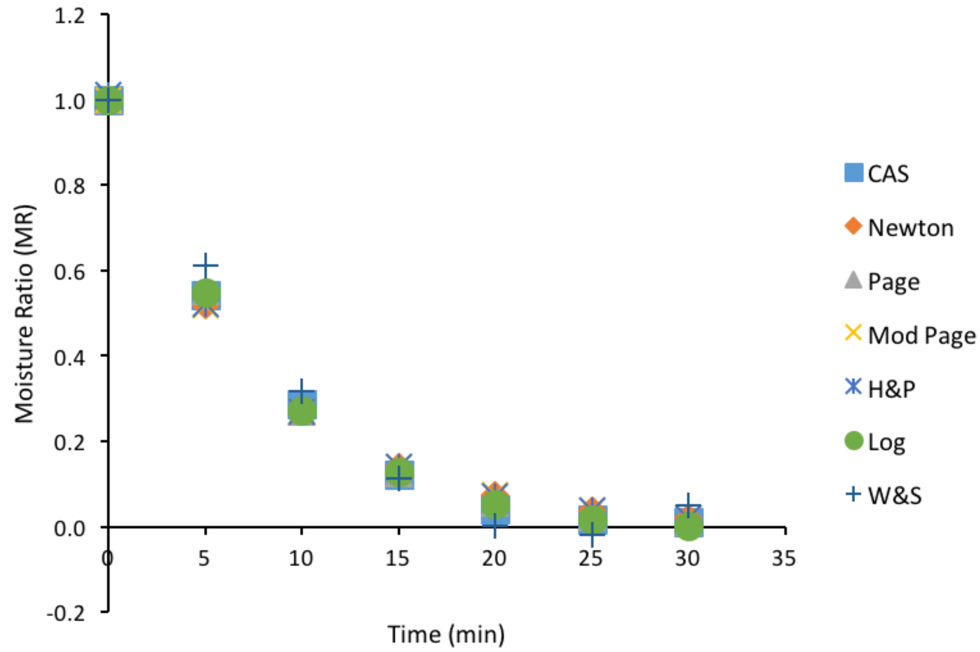

Figure 4. 9: The mathematical models fitting to the drying curve of (a) carrot slices pre-treated with water blanching (WB), (b) carrot slices pre-treated with 20% sugar solution (SS), and (c) carrot slices pre-treated with 1% citric acid solution (CAS), dried at the optimized drying conditions in MWFBD (initial microwave power density of 0.44 W/g, inlet air temperature of 55 °C). Mod Page: Modified Page model; H&P: Henderson & Pabis model; Log: Logarithmic model; W&S: Wang and Singh model.

4.3.5 Effective Moisture Diffusion Coefficient

The effective moisture diffusion coefficient (D_{eff}) of the drying of carrot slices at different conditions, and the drying of pre-treated carrot slices at the optimized drying conditions (power density of 0.44 W/g, drying temperature of 55 °C), are given in Table 4.9. It can be seen that the D_{eff} values were increased with the increase in inlet air temperature at the same initial microwave power density. At the same inlet air temperature, the D_{eff} values were slightly increased with the increase in the initial microwave power density. Pre-treatment of the carrot slices before drying improved the drying rate due to the significant increase in the D_{eff} values. The lowest D_{eff} value was found at the power density of 0.44 W/g with the inlet air temperature of 40 °C, and the highest was obtained for drying of carrot slices pre-treated with water blanching followed by the drying at the optimized drying conditions.

Table 4. 9: Effective moisture diffusion coefficient of drying of carrot slices at different drying conditions.

Initial microwave Power Density (W/g)	Inlet air Temperature (°C) and Pre-treatment	Effective Moisture Diffusion Coefficient (D_{eff} ± E-08)
0.44 W/g	40	0.720
	50	1.053
	60	1.489
0.77 W/g	40	0.900
	50	1.304
	60	1.588
1.21 W/g	40	1.079
	50	1.561
	60	1.890
0.44 W/g	55 (WB)	2.121
	55 (SS)	1.765
	55 (CAS)	2.009

4.3.6 Color Values of Pre-treated Carrot Slices

It can be observed that the application of pre-treatments remarkably affected the final color of dried carrot slices. In comparison to the color values of the dried carrot slices without any pre-treatment given in Table 4.2, the color values of the dried carrot slices with pre-treatment given in Table 4.10 have increased. The L^* and the b^* values were significantly increased, a^* values were slightly increased and the total color difference (ΔE) was significantly reduced. The dried carrot slices with pre-treatment were lighter and with more red and yellow hues than the dried carrot slices without any pre-treatment (Fig. 4.10). All the values (L^*, a^* and b^*) in Table 4.10 were close to the color values of the fresh carrot slices and show that the lightness, redness and yellowness were not changed by the drying process. The lowest total color difference was observed for dried carrot slices pre-treated with 20% sugar solution, hence sugar solution pre-treatment is the most effective way to maintain the original color compared with water blanching and citric acid solution pre-treatments.

Table 4. 10: Color values of pre-treated carrot slices dried at the optimized conditions in MWFBD.

Pre-treatment Method	Power Density (W/g)	Temperature (ºC)	Color values			
			L^*	a^*	b^*	ΔE
Fresh	-	Ambient	53.86	26.46	50.51	-
WB	0.44	55	54.17	28.27	55.76	5.57
SS			53.29	27.35	50.74	1.08
CAS			55.75	29.83	57.14	7.67

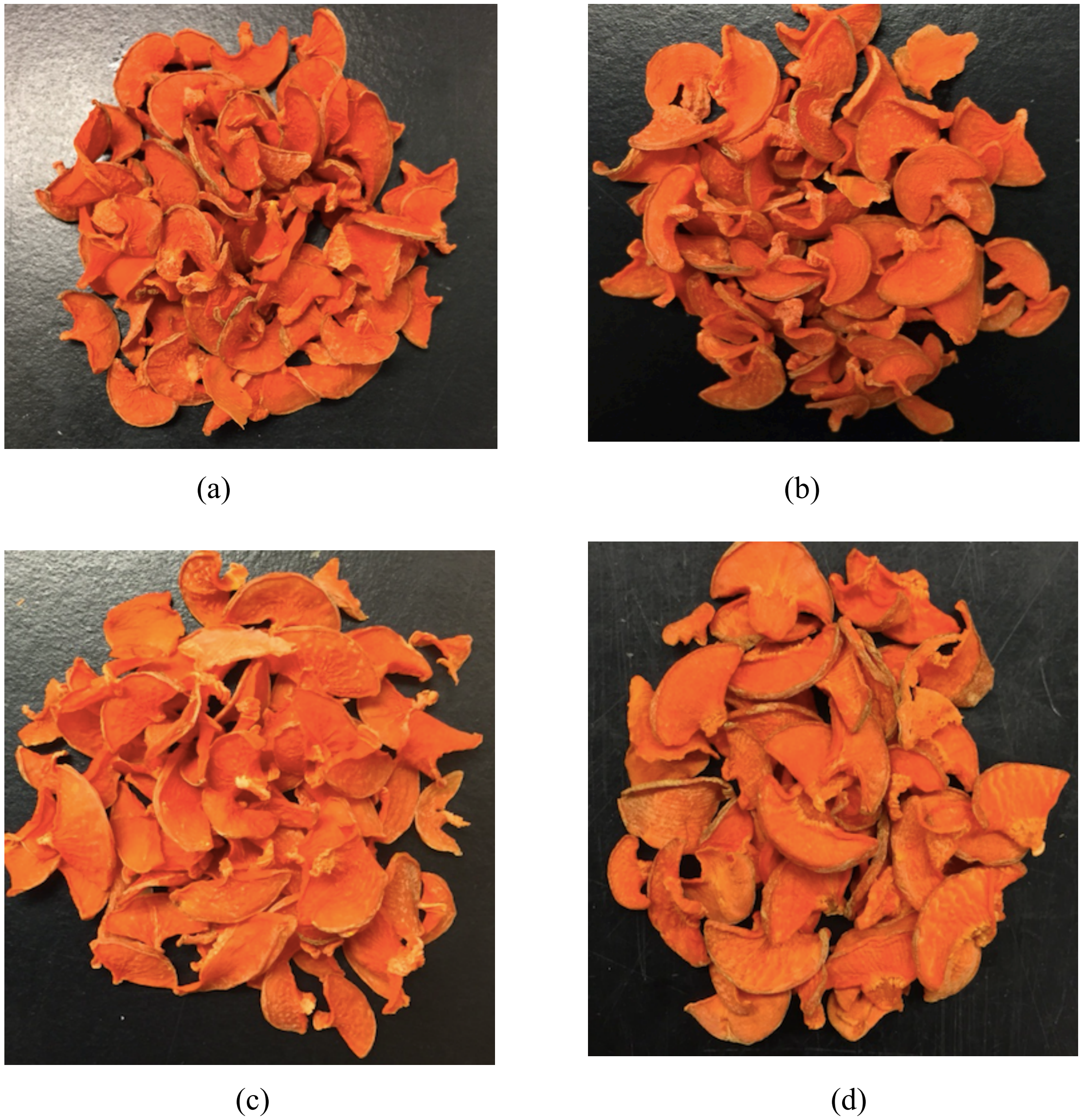

Figure 4. 10: The color of dried carrot slices with; (a) water blanching pre-treatment (WB) and dried at the optimized conditions, (b) sugar solution (SS) pre-treatment and dried at the optimized conditions, (c) citric acid solution (CAS) pre-treatment and dried at the optimized conditions and (d) without any pre-treatment.

4.3.7 Rehydration Characteristics

The rehydration capability (RC) were calculated using Equation (20) and are shown in Table 4.11. There was no significant difference among the RC values of the dried carrot slices without any pre-treatment. But the RC values of the carrot slices pre-treated with water blanching (WB) and citric acid solution (CAS) followed by the drying at the optimized conditions (0.44 W/g, 55 ºC) were higher than the RC values of others. It implied that the drying process caused less structural damage in carrot slices with the protection of water blanching and citric acid solution pre-treatments.

Table 4. 11: Rehydration capability (RC) of dried carrot slices at different drying conditions.

Initial Microwave Power Density (W/g)	Temperature (ºC) and Pre-treatment	Rehydration Capability (RC)
0.44	40	4.66
	50	4.40
	60	4.84
0.77	40	4.89
	50	4.76
	60	4.87
1.21	40	4.76
	50	4.60
	60	4.67
0.44	55 (WB)	5.79
	55 (SS)	4.50
	55 (CAS)	6.24

4.3.8 Textural Analysis

The results of textural strength analysis of the rehydrated carrot slices are presented in Figures 4.11–4.13. The Figures 4.11 and 4.12 show that after rehydration, the dried carrot slices with pre-treatment required more force and energy in comparison to the dried carrot slices without any pre-treatment. There was no significant difference in the textural properties among the carrot slices without any pre-treatment. Figure 4.13 shows the hardness of the rehydrated carrot slices from different drying conditions. It shows that, the higher the slope value is, the harder the carrot slices are. The dried carrot slices with pre-treatment were harder than the dried carrot slices without any pre-treatment after rehydration. This may be due to the pre-treatments enhanced the strength of the internal structure of carrot slices before drying (Zhang et al., 2006). The results implied that, the chewiness of the dried carrot slices with pre-treatment would be better, when they are used in making a soup, and therefore will be more acceptable by the consumers.

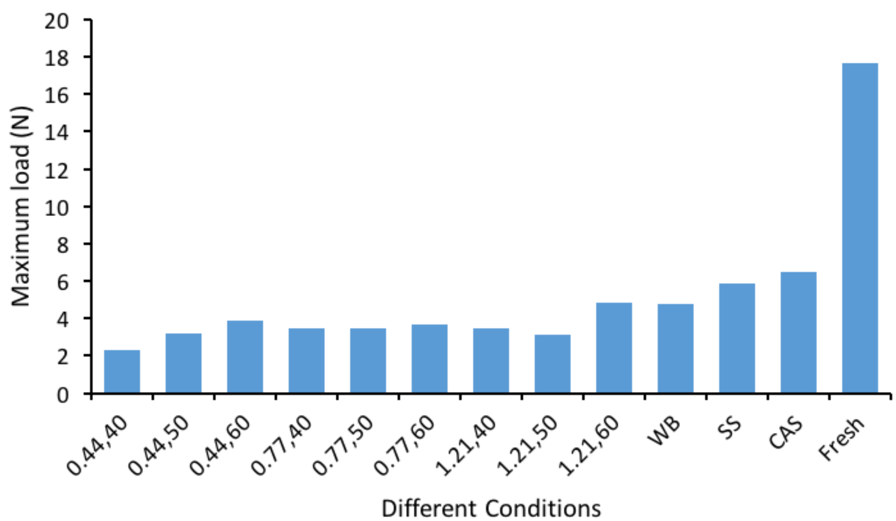

Figure 4. 11: Comparison of the maximum load (N) on the rehydrated carrot slices from different drying conditions.

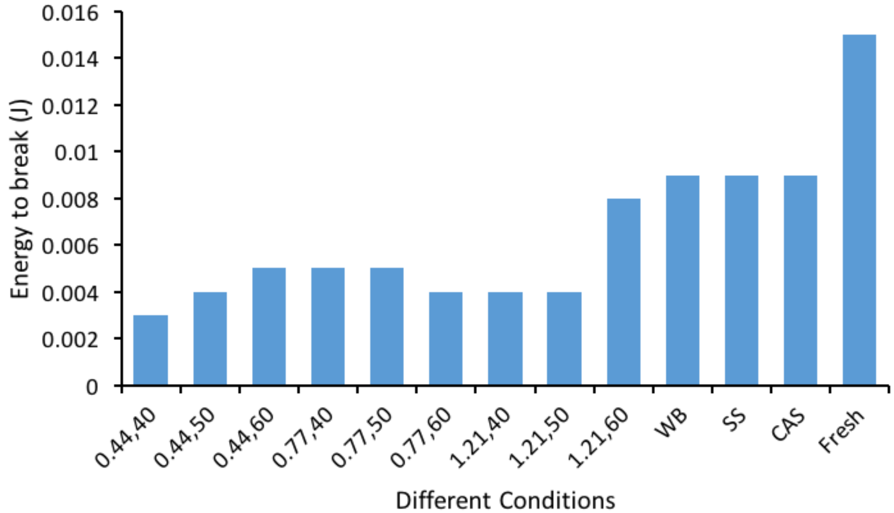

Figure 4. 12: Comparison of the energy to break (J) the rehydrated carrot slices from different drying conditions.

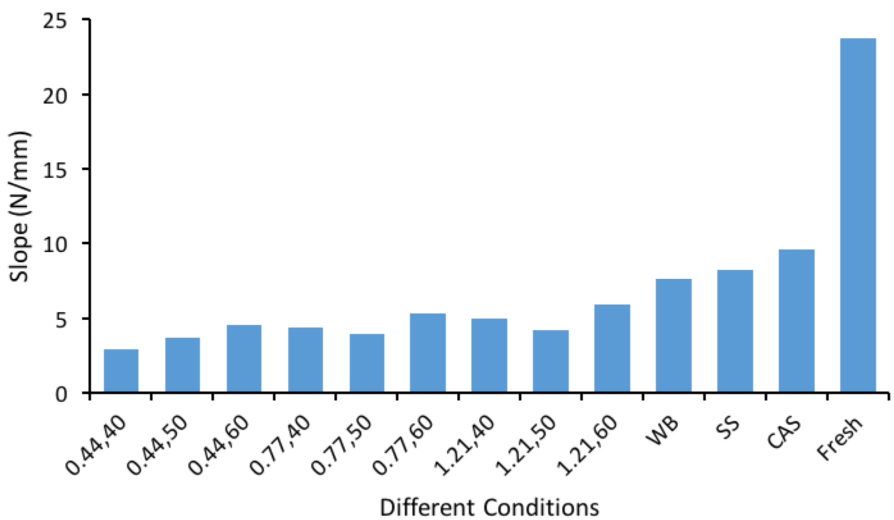

Figure 4. 13: Comparison of Slope (N/mm) value of the rehydrated carrot slices from different drying conditions.

4.4 Conclusion

In this study, the drying characteristics of carrot slices in microwave-assisted fluidized-bed drying at different initial microwave power densities and inlet air temperatures were investigated. The drying conditions in MWFDB system were optimized (initial microwave power density of 0.44 W/g and inlet air temperature of 55 ºC) based on the predicted drying time and the total color difference of dried carrot slices. The carrot slices with pre-treatment of water blanching (WB), 20% sugar solution (SS) and 1% citric acid solution (CAS) were dried at the optimized drying conditions in MWFBD system. The results showed that, with pre-treatments, the effective moisture diffusion coefficient (D_{eff}) was increased and the lightness, redness and yellowness of the dried carrot slices were also increased. Also, the pretreatment resulted in increased maximum load, energy to break and the hardness of the rehydrated carrot slices, in comparison to the carrot slices without any pre-treatment. This study can help to develop processes for the production of value added materials from the vegetable and fruit residues and thus to reclaim the value in them. Further studies have to be conducted using the MWFBD system for the processing of other vegetables and fruits to advance the application of this technology to industrial scales.

Acknowledgements

The authors are grateful to the Natural Sciences and Engineering Research Council of Canada (NSERC) and ministère de l'Agriculture, des Pêcheries et de l'Alimentation du Québec (MAPAQ) for the financial support (Grant No. IA113076).

References

Balbay, A., Şahin, Ö. 2012. Microwave drying kinetics of a thin-layer liquorice root. *Drying Technology*, **30**(8), 859-864.

Batchelor, W., Kibblewhite, R., He, J. 2008. A new method for measuring RBA applied to the Page equation for the tensile strength of paper. *Appita Journal*, **61**(4), 302.

Billmeyer, F.W., Saltzman, M. 1981. *Principles of color technology*. J. Wiley & sons.

Chen, G., Wang, W., Mujumdar, A.S. 2001. Theoretical study of microwave heating patterns on batch fluidized bed drying of porous material. *Chemical Engineering Science*, **56**(24), 6823-6835.

Crank, J. 1979. *The mathematics of diffusion*. Oxford university press.

Cui, Z.-W., Li, C.-Y., Song, C.-F., Song, Y. 2008. Combined microwave-vacuum and freeze drying of carrot and apple chips. *Drying Technology*, **26**(12), 1517-1523.

Doymaz, İ. 2010. Effect of citric acid and blanching pre-treatments on drying and rehydration of Amasya red apples. *Food and Bioproducts Processing*, **88**(2), 124-132.

Doymaz, I., Kipcak, A.S., Piskin, S. 2015. Microwave Drying of Green Bean Slices: Drying Kinetics and Physical Quality. *Czech Journal of Food Sciences*, **33**(4), 367-376.

Gekas, V., Lamberg, I. 1991. Determination of diffusion coefficients in volume-changing systems—application in the case of potato drying. *Journal of Food Engineering*, **14**(4), 317-326.

Giese, J. 1992. Advances in microwave food processing. *Food technology*, **46**(9), 118-123.

Goksu, E.I., Sumnu, G., Esin, A. 2005. Effect of microwave on fluidized bed drying of macaroni beads. *Journal of Food Engineering*, **66**(4), 463-468.

Gustavsson, J., Cederberg, C., Sonesson, U., Van Otterdijk, R., Meybeck, A. 2011. Global food losses and food waste. *Food and Agriculture Organization of the United Nations, Rom*.

Hovmand, S. 1995. Fluidized bed drying. *Handbook of Industrial Drying*, **1**, 195-248.

Kingsly, A., Singh, R., Goyal, R., Singh, D. 2007. Thin-layer drying behaviour of organically produced tomato. *Am. J. Food Technol*, **2**, 71-78.

Maskan, M. 2001. Drying, shrinkage and rehydration characteristics of kiwifruits during hot air and microwave drying. *Journal of food engineering*, **48**(2), 177-182.

Mayor, L., Sereno, A. 2004. Modelling shrinkage during convective drying of food materials: a review. *Journal of Food Engineering*, **61**(3), 373-386.

Midilli, A., Kucuk, H. 2003. Mathematical modeling of thin layer drying of pistachio by using solar energy. *Energy conversion and Management*, **44**(7), 1111-1122.

Midilli, A., Kucuk, H., Yapar, Z. 2002. A new model for single-layer drying. *Drying technology*, **20**(7), 1503-1513.

Mohapatra, D., Rao, P.S. 2005. A thin layer drying model of parboiled wheat. *Journal of food engineering*, **66**(4), 513-518.

Mujumdar, A.S. 2014. *Handbook of industrial drying*. CRC Press.

Murthy, K., Pandurangapp, T., Manohar, B. 2012. Microwave drying of mango ginger (Curcuma amada Roxb): prediction of drying kinetics by mathematical modelling and artificial neural network. *International Journal of Food Science & Technology*, **47**(6), 1229-1236.

Nair, G., Liplap, P., Gariepy, Y., Raghavan, G. 2011. Microwave drying of flax fibre at controlled temperatures. *Journal of Agricultural Science and Technology B*, **1**(8), 9-21.

Overhults, D., White, G., Hamilton, H., Ross, I. 1973. Drying soybeans with heated air. *Amer Soc Agr Eng Trans ASAE*.

Prabhanjan, D., Ramaswamy, H., Raghavan, G. 1995. Microwave-assisted convective air drying of thin layer carrots. *Journal of Food engineering*, **25**(2), 283-293.

Ratti, C., Mujumdar, A. 1997. Solar drying of foods: modeling and numerical simulation. *Solar energy*, **60**(3), 151-157.

Sanga, E., Mujumdar, A., Raghavan, G. 2002. Simulation of convection-microwave drying for a shrinking material. *Chemical Engineering and Processing: Process Intensification*, **41**(6), 487-499.

Singh, A., Nair, G.R., Rahimi, J., Gariepy, Y., Raghavan, V. 2013. Effect of static high electric field pre-treatment on microwave-assisted drying of potato slices. *Drying Technology*, **31**(16), 1960-1968.

Sumnu, G., Turabi, E., Oztop, M. 2005. Drying of carrots in microwave and halogen lamp–microwave combination ovens. *LWT-Food Science and Technology*, **38**(5), 549-553.

Wang, J., Xi, Y. 2005. Drying characteristics and drying quality of carrot using a two-stage microwave process. *Journal of food Engineering*, **68**(4), 505-511.

Xanthopoulos, G., Oikonomou, N., Lambrinos, G. 2007. Applicability of a single-layer drying model to predict the drying rate of whole figs. *Journal of Food Engineering*, **81**(3), 553-559.

Zhang, M., Tang, J., Mujumdar, A., Wang, S. 2006. Trends in microwave-related drying of fruits and vegetables. *Trends in Food Science & Technology*, **17**(10), 524-534.

SUMMARY AND CONCLUSION

Every year, the industrial processing and marketing of vegetables and fruits industries produces a lot of residues which need to be disposed off. These residues contain considerable amounts of essential nutrients such as vitamins, minerals and fibre for animal health. Therefore, drying processes can be applied to convert the vegetable and fruit residues into by-products with added value to make our agriculture more sustainable and environmentally friendly. Many types of drying methods such as hot air drying, microwave drying, solar drying and microwave-assisted convective drying have been applied to dry vegetables and fruits. But sometimes the high temperature applied in the drying process causes the loss of product quality. However, drying time and total expense may be higher when the materials are dried at low temperatures. Thus, in this study, the performance of fluidized-bed drying (FBD) and microwave-assisted fluidized-bed drying (MWFBD) of carrot slices were investigated.

The first objective of this study was to investigate the fluidized-bed drying of carrot slices at controlled temperatures. The carrot slices without any pre-treatment were dried at controlled temperature of 40 ºC, 50 ºC and 60 ºC. The results have shown that the drying time was significantly reduced with the increase of drying temperature. The Logarithmic model was the best fitted mathematical model for the drying curves obtained. The carrot slices with water blanching (WB), 20% sugar solution (SS) and 1% citric acid solution (CAS) pre-treatments were dried at the optimized temperature of 60 ºC. The pretreatment of the carrot slices before drying resulted in 60% reduction in drying time. Also the color difference was minimal in the pre-treated carrot slices after drying. In addition, the hardness of rehydrated carrot slices was higher from the application of pre-treatments.

The second objective of this study was to investigate the microwave-assisted fluidized-bed drying of carrot slices at different initial microwave power densities (0.44 W/g, 0.77 W/g and 1.21 W/g) and inlet air temperatures (40 ºC, 50 ºC and 60 ºC). The experimental data implied that the extent of reduction in drying time was more influenced by temperatures than the initial microwave power densities. The drying conditions were optimized (initial microwave power density of 0.44 W/g and inlet air temperature of 55 ºC) on the basis of the predicted drying duration and the color difference of the dried carrot slices. The drying time decreased with the application of pre-treatment (WB, SS and CAS) of the carrot slices. The effective moisture diffusion coefficient (D_{eff}) of the drying process and the lightness, the redness and the yellowness of the dried carrot slices were increased in the drying of carrot slices with pre-treatment. The dried carrot slices with pre-treatment were harder after rehydration and the chewiness would be better and more acceptable by the market than the dried carrot slices without any pre-treatment.

FUTURE WORKS

1) Drying of other vegetables and fruits can be conducted in the FBD and MWFBD systems to advance the application of these drying technologies.
2) Further study of the effects of different pre-treatments on the drying duration and quality of the dried products during FBD and MWFBD can be done to select the best pre-treatment for time saving and quality protection.
3) A comparison between FBD and MWFBD can be conducted to assess the effect of these technologies on the duration of drying, quality of the dried products, and the energy consumption.